Titre: Title:	Electrospinning as a Promising Technique for Stretchable Organic Electronics Fabrication
Auteur: Author:	Michaël Lerond
Date:	2022
Type:	Mémoire ou thèse / Dissertation or Thesis
Référence: Citation:	Lerond, M. (2022). Electrospinning as a Promising Technique for Stretchable Organic Electronics Fabrication [Ph.D. thesis, Polytechnique Montréal]. PolyPublie. https://publications.polymtl.ca/10333/

POLYTECHNIQUE MONTRÉAL

affiliée à l'Université de Montréal

Electrospinning as a promising technique for stretchable organic electronics fabrication

MICHAËL LEROND

Département de génie chimique

Thèse présentée en vue de l'obtention du diplôme de *Philosophiae Doctor*

Génie chimique

Mai 2022

POLYTECHNIQUE MONTRÉAL

affiliée à l'Université de Montréal

Cette thèse intitulée :

Electrospinning as a promising technique for stretchable organic electronics fabrication

présentée par **Michaël LEROND**

en vue de l'obtention du diplôme de *Philosophiae Doctor*

a été dûment acceptée par le jury d'examen constitué de :

Nick VIRGILIO, président
Fabio CICOIRA, membre et directeur de recherche
William SKENE, membre et codirecteur de recherche
Raphaël TROUILLON, membre
Manisha GUPTA, membre externe

DEDICATION

To my grandmother, who unwittingly helped me to stay in school as long as possible, from a very young age

À ma grand-mère, qui a involontairement contribué à ce que je poursuive mes études le plus longtemps possible, et ce, depuis mon plus jeune âge.

ACKNOWLEDGEMENTS

First, I would like to thanks my supervisor Fabio Cicoira for the opportunity he gave to me when I knocked at his office door few days after I failed my predoctoral exam from Université de Montréal. Fabio, you gave me the second chance I needed by letting me join your research group as a Ph.D. student. You also helped me to go through an endless spiral of failed experiments in June 2020, which might have led to the failure of my Ph.D. I will be always grateful for that. In your group I had the opportunity to work with amazing people and on interesting subjects.

I am grateful to the jury members, Nick Virgilio, Raphael Trouillon and Manisha Gupta for their time and interest in my work.

I am very grateful to the technicians at Polytechnique: Sébastien Chenard for his technical help fixing the electrospinning machine, Daniel Pilon for his support on the Labview software and Etienne Bousser for his time and help to get beautiful SEM pictures.

To my colleagues at Polytechnique: Michel, Ben, Mona, Jo'Elen, Mina, Noémy, Pierre, Erwan, Jeeyeon, Chi-hyeong, Jinsil, Derek, Cécile, Gayaneh, Kathel, Meijing and Sara, it was a pleasure to work with all of you all. A special thanks to Yang, Arun - *Superman* - and Xin - *Knife* -, more than lab mates I found friends, here in the group. I will always remember our "raclette" party during the 2018 New Year eve, our "meetings" and soccer games in Jarry's park. Your support, especially at the end, was very helpful and important to me. I also don't forget Eduardo Di Mauro, even though we never properly worked together, we created a strong friendship by playing soccer in the same team. Thank you a lot Eduardo for the life changer role you played in my life during our soccer games, talks and parties.

I have a special thanks to my wonderful girlfriend Yannice - *Yaya* -, who entered in my life at the beginning of my Ph.D. and always supported me in both good and bad times. Without your daily presence around me this adventure would have been definitely more complicated.

My friends here played a key role as they helped me to keep faith in my work during hard times.

To Yohan, I'm grateful we have met, your friendship is as important to me as our battle royal wins. Maxime, thank you very much for your support during my predoctoral exam and the writing of the

thesis. I also owe a big thanks to Anaëlle (one of the greatest soccer player I met) and Pierre Olivier - *PO* - for their invaluable help.

A special thank to my former flatmates Rémy – *BateauThon151* - and Zoé - *Zouille* -, I spent wonderfull days with you both, thanks you for all the laughs and the joy you brought in my life. I will never forget our improvised 2000's Friday night party. I also don't forget Heather and Bouchra, your friendship means a lot to me.

All my gratitude to my friends in France, our small talks during all these years were important to me, it is good to know our friendship won't die with the distance.

Finally, I would like to thanks my family, my parents Etienne and Isabelle Lerond who, despite the fact I told them every year that I will finish my Ph.D. the next year, always supported me. I don't forget my sisters Laetitia and Emilie and my nephews who have recently enlarged the family, Nolan and Celestine. I hope one day both of you will have the curiosity to read this small dedication.

RÉSUMÉ

Nous sommes à l'aube d'une nouvelle révolution technologique ; la commercialisation des premiers appareils électroniques flexibles tels que les smartphones, les écrans et les téléviseurs a débuté il y a seulement 5 ans. Alors que cette nouvelle technologie fera partie de l'électronique grand public dans les prochaines années, l'intérêt pour l'électronique étirable ne cesse de croître. Ces dispositifs sont prometteurs en tant que capteurs corporels, car ils seront moins invasifs pour le patient, mais aussi dans le domaine des écrans, des batteries et de l'internet des objets, pour n'en citer que quelques-uns. La production à grande échelle de tels dispositifs électroniques doit être assurée par une technique de production rentable et rapide. Dans le cadre de cette thèse, nous avons étudié la fabrication de deux types de dispositifs électroniques étirables en combinant un polymère conjugué disponible dans le commerce avec une méthode de production bien connue dans l'industrie : l'électrofilage.

Tout d'abord, nous avons étudié la viabilité de l'électrofilage comme méthode de fabrication pour produire des transistors électrochimiques organiques étirables (OECTs). Des nano et micro fibres de poly(3,4-éthylènedioxythiophène) : tosylate de fer (PEDOT:Tos) ont été produites par une combinaison d'électrofilage et de polymérisation en phase vapeur (VPP). Brièvement, un mélange constitué d'un polymère porteur et d'un oxydant (tosylate de fer) a été électrofilé et soumis à une vapeur d'éthylènedioxythiophène (EDOT) sous pression réduite pour assurer la formation de PEDOT autour des fibres. Deux polymères porteurs, soit le poly(oxyde d'éthylène) (PEO) ou le poly(vinyl pyrrolidone) (PVP) et différents temps d'électrofilage ont été étudiés pour optimiser la conductivité et l'étirabilité des fibres. Nous avons observé deux morphologies de fibres distinctes, liées à l'utilisation de PEO ou de PVP dans le mélange utilisé pour l'électrofilage et nous les avons corrélées avec des propriétés mécaniques et électroniques différentes. Des OECTs ont été préparés à partir des deux polymères porteurs et leurs performances mécaniques et de transistors se sont avérées directement dépendantes de la morphologie des fibres.

Afin d'augmenter la conductivité des fibres de PEDOT et de simplifier la production des fibres, nous avons par la suite travaillé avec des fibres de poly(3,4-éthylènedioxythiophène) : poly(styrène sulfonate) (PEDOT:PSS) au lieu de fibres de PEDOT:tos. L'utilisation du PEDOT:PSS offrait deux avantages principaux : 1) de produire des fibres à partir d'un mélange disponible dans le commerce

sans avoir besoin de VPP et 2) de doper davantage les fibres pour ajuster leurs propriétés électroniques et mécaniques.

Nous avons assemblé avec succès des dispositifs électrochromiques étirables tout-polymère, préparés à partir de fibres PEDOT : PSS. Les traditionnelles électrodes d'oxyde d'indium et d'étain (ITO) ont été remplacées par des fibres de PEDOT:PSS déposées sur des substrats de poly(diméthylsiloxane) (PDMS). Les fibres sont pertinentes pour produire des électrodes étirables et transparentes : elles sont mécaniquement souples en raison de leur morphologie et elles nécessitent de petites quantités de matériau pour maintenir une transparence élevée et une bonne conductivité. Les fibres de PEDOT : PSS ont été rincées avec de l'éthanol absolu (EtOH) pour éliminer le PEO (polymère porteur) et pour améliorer la conductivité en tant que dopant secondaire. Nous avons ajouté un trimère organique comme chromophore à l'intérieur des dispositifs. Celui-ci peut être successivement commuté de l'orange au bleu dans ses états OFF et ON, respectivement. Les dispositifs électrochromiques résultants sont capables de passer du jaune au bleu même sous une contrainte de 100% d'élongation, ce qui prouve l'utilisation réussie des fibres PEDOT:PSS pour produire des électrodes transparentes étirables.

La transparence et la conductivité améliorées des fibres PEDOT:PSS par rapport à leurs homologues PEDOT:tos en font un matériau prometteur pour les OECTs étirables. La ductilité du PEDOT:PSS peut être améliorée par l'ajout d'éthylène glycol (EG) et d'autres dérivés de poly(éthylène glycol) PEG, ce qui conduit à des films minces étirables. La conductivité de ces films peut également être dopée par un post-traitement sans aucune perte des propriétés mécaniques.

L'amélioration in situ de l'étirabilité et de la conductivité, combinée avec la souplesse mécanique offerte par la morphologie des fibres, a été exploitée pour assembler des OECTs hautement étirables et transparents. Le mélange d'électrofilage a été conçu pour contenir un copolymère poly(éthylène glycol)-poly(propylène glycol)-poly(éthylène glycol) (PEG-PPG-PEG). Ce copolymère PEG a agi comme un plastifiant pour améliorer l'étirabilité du PEDOT:PSS. Les fibres électrofilées ont ensuite été traitées à l'acide sulfurique (H_2SO_4) lors d'un post-traitement. L'acide sulfurique a été choisi car il est connu pour augmenter drastiquement la conductivité du PEDOT:PSS, amenant à des valeurs de conductivité nettement plus élevées par rapport aux post-traitements à l'EtOH ou au diméthylsulfoxyde (DMSO).

Les mesures électromécaniques ont mis en évidence une amélioration de l'étirabilité et de la conductivité des fibres de PEDOT:PSS post-traitées par rapport aux fibres de PEDOT:PSS non traitées. Les premières ont pu être étirées jusqu'à 200% d'élongation avec une perte minimale de 20% du courant initial, alors que les secondes ont été limitées à seulement 120% d'élongation et à une perte de 25% du courant initial. Les OECTs préparés à partir de fibres de PEDOT:PSS se sont avérés fonctionner sous une déformation de 100% et avec de meilleures performances que celles que nous avions précédemment mentionnées avec les fibres de PEDOT:tos. Nous avons également observé que la perte des propriétés électroniques est peu corrélée aux nombre de cycles d'étirement/relâchement, mais est plutôt lié à l'intensité de la contrainte mécanique appliquée. En effet, une grande stabilité lors des tests de cycles a été démontrée et la récupération de la performance électronique une fois libérée, a été observée.

La fabrication de composants électroniques hautement étirables tels que les dispositifs électrochromiques et les OECTs à partir de fibres électrofilées, démontrés dans cette thèse, contribue au dévelopement des méthodes de fabrication et à l'accumulation de nouvelles connaissances afin ouvrir la porte à la production à grande échelle de la prochaine génération de dispositifs électroniques organiques. La polyvalence de l'électrofilage, combinée aux récents développements dans l'amélioration des propriétés du PEDOT:PSS, rend la production de dispositifs électroniques étirables plus facile et plus abordable.

ABSTRACT

We are at the dawn of a new technological revolution; the commercialization of the first flexible electronic devices such as smartphones, displays, and TVs started only 5 years ago. While this new technology will be a part of consumer electronics in the next few years, the interest in stretchable electronics is rising. Such devices are promising as body sensors since they will be less invasive for the patient but also in the field of displays, batteries, and the internet of things to name but a few. The large-scale production of such electronic devices needs to be insured by a cost-effective and fast technique. In the scope of this thesis, we investigated the fabrication of two types of stretchable electronic devices by combining a commercially available conjugated polymer with a well-known production method in the industry: electrospinning.

First, we investigated the viability of electrospinning as a processable method to produce stretchable organic electrochemical transistors (OECTs). Nano to micro-poly(3,4-ethylenedioxythiophene: iron tosylate) PEDOT:tos fibers were produced by a combination of electrospinning and vapor phase polymerization (VPP). Briefly, a mixture consisting of a carrying polymer and an oxidant (iron tosylate) has been electrospun and subjected to ethylenedioxythiophene (EDOT) vapor under reduced pressure to ensure the formation of PEDOT around the fibers. Two carrying polymers, either poly(ethylene oxide) (PEO) or poly(vinyl pyrrolidone) (PVP) and different electrospinning times were studied to optimize the fiber mat's conductivity and stretchability. We observed two distinct fiber morphologies, related to the use of either PEO or PVP in the electrospinning mixture and we correlated them with different mechanical and electronic properties. OECTs were prepared from both carrying polymer and their mechanical and transistor performances were found to be directly dependent on the fibers' morphology.

To increase the conductivity of the PEDOT fibers and to simplify the fiber production, we further started to work with poly(3,4-ethylenedioxythiophene): poly(styrene sulfonate) (PEDOT:PSS) fibers instead of PEDOT:tos fibers. The use of PEDOT:PSS offered two main advantages: 1) to produce fibers from a commercially available mixture without the need of VPP and 2) to further dope the fibers to tune their electronic and mechanical properties.

We successfully assembled stretchable all-polymeric electrochromic devices prepared from electrospun PEDOT: PSS fibers. Traditional indium-tin oxide (ITO) electrodes were replaced by

PEDOT:PSS fibers deposited on poly(dimethylsiloxane) (PDMS) substrates. Fibers are relevant to produce stretchable and transparent electrodes: they are mechanically compliant due to their morphology and they required small amounts of material to maintain high transparency and good conductivity. PEDOT: PSS fibers were rinsed with absolute ethanol (EtOH) to remove PEO (carrying polymer) and to enhance the conductivity as a secondary dopant. We added an organic trimer as a chromophore inside the devices. This one can be successively switched from orange to blue in its OFF and ON states, respectively. The resulting electrochromic devices were shown to switch from yellow to blue even under 100% strain, proving the successful use of PEDOT:PSS fibers to produce stretchable transparent electrodes.

The transparency and the improved conductivity of PEDOT:PSS fibers versus their PEDOT:tos counterparts made them a promising material for stretchable OECTs. The ductility of PEDOT:PSS can be improved by the addition of ethylene glycol (EG) and other poly(ethylene glycol) PEG derivatives, leading to stretchable thin films. The conductivity of these films can also be doped by a post-treatment without any loss in the mechanical properties.

The combination of intrinsically improved stretchability and conductivity with the mechanical compliance offered by the fiber morphology was exploited to assemble highly stretchable and transparent OECTs. The electrospinning mixture was designed to contain poly(ethylene glycol)-poly(propylene glycol)-poly(ethylene glycol) copolymer (PEG-PPG-PEG). This PEG copolymer acted as a plasticizer to enhance the stretchability of the PEDOT:PSS. Electrospun fibers were further treated with sulfuric acid (H_2SO_4). Acidic treatment was chosen to drastically increase the conductivity of PEDOT:PSS, leading to higher conductivity compared to EtOH or dimethyl sulfoxide (DMSO) post-treatment. Electromechanical measurements highlighted an improved stretchability and conductivity of post-treated PEDOT:PSS fibers compared to untreated PEDOT:PSS fibers. The former could be stretched up to 200% strain with a minimal loss of 20% of the initial current while the latter was limited to 120% strain and a loss of 25% of the initial current. OECTs prepared from PEDOT:PSS fibers were shown to work under 100% strain and with better performances than we previously mentioned with PEDOT:tos fibers. We also observed that the loss of electronic properties is barely due to the number of stretching/releasing cycles, but rather due to the applied strain. Indeed, great stability over cycling tests has been demonstrated and recovery of the electronic performance once released, has been observed.

The fabrication of highly stretchable electronics such as electrochromic devices and OECTs from electrospun fibers, demonstrated in this thesis, contributes to valuable methods and knowledge to open the door to large-scale production of the next generation of organic electronics. The electrospinning versatility, combined with the recent developments in tuning the properties of PEDOT:PSS makes the production of stretchable electronics easier and more affordable.

TABLE OF CONTENTS

LIST OF FIGURES

LIST OF SYMBOLS AND ABBREVIATIONS

CB	Conduction Band
CE	Coloration efficiency
CP	Conjugated polymer
DMF	Dimethyl formamide
DMSO	Dimethyl sulfoxide
ECD	Electrochromic device
EG	Ethylene glycol
E_g	Band gab
EtOH	Ethanol
g_m	Transconductance
H_2SO_4	Sulfuric acid
HSO_4^-	Hydrogen sulfate
HOMO	Highest Occupied Molecular Orbital
I_{ds}	Drain-source current
ITO	Indium tin oxide
JFET	Junction-gate field-effect transistor
LUMO	Lowest Occupied Molecular Orbital
M_n	Molecular weight
MOSFET	Metal–oxide–semiconductor field-effect transistor
NaCl	Sodium chloride
OECT	Organic electrochemical transistor
OFET	Organic field effect transistor
OLED	Organic light emitting diode

OPV	Organic photovoltaics
PDMS	poly(dimethylsiloxane)
PEDOT	poly(3,4-ethylenedioxythiophene)
PEDOT:PSS	poly(3,4-ethylenedioxythiophene) doped with poly(styrene sulfonate)
PEDOT:Tos	poly(3,4-ethylenedioxythiophene) doped with iron tosylate
PEG	poly(ethylene glycol)
PEG-PPG-PEG	poly(ethylene glycol)-poly(propylene glycol)-poly(ethylene glycol) copolymer
PEO	poly(ethylene oxide)
PET	poly(ethylene terephtalate)
PSS	poly(styrene sulfonate)
PU	poly(urethane)
PVP	poly(vinyl pyrrolidone)
SEM	Scanning electron microscopy
TCE	Transparent conductive electrode
THF	Tetrahydrofuran
Tos	Iron tosylate
T_{ox}	Transmittance of the oxidized state
T_{red}	Transmittance of the reduced state
V	Voltage
VB	Valence Band
V_{ds}	Drain-source voltage
V_{gs}	Gate-source voltage
VPP	Vapor phase polymerization

LIST OF APPENDICES

CHAPTER 1 INTRODUCTION

1.1 Stretchable Organic Electronics

Electronics are crucial components in our daily life as well as they are in the heart of technological breakthroughs. Traditional silicon-based semiconductors were at the origin of the television, the computer and the cellphone technologies to name but a few.[1] Such components could be miniaturized to produce more powerful and smaller devices. While being performants, they suffer of a lack of mechanical compliance, making them impossible to use in wearable devices nor in the robotic field as electronic skin. During the past two decades, many efforts have been made to produce flexible electronics.[2-4] Nowadays, some electronic devices can be bent and/or stretched with the merit of being light-weight and cost effective.[5] Their application potential is wide: wearable devices for body monitoring, Organic Light Emitting Diodes (OLEDs), [6] electronic skin,[7] implantable health monitoring devices and batteries.[8]

Stretchable electronics can be made out of inorganic materials, organic molecules or a combination of both in composite materials. Inorganic materials like metallic oxides, silver nanowire or sulfur-based nanoparticles exhibit a higher conductivity and a better stability under mechanical and electrical stresses than their organic counterparts.[9] The latter, however, are lighter, easier to manufacture, scalable, naturally biocompatible and cheaper.[10] Stretchable organic electronics involve the use of conjugated polymers (CPs) which are either deposited on or blended with an elastomeric matrix at room-temperature. These can be prepared from solution processed methods like polymer blending,[11-13] and deposition on a pre-strained substrate,[14, 15] or from shaping techniques like Kirigami [16-18] and electrospinning.[19-21] All of these technics involve a deposition or a blend with an elastomeric matrix, except for the Kirigami method where the substrate unfolds to increase its length.

Conjugated polymers have the ability to allow electron transportation along their alternating backbone thanks to a π system and the formation of delocalized charges. The conduction principles of conjugated polymers will be discussed in more details in the literature section of this thesis. Conjugated polymers are also known as conductive polymers and they are the key component of stretchable organic electronics. The versatility of their synthetic pathways and the simple processing methods they require allow them to be used in a wide range of devices like OLEDs,[22-

24] field effect transistors (OFETs) [25-27], electrochromic devices (ECs),[28-30] sensors [31, 32] or even organic photovoltaics (OPVs),[33, 34] with scale-up capability. CPs are compatible with large scale manufacturing techniques such as roll to roll [35, 36] or screen and inkject printing,[37-39] owing to their solution processability at room temperature. Different post treatments and functionalizations are known to enhance or tune their mechanical and electronic properties, allowing to produce a range of CPs capable to respond to different needs. [40-42] Polymer precursors can also be tailored to tune the final polymer properties, e.g. in the case of electrochromic polymers, where side chains or functional groups are added to the monomers in order to form polymers exhibiting different colors upon oxidation. [43, 44]

Among existing conducting polymers, poly(3,4-ethylenedioxythiophene) doped with poly(styrene sulfonate) (PEDOT:PSS) is the most famous and used one for its solution processability, its good oxidation stability and its high conductivity.[45] PEDOT:PSS was invented in 1986 and is still studied to improve its conductivity ever since. More than 30 years after its first synthesis, this copolymer evolved a lot: the mixture is commercially available, the ratio PEDOT/PSS is tuned in order to produce mixtures with different electronic properties and viscosities, post treatments have been found to enhance the conductivity of PEDOT:PSS films by soaking or mixing high boiling point solvents or highly polar chemicals[45]. Stiffness of as-prepared films can also be reduced by blending PEDOT:PSS with plasticizing agents or elastomers in order to produce intrinsically bendable or stretchable films.[46, 47] The interest for PEDOT:PSS doesn't decrease over the years, its vast capabilities and potential commercialization in electronic devices, as well as its intriguing conductivity mechanisms are fascinating research teams.

Nowadays, the demands for consumer electronics has sharply increased and the need for large scale production is felt. The use of organic materials is a long-term strategy towards efficient, recyclable and cost effective electronic devices. PEDOT:PSS is a material of choice, owing to the afford mentioned advantages and electrospinning offers a large-scale processability while minimizing the quantities of materials involved in the fabrication process.

1.2 Motivations

The need for mechanical compliance in the field of electronic devices originates from the applications. Bioelectronics are the link between the human body and electronic monitoring

systems. Human body is soft and the skin, in particular, can be bent and stretched up to 30% of its initial length. Wearable monitoring devices enduring motion-induced strain while maintaining stable electrical performance is a real concern for the medical patient's comfort. Flexible batteries are also of great interest to power future wearable devices. Rollable computers or cellphones fascinate the high-tech industries and these devices have to be made from flexible components such as batteries, displays, memories or even microchips.

Electrochromic devices (ECDs) and (OECTs) also benefit from the mechanical compliance of organic electronic materials. ECDs has been extensively studied in order to improve their performances in terms of color contrast, response time and life time, but very few efforts have been made on the improvement of their flexibility. Bendable or stretchable ECDs would have been of great interest for sensing applications due to their visual color change upon a redox reaction but also for low power consumption displays. Flexible OECTs are on the opposite a hot topic since their use as transistors or logic gates in bioelectronics or as sensors for health signals monitoring is a promising technological breakthrough with a high commercial potential.

This thesis is dedicated to the fabrication and characterization of stretchable organic electronics via electrospinning of a conjugated polymer.

1.3 Hypotheses and Objectives

The very high aspect ratio of nano-to micro fiber naturally gives them a certain mechanical compliancy, regardless of the brittle nature of the material they are made of. Electrospinning offers the opportunity to make non-woven fiber mats from a polymeric mixture, allowing to produce highly stretchable films (more than 2 times the original length), even from ductile and brittle polymers such as PEDOT:PSS. This conjugated polymer can be mixed with plasticizers in order to increase its stretchability around 30 to 50 % while retaining a high conductivity. We further hypothesize that PEDOT based fibers can be integrated in OECTs and ECDs in order to assemble highly stretchable devices by a combination of electrospinning and chemical secondary doping of PEDOT:PSS. The as-assembled devices will fill a lack in the needs for highly stretchable conducing polymers with a promising large-scale processability.

Hence, the primary objective of this thesis is to enhance the stretchability of PEDOT based on conjugated polymers: PEDOT:tosylate (PEDOT:Tos) and PEDOT:PSS by exploiting the fiber

morphology acquired by electrospinning. This shaping technique requires the use of a polymeric mixture with a specific composition in order to produce defect-free and smooth fibers in combination with experimentally defined processing parameters. The tunability of PEDOT:PSS will also be exploited to enhance both the conductivity and the stretchability of spun fibers by using secondary dopants.

Therefore, the main specific objectives of this thesis are:

1) To demonstrate the benefit of the fiber morphology by turning a brittle copolymer i.e. PEDOT:Tos into a stretchable one and to fabricate stretchable OECTs on a poly(dimethylsulfoxide) (PDMS) elastomeric substrate. The effect of the polymer mixture composition on the fibers morphology as well as the impact of the fibers morphology on the electromechanical properties will be investigated.
2) To fabricate a stretchable all-organic electrochromic device exploiting an organic chromophore to exhibit two distinct colors. PEDOT:PSS fibers deposited on PDMS substrates will be used as stretchable transparent electrodes to replace ITO in the device fabrication.
3) To fabricate highly stretchable OECTs made of secondary doped PEDOT:PSS fibers. A combination of a plasticizing agent and an acidic post treatment will be used in order to increase the stretchability and the conductivity of the fiber mats, respectively. The combination of intrinsically doped PEDOT:PSS and the stretchability gained by the fiber morphology will be investigated to enhance the transistor performances and the stretchability of OECTs.

1.4 Organization of the work

This PhD thesis contains 8 chapters. Chapter 1 discusses the background of stretchable organic electronics, the research project motivations, and objectives of this PhD work. The Chapter 2 is an introduction to the electrospinning technique and the conducting polymers. Electrospinning processing parameters and their impact on the fibers' diameter and morphologies are presented. Conducting polymers principles and doping process are discussed and PEDOT:PSS is introduced with a special attention to its electrical and mechanical properties. Operation mechanisms and figure of merits of OECTs and ECs are presented. Chapter 3 is dedicated to the introduction of the

research work and the material processing. Chapters 4 to 6 are reprints of three articles of which I was the first author.

-**Article 1** Michael Lerond, Subramanian Arunprabaharan, Skene William G, Cicoira Fabio, Combining Electrospinning and Electrode Printing for the Fabrication of Stretchable Organic Electrochemical Transistors. *Frontiers in Physics* (2021).

-**Article 2** Michael Lerond, Anthony Raj Mohan Raj, Veronica Wu, W. G. Skene, Fabio Cicoira, An Intrinsically Stretchable and Bendable Electrochromic Device. *IOP Nanotechnology* (2022) (Manuscript ID : NANO-131602, under review)

-**Article 3** Michael Lerond, Skene William G, Cicoira Fabio, Enhancing the performance of transparent and highly stretchable organic electrochemical transistors by secondary acid doping and copolymer blending of electrospun PEDOT:PSS fibers. *Journal of Material Chemistry C* (2022) (Manuscript ID : TC-ART-03-2022-001134 under review)

In **Article 1**, we prepared PEDOT:Tos stretchable transistors by a combination of electrospinning and vapor phase polymerization (VPP). We first studied the impact of the carrying polymer nature and molecular weight in the electrospinning polymer mixture on the fibers morphology. The as-prepared fiber mats were characterized by electrochemistry and the evolution of the current under strain was recorded. They were further used as channel material in stretchable OECTs, exhibiting a stable transistor behavior from 0 to 50 % strain. In **Article 2**, we reported the fabrication of stretchable all organic electrochromic devices by electrospinning a mixture of PEDOT:PSS with PEO. We first prepared transparent and stretchable organic electrodes from electrospun PEDOT:PSS nanofibers on a PDMS substrate. They were further used as both anode and cathode in the electrochromic devices and the electrospectrophotometric performances were recorded and compared to a solid state device. The evolution of the chronoamperometric response when the devices were bent and stretched was also recorded. Finally, in **Article 3** we prepared highly stretchable OECTs by electrospinning a mixture of PEDOT:PSS, PEO and PEG-PPG-PEG. Electrospun fibers were post-treated with sulfuric acid to increase the conductivity of the fiber mat. Electromechanical measurements showed a high stretchability of 200% strain with a minimal loss of the current of 20%. As prepared OECTs demonstrated a transistor behavior from 0 to 100%

strain. Moreover, OECTs prepared from electrospun fibers exhibited better transistor performances than their counterparts prepared from homogenous thin PEDOT:PSS films.

In Chapter 7, the results of this thesis are discussed as a whole, supported by the literature review and the published articles. In Chapter 8, conclusions are drawn and perspectives on future work are also given here.

CHAPTER 2 LITERATURE REVIEW

The aim of this section is to introduce the production of non-woven fibers by electrospinning and to give a general overview of the history of conductive polymers. OECTs and ECDs working principles and figure of merits will be also discussed.

1.1 Electrospinning

Electrospinning is a low cost, reproducible, and simple method to produce homogenous fibers at the nanometer scale for various applications such as batteries,[48-50] gas sensors,[51-53] and light emitting diodes[54-57] to name but a few. Such fibers with diameters down to the nanometer scale, can be composed of natural-based,[58-60] organic[60, 61] and inorganic materials.[62, 63] They are assimilated as one-dimensional objects since their length is much larger than their diameter and their composition can be very simple or relatively complex.[64] Fibers can either be homogeneously distributed along their entire length and thus have the same internal structure or either be a mixture of materials and offering different internal and surface structures.[65, 66] The latter type of fibers is extensively investigated thanks to the wide properties combination and tuning they provide.[67-69] They can be prepared directly from a solution mixture or via a special spinneret composed of a double thread. This second technic is named co-axial electrospinning and allows the production of core-shell type fibers.[70-72]

Electrospinning principle is based on the overcoming of the surface tension of a solution under a strong electric field to produce a spinning jet. A high voltage is applied between a polymer solution (or melt) contained in a spinneret and a collector[73], allowing the production of continuously long fibers (**Figure 2-1**).

The theoretical understanding of the influence of an electric field on a small volume of liquid was settled by Taylor,[74] 67 years after the first patent of an electrospinning machine, in 1902. Under a high voltage, the polymer droplet forming at the tip of the nozzle is electrostatically charged. The charge repulsion works against the surface tension of the polymer solution or melt and the droplet shape changes from a spherical to a conical shape called a Taylor Cone. A rectilinear jet is then released from the tip of the nozzle and follows a complex path, subjected to instabilities induced by the electric charges to finally reach the collector. Different types of collectors can be used to control the orientation of the fibers. These will be randomly oriented when electrospun on a

stationary plate, in order to produce nonwoven mats. On the other hand, the use of a rotating disk, drum or a frame can provides align fibers.

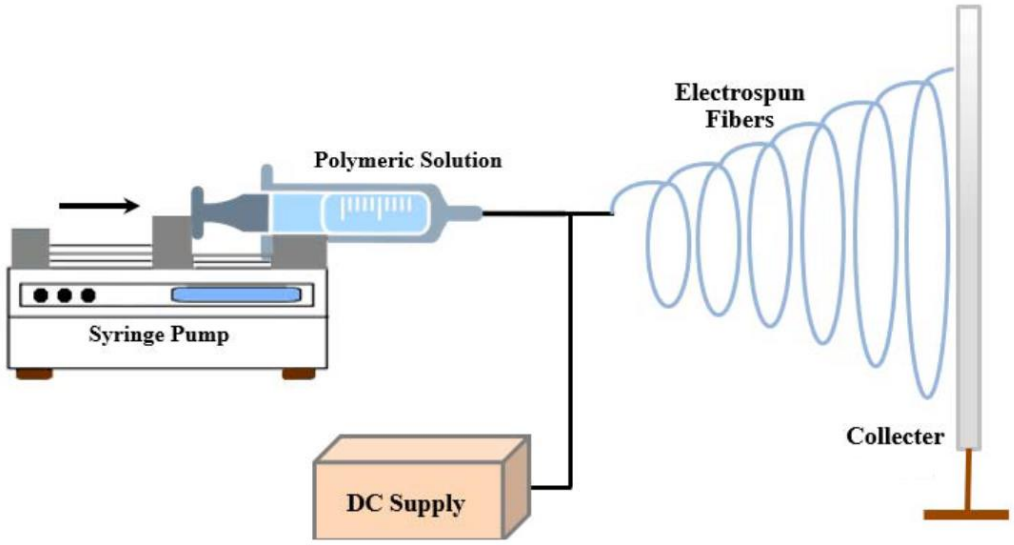

Figure 2-1. Scheme of electrospinning setup.[75] Reprinted with permission.

1.1.1 Electrospinning solution properties

Solution concentration and viscosity

The polymer concentration in the electrospinning mixture is of great importance since it drastically impacts the formation of the fibers. Numerous studies have been made on the fiber formation during electrospinning in function of the polymer concentration solubilized in a given solvent and for different molecular weights.[76-80] These revealed the existence of a critical concentration (C*) representing the minimum polymer concentration required to produce smooth fibers. Below this, isolated beads were observed. The production of beads is called electrospraying and won't be discussed in this thesis. Interestingly, it was demonstrated that C* can be lowered by increasing the molecular weight of the polymer. However, as the molecular weight of a polymer in solution increases, the viscosity of the solution also increases. This relationship is described by the Mark-Houwink-Sakurada (MHS) equation.

$$[\eta] = KM^{\alpha}$$

This equation gives a relation between the intrinsic viscosity [η] of a solution and the molecular weight *M*. The two Mark-Houwink-Sakurada parameters K and α are dependent of a given solvent-polymer system and are empirically determined.

The increase in viscosity caused the average fiber diameter to increase due to a higher quantity of polymer chains in the Taylor cone, leading to more polymer in the fiber jet and hence a thicker fiber after drying.

Electrical conductivity

Electrical conductivity of the electrospinning solution can be tuned in order to produce thinner fibers. The conductivity of the electrospinning solution is inherently linked to the conductivity of its solvent. The solvent is mainly chosen for solubility reasons, and ionic salts may be used to increase the conductivity of the electrospinning solution.

C.J. Angammana et al. showed that the Taylor cone formation is governed by the electrostatic force created by the surface charges formed under an external electric field.[81] The increase in ions through the use of salts hence drastically increase the electrostatic force induced on the fluid surface and facilitates the Taylor cone formation.[82] A decrease in the average fiber diameter is reported as the conductivity of the solution increases. The combination of two phenomena is at the origin of the decreasing in fiber diameter:

1. The fluid jet undergoes a higher stretching due to the larger quantity of surface charges, thinning the diameter.
2. A reduction in the tangential electric field has been observed, leading to an increase in the flying time of the fluid jet. During this overtime, the jet is over stretched, reducing the diameter of the electrospun fibers.

1.1.2 Experimental setup

Electric voltage

The principal goal of applying an electric field during an electrospinning process is to break the surface tension of the Taylor cone. A voltage range is then defined for a given solution composition which lead only to the formation of defect-free fibers. [83, 84] Below the voltage window, beaded

fibers or electrospraying is observed, while beyond the upper voltage, the polymer jet stops being stable and starts forming multiple jets and electrospraying.

It was reported that the increase in voltage resulted in the formation of thicker fibers as the volume of ejected fluid increased, leading to a thicker polymer jet. Similarly, an increase in ejected volume leads to a higher deposition rate.[83]

In a general way, the choice of the applied voltage has to be experimentally defined since it's highly correlated to the polymer solution parameters such as: conductivity, polymer concentration and surface tension.

Tip to collector distance

The tip to collector distance is used to control the morphology of the electrospun fibers. The distance might ensure a sufficient time of flight for the solvent to be evaporated before reaching the surface of the collector. Too short time-of-flight results in thick and sticky fibers merging together on the collector, making the fiber shape disappearing to the benefit of a film.[85-87] On the other hand, too long distance results in too high decrease of the electric field produced by the power supply, leading to no fiber formation on the collector. The right tip to collector distance has to be experimentally determined. In most of the time, a distance between 10 and 20 cm is a good lead to start with a voltage defined as 1 kV/cm.

Flow rate

The flow rate is defined as the rate at which the polymeric solution is fed into the nozzle. Just as the electric voltage, the adequate flow rate exists over a range. The flow rate has to be adjusted to keep the polymer droplet at a constant size and shape to ensure the stability of the jet. The tip should be fed enough to keep the Taylor cone intact during the electrospinning, without any excess or lack of supply. Such variations will result in an unstable polymer jet, leading to beaded, spitted or thick fibers.

An excessively high flow rate causes an increase in the average fiber diameter as well as a beaded fiber morphology.[88, 89] Generally, the flow rate varies between 0.1 and 2 mL/h for the nozzle with an inner diameter of 0.3 mm. It's necessary to adjust this last parameter for a given solution and voltage to produce thin and smooth fibers.

1.1.3 Electrospun induced stretchability in polymers

Electrospinning led to recent advances in the field of organic electronics and bioelectronics. Verpoorten E. et al. produced a flexible sensor based on PEDOT:PSS microfibers to monitor the deformation of the human body as well as the pH of the skin.[90] The piezoresistive and electrochemical active properties of the PEDOT:PSS were combined in a single device for human body monitoring. Similarly, PEDOT:PSS/graphene oxide fibers were used for electrocardiography and electromyography monitoring in smart clothing.[91] Electrospinning is highly investigated in the field of conductive textiles for its great compatibility with fabrics.[92] Organic strain sensors are also widely studied because of their biocompatibility.[93] PEDOT:PSS mixed with various amounts poly(vinyl alcohol) (PVA) led to sensors with adjustable conductivities.[94] Similarly, carbon nanofibers were blended with PEDOT:PSS prior to electrospinning to produce highly stretchable thermoelectric strain sensors.[95] The mechanical compliancy gained by the fiber shape led to various studies in order to produce flexible energy storage devices such as supercapacitors.[96-98]

1.2 : Conductive Polymers

The history of electrically conductive polymers is quite recent in the field of polymer research and industry. The discovery of this new type of materials begun after the pioneering work of Hideki Shirakawa, Alan Heeger and Alan MacDiarmid in 1997.[99] They showed that the conductivity of polyacetylene can be increased by seven orders of magnitude via doping by iodine. Conducting polymers are described as materials exhibiting electrical and optical properties of metals or semiconductors while retaining the mechanical properties and processing advantages of polymers.[100]

Electrically conducting polymers are also called organic semiconductors or more generally, conjugated polymers (CPs). Those polymers are made of repetitive units where atoms are covalently bonded to each other with alternating single and double bonds. This particular backbone promotes the electron transportation along the polymeric chains but the intrinsic conductivity is very low (less than 10^{-5} $S.cm^{-1-}$).[101] To enhance the conductivity and the carrier density of the conjugated polymers, a chemical doping is required.

1.2.1 Conductivity in conjugated polymers

The conjugated polymer backbone is at the origin of their electrical properties. As mentioned before, alternating single and double bonds give rise to the electrical properties by delocalizing π electrons. In organic semiconductors, electronic performances are closely related to their solid-state packing structure. Indeed, intermolecular organic coupling drives the stacking, and thus charge transport properties too.[102] A small π-π stacking distance will result in high electron mobility, which is the case with crystals and aggregates, while in amorphous polymers, the charge transport is lowered.[103] Unfortunately, these crystallites and aggregates are known to lead to brittle materials compared to amorphous polymers.

Conductivity in materials can be classified in to three categories according to width of the band gap: (I) metals, (II) semiconductors and (III) insulators. The band gap of a material is designed by the distance between its conduction band (CB) and its valence band (VB) (**Figure 2-2**). The band theory originates from the atomic orbitals of atoms which have discrete energy levels. Orbitals overlap and hybridize when 2 or more atoms join together. By increasing the number of atoms in a macroscopic material, the number of orbitals is increased and thus become closely spaced in energy, leading to the formation of energy bands separated by forbidden bands.

In the case of a metallic type material, there is an overlap between the two bands. This allows the electrons from the Highest Occupied Molecular Orbital (HOMO) in the VB to jump into the Lowest Unoccupied Molecular Orbital (LUMO) of the CB. This leads to an easy electron flow and thus, electrical conductivity.[45] In contrast, the band gap is wide for an insulator. Therefore, the electrons cannot move from the HOMO to the LUMO, inhibiting the electrical conductivity.

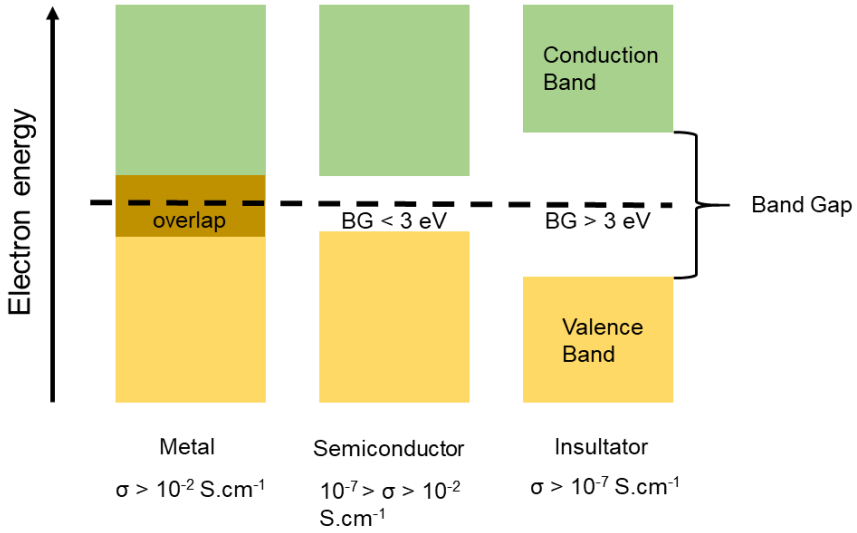

Figure 2-2 : Band gap diagram for a metal, a semiconductor and an insulator material.

Finally, the most interesting case concerns the semiconductors. They also show a band gap, but it is smaller than that of the insulators. As a result, few electrons can go through it, resulting in a low but existing electrons flow. As a consequence, the electrical conductivity is very low but still interesting in electronic devices for specific applications.

The conductivity of a material can be explained by the Sommerfeld equation: $\sigma = ne^2\tau/m$, where n is the conduction electron density, e the electronic charge, τ the relaxation time between two electrons collision, and m their mass.

In metal type electrical conductors, temperature leads to the decrease of electrical conduction. This phenomenon is due to an increase in collisions while the conduction electron density remains the same, as consequent, the relaxation time τ decrease. On the other hand, the thermal activity enhances the electrical conductivity in semiconductors. This is because the electrons from the valence band move to the conduction band and so the electron density *n* increase. This phenomenon is much more important than the τ variation, leading to an increase in conductivity.

1.2.2 Doping and structural effects on electrical conductivity

The first doping on a conjugated polymer was a real breakthrough in this area. It appeared in 1977, and once again, polyacetylene was the subject of this discovery.[104] Its conductivity was found to increase by 7 orders of magnitude when exposed to oxidizing or reducing agents. This process

is called “doping” by analogy of the doping of inorganic semiconductors. In fact, the doping process is a redox reaction. Two types of doping are possible: *p* and *n*. In the case of a *p* doping, the neutral polymer (and thus insulator) is partially oxidized to an ionic complex: a polymeric cation plus a counterion which is the reduced form of the oxidizing agent. The *n* type is the opposite phenomena: the polymer is reduced to a polymeric anion and it is stabilized with a counterion which is the oxidized form of the reducing agent. The most famous conjugated polymers such as polyaniline, polythiophene and their derivatives are produced through an oxidative chemical or electrochemical polymerization, leading to oxidized polymers.

In a *p* type doping, electrons are removed from the top of the valence band, while in *n* doping, they are added to the bottom of the conduction band. Once doped, the equilibrium energy is different from the ground state, leading to an ionized state. In the ground state, the structure is benzenoid where it can be represented with benzenes and their unsaturations. In contrast, the quinoid form is adopted when doped. In this one, electrons are delocalized and the double bonds appear outside the benzene ring. An example of the benzoid and quinoid forms is given in **Figure 2-3**.

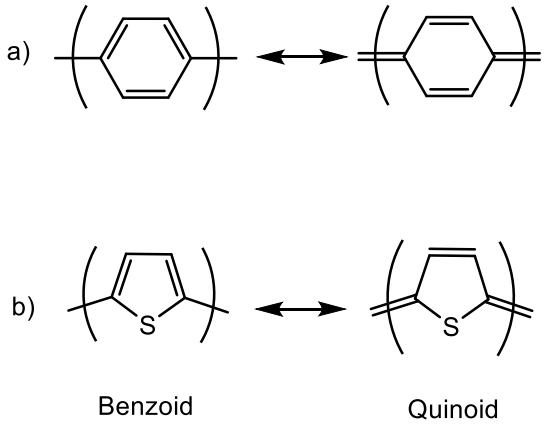

Figure 2-3 : Two examples of benzoid and quinoid form for a benzene ring (a) and a thiophene (b).

The doping induces the presence of localized electronic states in the band gap. These are due to a local upward shift of the HOMO and a downward shift of the LUMO.[105] This process is due to a localization of charges on the polymeric chain, which need to relax by a lattice distortion. The association of a localized charge and a lattice deformation is called a polaron, assimilated in chemistry to a radical ion. The localized electronic states present in the gap are called polaronic

states. Although polymeric chains can reach lengths of several microns, the conjugation length rarely exceeds ten repeating units. This is due to the presence of structural defects (cis-trans, sp3 carbon), polymerization or purity.[106] The delocalization of the σ electronic cloud is therefore limited to these few units and the need for electronic conduction between chains is then felt.

The ability of a charge to deform the lattice around itself is characteristic of strong electron-phonon coupling. When a second electron is removed from the polymeric chain, a bipolaron is formed. This entity is defined as a pair of identical charges, associated with a strong distortion of the network. The coulombic repulsion between the two charges of the same sign is exceeded by the energy gain generated by the relaxation of the network during the formation of the bipolaron. Moreover, the latter is thermodynamically favored compared to the formation of two polarons, since the decrease of ionization energy is more important.

In a conjugated polymer, the strong electron-phonon coupling implies that the charges introduced into the polymer interact with certain molecular vibrations and are therefore able to reduce their energy by forming localized polarons.[107] The electron-phonon coupling is quantified by the binding energy of the polaron, which corresponds to the energy reduction due to polarization and lattice deformation[108]. The interaction of an electron (or a hole) with lattice vibrations induces a jump of the charge carrier from a given atom to a neighboring atom. This is called hopping conduction and gives rise to conduction between polymer chains.[109] This process strongly limits the charge transport. In the particular case of high concentration doping, the wave functions of the polarons start to overlap, giving rise to the appearance of semi-filled polaronic bands within the gap, approaching then a metallic character. [110]

When an electric field is applied, the polarons move within the material creating an electric current. Therefore, they act as charge carriers and it has been experimentally demonstrated that they are at the origin of electrical conduction in conjugated polymers.[107] Thus, a conjugated polymer can adopt the behavior of a semiconductor or a metal, depending on its doping level.

1.2.3 Doped conjugated polymer

The process of doping a conjugated polymer refers to a redox reaction where electrons are removed (or added) to the backbone to forms polymeric cations (or anions) with counterions. The most famous conjugated polymers such as polyaniline, polythiophene and their derivatives are produced

through an oxidative chemical or electrochemical polymerization, leading to oxidized polymers. During the oxidation, positive charge carriers are generated (holes) and hence give a *p*-type character to the as-formed polymer. In their oxidized form, conjugated polymers are referred to *p*-doped in analogy to *p*-doped inorganic semiconductors. *P*-doped polymers are polycationic materials and anionic species must be incorporated as counterions to balance the excess of positive charges and hence maintained the charge neutrality. Although less common, some conjugated polymers can undergo a reduction reaction to be *n*-doped.[111, 112] In this case, the electrons are the charge carriers and cationic species need to be incorporated. The species acting as counterions during *p*-doping (or *n*-doping) are also called dopants since they are mandatory to generate the oxidized (or reduced) form of conjugated polymers, leading to conductive materials.[113]

1.3 : PEDOT and PEDOT:PSS

1.3.1 From polyacethylene to PEDOT

Historically, the first conjugated polymer (CP) is recognized to be the iodine doped polyacetylene. It's simple alternating structure of single and double carbon bonds unfortunately makes it unsuitable for large-scale industrial applications. Polyacetylene suffers of both air instability and a poor processability due to its insolubility in solvents once doped. Fortunately, in the early 1980s, many research led to the development of new monomers for electropolymerization into conjugated polymers. Among them, polyaniline[114], polypyrrole[115] and polythiophene[116] were the most studied. The introduction of heteroatoms (N or S) into a heterocyclic conjugated structure led to a more electro-donating behavior and hence help to stabilize the π-electron system. Electropolymerization consists of applying a given potential over time to a mixture of the monomer and an electrolyte in solution to form thin immiscible polymer conjugated films.

These first conjugated polymers could not be processable, their electrical properties were poor and their mechanical ones were not compatible with industrial processing methods. To be interesting for industrial scale up, these polymers have to combine the electrical properties of metal/semiconductors with the mechanical properties and processability of polymers. A breakthrough in 1986 by McCullough was the first step to developing conjugated polymers as we know them nowadays.[117] His works led to the synthesis of polythiophene and its alkyl derivatives by a metal cross-coupling polymerization (Kumada). He developed new synthetic

routes to processable conjugated polymers by increasing their solubility and stacking, mainly by adding a solubilizing side chain. These have made possible the formation of highly conductive polythiophenes but long-term air and humidity stability was still not achieved. Even if polythiophenes successfully increased the environmental stability in the field of conjugated polymers, the bi-polaron state cannot be maintained over long exposure to air and humidity. The synthesis of poly(alkoxythiophenes) was investigated in order to stabilize the bipolaronic state through a mesomeric effect. The stabilization was only achieved by a ring closure of the 3,4-thiophene group with an ethylene unit, leading to 3,4-ethylenedioxythiophene (EDOT) and hence to poly (3,4-ethylenedioxythiophene) (PEDOT).

The insolubility of PEDOT in most solvent was still limiting its processability and its further use in large-scale applications. The solution to this issue was the addition of polystyrene sulfonate (PSS) as a water-soluble polyanion. PSS acts as a counterion for PEDOT, forming a stable micro-dispersion in water and a highly processable complex PEDOT:PSS. Aqueous PEDOT:PSS dispersions are commercially available from H.C. Starck Clevios GmbG under the trade name Clevios™, from Bayer™ (Baytron) and from Agfa™ (Orgacon) with conductivities ranging from 10^{-5} S/cm to 1000 S/cm for different usages.

1.3.2 Secondary Doping

The secondary doping of conjugated polymers arose with the democratization of polyacetylene and polyaniline, which were systematically treated with organic solvents to increase their conductivity. The concept of secondary doping was stated by MacDiarmid et al. as a treatment of an already primary doped polymer by an apparently “inert” substance which increases the conductivity with concomitant changes in the electronic spectra and/or degree of crystallinity.[118] The primary doping occurs by definition during the oxidative polymerization of the conjugated polymer. Here, the PEDOT is primarily doped by the PSS in the complex PEDOT:PSS, or by metallic cations such as Fe^{+3}, which is released during the oxidation reaction of EDOT with an oxidative agent like iron tosylate.

Dimethyl sulfoxide (DMSO) was the first secondary dopant which led to an increase of the conductivity by 2 orders of magnitude (from 0.8 to 80 S/cm).[119] A screening effect induced by the DMSO was assumed to be responsible of the increase in conductivity while no conformational

chain change nor doping level change were evidenced. Later, an increase in the PEDOT-to-PSS ratio was highlighted by addition of solvents in doped PEDOT:PSS, which was attributed to the segregation and the removal of PSS excess.[120] A better connection between PEDOT and PSS grains is induced and hence a more efficient electronic pathway is created. Other polar solvents were also investigated as secondary dopants: ethanol (EtOH), methanol, glycerol, poly(ethylene glycol) (PEG) and ethylene glycol (EG), to name but a few. The latter was found to increases the conductivity by inducing a structural change in PEDOT:PSS, from a coil to linear or expanded coil structure.[121] The three proposed mechanisms: screening effect, PSS excess segregation /removal and structural change were found to be complementary. Indeed, Müller-Meskamp et al. reported a conductivity of about 1400 S/cm by optimizing the solvent and thermal post treatment using EG in a PEDOT:PSS dispersion.[122] The removal of PSS excess together with conformational changes were assumed to be at the origin of the breakthrough. Even though the efficiency of the addition of polar solvents and post-treatments is admitted, the real mechanism of the enhancement of the conductivity is still subject to debates and studies.[123, 124] Ionic liquids were found to increase the conductivity up to 2084 S/cm, following the same mechanisms as described above.[125] In 2010, Ouyang et al. studied various acids as secondary dopants, leading to an increase from 0.2 to more than 200 S/cm.[126] The proposed mechanism was a combination of an enhanced aggregation of PSSH particles that were easily washed off as long as conformational changes of the PEDOT chains. More recently, acidic treatment with sulfuric acid increased the PEDOT:PSS conductivity up to 4839 S/cm.[127] It is commonly admitted that PSS^- anions are protonated by protons from the acid and some of them are also replaced by hydrogenosufate.[128] (**Figure 2-4**) Here again, this proposed mechanism is subjected to debates as some studies assessed that no ions derived from acid were present after the secondary doping treatment.[129, 130]

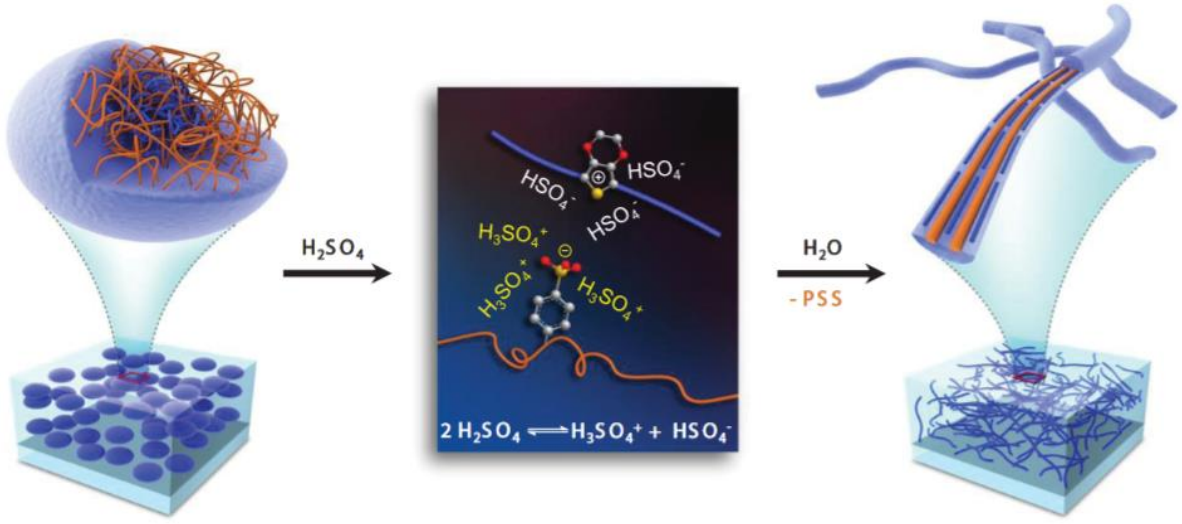

Figure 2-4. Diagram of the structural rearrangement of PEDOT:PSS. The amorphous PEDOT:PSS grains (left) are reformed into crystalline PEDOT:PSS nanofibrils (right) via a charge-separated transition mechanism (middle) via a concentrated H2SO4 treatment[129]. Reprinted with permission.

1.3.3 Flexibility and stretchability

One of the major advantages of using conjugated polymers over inorganic materials and metal oxides is their intrinsic flexibility upon bending. In the case of PEDOT:PSS, the strain energy generated during a deformation is dissipated either by weak Van der Waals or electrostatic interactions inside the polymer domains. However, pristine PEDOT:PSS exhibits a low strain at break, around 5% only, limiting its use in stretchable devices. Mechanical properties of free-standing PEDOT:PSS were investigated by Lang et al.[131] They found that the relative humidity (RH) strongly impacts the Young modulus (*E*) of the free-standing films. It can be decreased from 2.8 GPa to 0.9 GPa by increasing the RH level from 23% to 55%, leading to an increase of strain at break from 2.3% to 5.8%. This limited compliance to tensile strain can be improved by the use of surfactants, plasticizers, elastomeric blends or by engineering methods to name but a few.

A.Amassian et al. used Zonyl FS 300 as a surfactant to improve both the conductivity and the stretchability of PEDOT:PSS.[132] They showed that the surfactant interacted with the PSS, inducing pathways for phase separation and order into PSS domains. They successfully decreased the Young modulus from 1.15 GPa to 0.338 GPa by blending PEDOT;PSS with 1w% of Zonyl.

They further decreased a bit more *E* to a value below 100 MPa by adding few amounts of DMSO. Lipomi et al. also reported the plasticization of PEDOT:PSS by introduction of 10 w% of Zonyl FS 300 and 5 w% of DMSO.[133] The as-prepared samples showed a maximum tensile strain of 28%. Low molecular weight polyethylene glycol (PEG) is also a suitable plasticizer to improve both electrical conductivity and stretchability of PEDOT:PSS.[134] High transconductance OECTs exhibiting a similar performance between 0% and 45% strain were easily prepared by mixing PEG 400 with commercially available PEDOT:PSS mixture from Clevios™.

The simplest engineer method to produce stretchable conjugated polymers is the buckling technique. This one consists to pre-strain an elastomeric substrate prior to the deposition of a thin film of CP, leading to the formation of buckles upon releasing the strained substrate. This method was notably used to fabricate stretchable OECTs[135] and triboelectric nanogenerator[136]. However, beyond its simplicity, this technique suffers of a limited stretchability in a range of 10 to 15 % strain[137, 138] and a limited possibility of integration in flexible/stretchable electronics that commonly require planar configurations or low profiles.

The second widely used route to make stretchable CPs is the elastomeric blend. Conductive fillers are embedded into an insulating elastomeric matrix, leading to the formation of nanocomposites. This strategy provides good mechanical improvements but also has the inconvenient of reducing the conductivity of the CPs. A PEDOT:tosylate/poly(urethane) (PU) blend prepared by Larsen et al. was allowed to be stretched up to 50% strain but showed a moderate conductivity of 150 S/cm.[139] Similarly, a PEDOT:PSS/PDMS composite was prepared by Teng et al.[140] A PEDOT:PSS aerogel was formulated and PDMS oligomers and curing agent were embedded prior to being cross-linked. The 3D elastomeric network formed by the cured PDMS serves as a support for the brittle aerogel. The as-prepared material showed a strain at break around 52%, a conductivity similar to pristine PEDOT:PSS, and can undergo more than 5000 cycles of bending or stretching without any irreversible damage.

The Kirigami method is also a suitable strategy to increase the stretchability of CPs. S.Gandla et al.[16] fabricated biocompatible and transparent electrodes for human-machine interaction by creating kirigami patterns. (**Figure 2-5**) A PEDOT:PSS thin film was encapsulated between two poly(lactic acid) layers and Y shapes were formed by laser cutting. These discontinuities in the film allowed it to relax the strains upon pressing or stretching. The as-prepared electrode showed

a strain at break of 33%, which is above the maximum stretchability of the human skin (30% strain). A humidity dosimeter exhibiting a maximum strain of 170% was prepared using Kirigami's method.[18] EDOT was polymerized by vapor phase polymerization (VPP) directly on a laser cut poly(ethylene terephthalate) (PET) layer. Upon stretching, cut channels in the PEDOT free-standing film allowed it to be unfolded, avoiding a strain concentration and hence the breakage of the film.

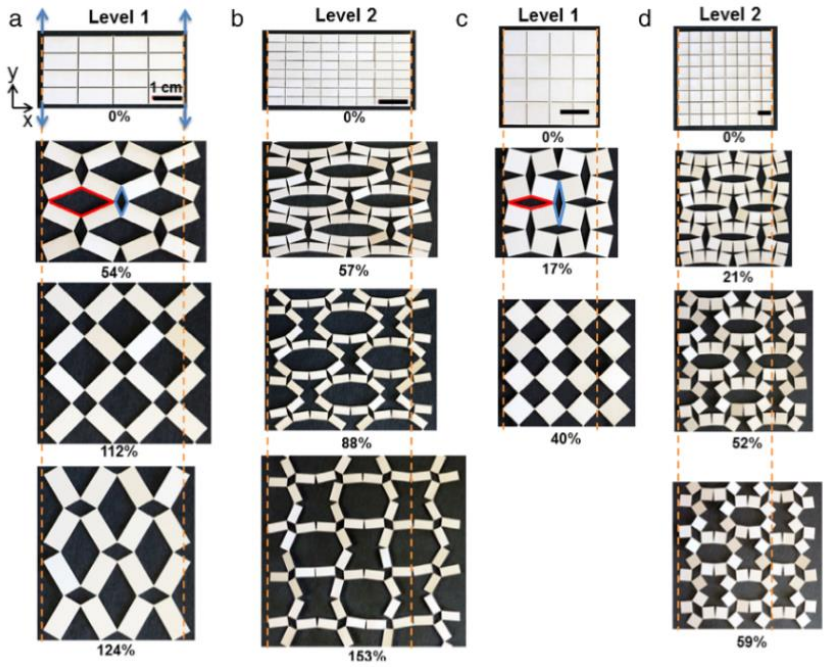

Figure 2-5. Evolution of structural reconfiguration in hierarchical paper kirigami metamaterials constructed from rectangle (a–b) and square (c–d) cut units with the stretching along y-axis. (a) and (c): level 1 structure; (b) and (d): level 2 structure. Reprinted with permission from [141].

Finally, electrospinning is known to produce fiber mats which can be stretched without showing irreversible structural damage.[142, 143] Poly(3-hexylthiophene) (P3HT) is another famous conjugated polymer from the polythiophenes family. P3HT nanofibers produced by co-axial electrospinning showed a huge stretchability up to 500% strain without showing any structural damage.[144] According to the authors, two key points explain such increase in the stretchability : 1) crystalline domains in the semi-crystalline nature of P3HT are lowered in the nanofiber during the electrospinning, leading to more ductile fibers and 2) the preferential orientation of crystal lamellae along the fiber axis due to the electrospinning force. Another strategy consists of the

polymerization of a CP around intrinsically stretchable electrospun fibers. PEDOT was chemically polymerized around a fiber mat of nitrile butadiene rubber, resulting in a conductive and stretchable material up to 75% strain.[93] Similarly, PEDOT:tosylate fibers were obtained by a combination of electrospinning and VPP.[145] A polymer mixture consisting of poly(vinylpyrrolidone) (PVP) and iron tosylate (Tos) were electrospun and subjected to EDOT vapor to allow the formation of a PEDOT shell around the fibers. Such PEDOT:tos fibers showed a strain at break of 140% while retaining 15%-20% of the initial conductivity.

1.4 Organic electrochemical transistors (OECTs)

The first transistor in history is attributed to Bell lab researchers J.Bardeen, W. Shockley and W.Brattain in 1947.[146] A transistor is an electronic device used to amplify or switch electronic signals and electrical power. It has a great impact on consumer electronics, allowing the large-scale commercialization of personal computers in the late 50's. Transistors are also the main components of microchips where nowadays billions of them are working in a small area of 400 mm^2. Organic Field Effect Transistors (OFETs) are a subcategory of transistors where a potential is used to tune the current flowing through the device, in opposition to bipolar transistors which are driven by a current. OFET is a large family regrouping Metal Oxide Semiconductor Field Effect Transistors (MOSFETs), Junction Field Effect Transistors (JFETs) and Organic Electrochemical Transistors (OECTs). OECTs are involving a combination of an electrolyte and a conjugated polymer to replace dielectric and semiconductors materials used in "classic" transistors. The ionic/electronic coupling property of CPs is the core of the working principle of OECTs, allowing a modulation of the current by electrochemical doping and de-doping process.

1.4.1 Working principle

The fabrication of the first OECT was attributed to White and coworkers in 1984, when they assembled two gold electrodes and a poly(pyrrole) channel.[147] This transistor involved two electrodes called source and drain, separated by a channel made of a semiconductor material (**Figure 2-6 a**). As mentioned before, the role of a transistor is to modulate the current by the application of a given voltage bias. The current caused by the flow of charge carriers between the electrodes source and drain is called the drain current (I_D). The intensity of I_D can be tuned by the application of a voltage at a third electrode immersed in an electrolyte solution and called the gate

electrode. The electrolyte creates an ionic path between the gate and the semiconductor, while the semiconductor channel ensures the electronic conduction. Conjugated polymers are promising channel materials because of their ambivalent character by conducting electrons as well as ions.[148, 149]

OECT working principle is based on a change in the doping state of the conjugated polymer composing the channel of the device. This change is made possible by electrolyte-ion injections at the gate electrode under the application of a voltage (V_{GS}), which modify the electrical conductivity.[150] When V_{GS} is removed, ions go back into the electrolyte and I_{DS} returns to its initial value. In the case of a typical PEDOT:PSS based OECT, a channel made of a PEDOT:PSS layer is in contact with the electrolyte where a gate electrode is immersed inside. Source and drain electrodes define the charge carrier path and are located below or above the channel. As a *p*-type doped polymer, PEDOT:PSS charge carriers are holes. They can hop to nearby chains under a voltage bias. Once a voltage is applied between the source and drain electrodes (called drain voltage, V_{DS}), the transistor allows to the charge carriers to freely move from the source to the drain electrodes, through the channel (ON state). The application of a positive gate voltage V_{GS} leads to the diffusion of the cations (M^+) from the electrolyte and their penetration in the polymer matrix. During this process, PEDOT undergoes a reduction, decreasing the number of mobile holes and hence leading to a drop of the drain current (OFF state). The (Equation 1) below summarizes the reduction of the PEDOT and the charge balancing with the PSS caused by the application of V_{GS}.

$$PEDOT^+ : PSS^- + M^+ + e^- = PEDOT^0 + M^+ : PSS^- \qquad \text{(Equation 1)}$$

A transistor showing a transition between the ON and OFF states upon the application of a positive V_{GS} is called “depletion mode OECT” (**Figure 2-6 b**), in opposition to “accumulation” or “enhancement mode OECT”. In the accumulation mode, I_{DS} is increased when a positive bias is applied and anions penetrate into the polymer matrix to dope it, resulting in a switch of a transistor from its OFF to ON state. (**Figure 2-6 c**)

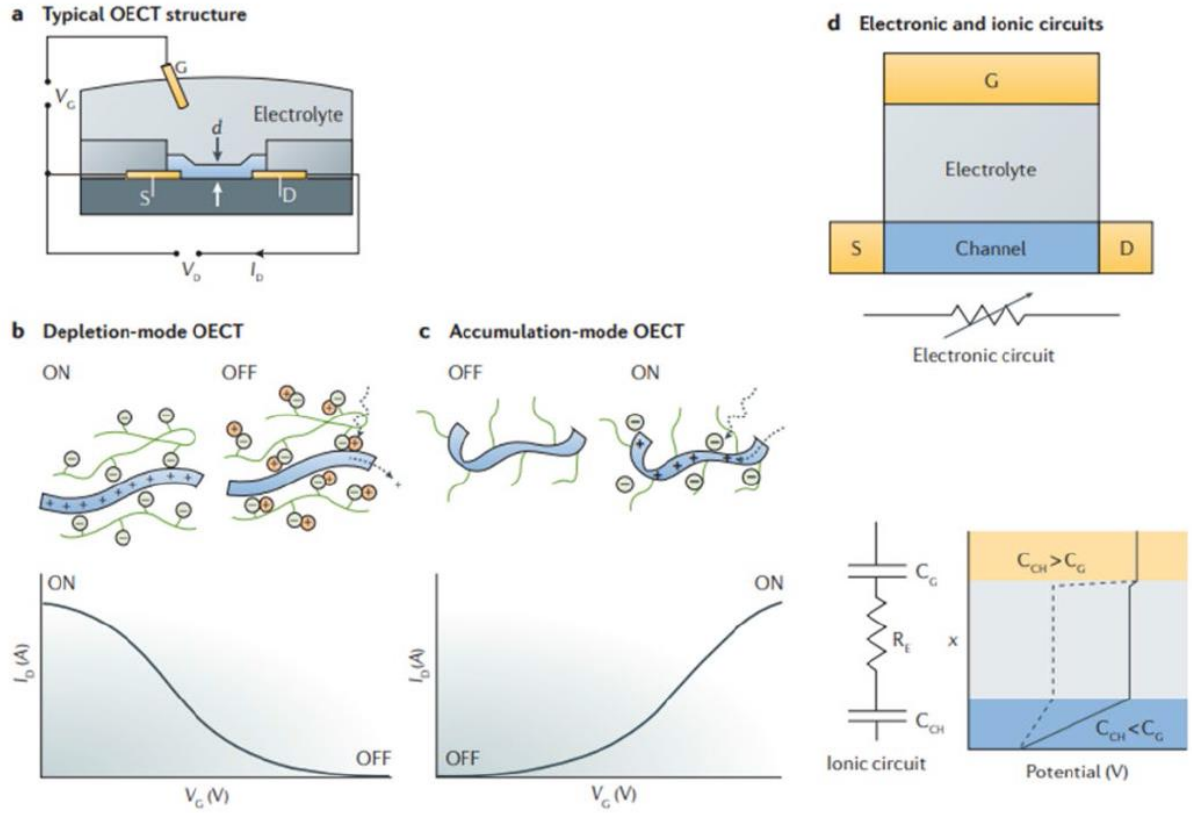

Figure 2-6. The device physics of organic electrochemical transistors. (a) The typical structure of an organic electrochemical transistor (OECT), showing the source (S), drain (D), electrolyte and gate (G). (b) Transfer curve showing depletion-mode operation of an OECT with a conducting polymer channel. At zero gate voltage, holes on the conducting polymer contribute to a high drain current and the transistor is ON. When a gate voltage is applied, the holes are replaced by cations and the transistor is OFF. (c) Transfer curve showing accumulation-mode operation of an OECT with a semiconducting polymer channel. At zero gate voltage, the channel has few mobile holes and the transistor is OFF. When a gate voltage is applied, holes accumulate and compensate injected anions, and the transistor is ON. (d) Ionic and electronic circuits used to model OECTs. The electronic circuit, shown below the device layout on the left, is modelled as a resistor with a resistance that varies upon gating. The ionic circuit, shown in the middle, consists of capacitors corresponding to the channel, CCH, and gate, CG, respectively, and a resistor corresponding to the electrolyte, RE. The panel on the right shows the distribution of potential in the ionic circuit. The solid line corresponds to the case of efficient gating, in which most of the applied gate

voltage drops at the electrolyte-channel interface, driving ions inside the channel. The dashed line corresponds to the case of poor gating, where most of the applied gate voltage drops at the gate-electrolyte interface. d, channel thickness; ID, drain current; VG, gate voltage; VD, drain voltage; x, distance[151]. Reprinted with permission.

1.4.2 Figure of merits of OECTs

Output and transfer characteristics

V_G directly controls the ion infiltration into the channel and, consequently, the material's doping degree through a redox reaction. The intensity of the drain current I_{DS} is determined by the difference in potential applied to the source and drain electrodes, called the drain source voltage (V_{DS}). The figure of I_{DS} *vs* V_{DS} is called the output curve and shows a decrease of I_{DS} when V_G is increased in the case of a depletion mode OECT. Usually, the variation of I_{DS} *vs* V_{DS} is recorded for different values of V_G to highlight the operation mode of the transistor.

A transistor can be used as an amplifier, converting low signals in gate voltage (V_G) into large changes in drain current. The variation of I_{DS} versus V_G is called a transfer curve and reflects a transistor switching from its ON state to its OFF state (in depletion mode). The efficiency of this amplification is depicted by the term "transconductance".

Transconductance

The transconductance g_m expresses the fact that I_{DS} is controlled by V_{GS} by the relation $g_m = \frac{\Delta I_{DS}}{\Delta V_{GS}}$, where ΔI_{DS} and ΔV_{GS} are the change in drain current and in gate-source voltage, respectively. If ΔI_{DS} is given in mA and ΔV_{GS} in volts, g_m is in millisiemens (mS) or simplified in mA/V. This second unit form clearly expresses what is the transconductance: if an OECT has a g_m of 3 mA/V, then a change in V_{GS} of 1 V causes a I_{DS} variation of 3 mA. A transconductance curve of g_m *vs* V_{GS} is often plotted alongside the transfer curve as a convenient graph expressing the efficiency of the switching of the transistor.

ON/OFF ratio

The ON/OFF ratio is the ratio of the drain current in ON state and OFF state for a given voltage range. The higher is this ratio, the more precise is the control of the gate voltage on current flowing from the source to the drain electrode.

Response Time

The response time of an OECT is defined as the time required to switch the transistor from its OFF state to its ON state. It also corresponds to the elapsed time between the application of V_{GS} and the achievement of the stable state in I_{DS}. The response time is dependent on one hand of the electronic charge carriers along the channel and, on the other hand, of ions transportation from the electrolyte to the channel. The latter is known to be the limiting process since the hole (or electron) transport ($\sim 10^{-1}$ cm^2 V^{-1} s^{-1}) in OECTs is 10 to 100 times faster than the ionic transport ($\sim 10^{-3}$ cm^2 V^{-1} s^{-1}).[152] The response time is hence strongly dependent of the thickness of the channel and of the transistors dimensions.

1.4.3 PEDOT based OECTs

In addition to being potentially an important component in the future of electronics, OECTs are currently used as chemical sensors. It was established in 2000 that OECTs can act as multi-parametric sensors thanks to their capacity to measure simultaneously the variation of four electrical parameters: the field effect mobility, the on/off ratio, the threshold voltage and the bulk conductivity of an organic film.[153] pH monitoring is an important feature of bioelectronics since this stimulus is very common in vivo reactions [154]. To this end, many examples of OECTs were developed for pH sensing applications [155-157] E.Scavetta and coworkers investigated the use of two pH-sensitive PEDOT composites.[31] The PSS counter ion has been replaced by two pH dyes: Bromothymol Blue and Methyl Orange, which change their electronic charge with pH, influencing the doping of the composite PEDOT:dye. They assembled a flexible OECT/pH sensor using PEDOT:PSS as the channel material and the composite PEDOT:dye as the gate material, proving its applicability in wearable electronics. A pH sensor was described by G.G. Malliaras et al. by combining two OECTs in the same device.[154] This typical layout, called Wheatstone bridge allowed the use of a reference solution instead of a reference electrolyte in order to calibrate the pH sensor. Here, a first OECT is calibrated with a pH tampon solution and a second one received the analyte, i.e another pH solution or human sweat. The difference recorded in the output voltages of the two OECTs was used to plot a linear dependence of the variation of pH vs output voltage. The as-prepared pH sensor was successfully used to determine the pH of a sweat sample with a higher precision than a commercial pH meter. The integration of ion-selective membranes to

OECTs led to devices capable of sensing and selecting cations in sweat.[158] The drain current of such devices will be decreased in presence of the desired cations and for a constant gate voltage, allowing the monitoring of biomarkers to help the early diagnosis of diseases. Similarly, A.Zappettini and coworkers prepared ion selective OECTs on textiles for wearable sweat monitoring.[159] They demonstrated an easy protocol to assemble on-fabric OECTs consisting of subsequent soaking and drying of a commercial fabric in a PEDOT:PSS and in an ion-selective solution, respectively.

All the above devices are working in depletion mode thanks to commercially available *p-type* PEDOT:PSS solutions. Very few examples of PEDOT:PSS OECTs working in enhancement or accumulation mode can be found in the literature. Enhancement OECTs have the advantage of a reduced power consumption since they are initially in the OFF state and hence only require a voltage bias to be turned ON. The demand for enhancement OECTs is real, especially in bioelectronics and wearable devices, where the power consumption is a major concern for a future large scale commercialization of consumer electronics. However, producing an enhancement OECT from PEDOT:PSS is still challenging since this mixture needs to be de-doped or reduced, leading to decrease of both its conductivity and oxygen stability.[160] Van de Burgt and coworkers prepared enhancement OECTs from commercially available PEDOT:PSS mixture and amine-based molecular de-dopants.[161] They successfully assembled OECTs with a mobility near that of pristine PEDOT:PSS with stable operation over 1000 ON/OFF cycles. The PEDOT:PSS de-doping mechanism is still under investigation and a lot of work is still required to achieve fully functional enhancement mode transistors, but this promising result opens the door for the development of more complex organic electronics based on both depletion and enhancement OECTs.

1.5 : Electrochromism

Electrochromic materials are by definition a class of materials able to exhibit a color change in the UV-visible-NIR window under a voltage bias and through a redox process. The first electrochromic device (ECD) was described in 1969 when it was discovered that thin films of WO_3 reversibly changed color.[162] Since then, a lot of efforts were dedicated to development of new electrochromic materials in order to span the entire visible spectrum[163, 164] and to optimize the

fabrication process and performances of the devices.[165, 166] They are classified into three major types, depending on the physical state they adopt in their neutral and colored state.[167]

- Type I electrochromes exist in their solution states during the whole redox process. An electron transfer undergoes at the solid-liquid interface between a conductive layer (an electrode) and the electrochromic material respectively, revealing a color change. This process can take place either at the anode or at the cathode by an oxidation or reduction reaction, respectively. Reacted species then diffuse back from the electrode to the bulk solution.
- Type II electrochromes are initially soluble in their neutral state and form insoluble species while oxidized or reduced. A colored deposit is formed on the surface of the electrode toward an electron transfer from the liquid electrochrome
- Type III electrochromes are in their solid state through the whole electrochromic operation, regardless of their redox states. They exist under the form of particles or films deposited on the surface of the electrode.

This thesis is dedicated to organic materials, even though metallic oxides are also promising electrochromic materials. Therefore, we will focus here on the specific case of conjugated polymers and small organic molecules as electrochromes.

1.5.1 Class of electrochromic materials:

Electrochromic materials can be distinguished according to the redox process required to reveal a color change. Electrochromes that are colored in their oxidized states are referred to as anodically-coloring materials. On the other hand, materials that are colored in their reduced states are cathodically-coloring. Also, while most of the electrochromic materials exhibit only one colored and bleached state, some can be switched to different colors. Those are referred as polyelectrochromic or multichromic materials.[168-170] More generally, the nature of the electrochromic material is the number one criterion to differentiate the type of device. Among them we can list, inorganic or organic molecules, and small molecules or macromolecules and polymers.

1.5.2 Conjugated electrochromic polymers:

This category of electrochromic materials offers several key advantages over their small molecules and inorganic compounds counterparts. Their color can be easily tuned through a chemical structural modification of their backbone and the combination of monomers of different natures is a successful strategy to design polyelectrochromic materials.[169] These can often be readily processed from a simple solution to form a thin film, lowering fabrication costs and making a large scale production of electrochromic devices feasible. In terms of intrinsic properties, better electrochromic performances such as high coloration efficiency, high optical contrast and rapid response times are revealed than their inorganic counterparts. Finally, the possibility of tailoring the mechanical properties of the polymers without lowering their electrochromic ones is of great interest in order to produce wearable and adaptive electronics.

Among the large variety of electrochromic conjugated polymers reported in the literature, polyaniline was the first to be characterized.[171] Polyaniline is known to be able to adopt four different redox forms: leucoemeraldine, emeraldine salt, emeraldine base and pernigraniline, all of them exhibiting four different hues: yellow, green, blue and black respectively. Polypyrroles and polythiophenes were also extensively studied and numerous electrochromic materials have been emerged from derivative molecules of these three main polymers. Among them, PEDOT is the most established and widely studied electrochromic conductive polymer. Derived from substituted polythiophene, this cathodically-coloring material exhibits a deep-blue color while being reduced and a sky blue color in its oxidized st ate.[172]

Electrochromic conjugated polymers are composed of a well-defined molecular backbone. This one can be either a repetition of electron-donating monomer units or an alternating combination of electron-donating and electron-withdrawing units, leading to an all donor polymer or a donor-acceptor polymer type respectively.[173] Donor-acceptor conjugated polymers offer the advantage of having a dual absorption band, leading to a wide variety of colors. Actually, the whole color palette has been achieved using the donor-acceptor strategy by tuning the hues via controlling the electronic transfer and the steric chain interaction of the polymer chains. Such parameters can be tailored by using heterocyclic units, substituents and side chains on the π system, physically blending different polymers and the copolymerization of several monomers.

The source of electrochromic changes in conjugated polymers originates from the addition or the withdrawing of electrons. Their initial color in the neutral state is determined by their intrinsic π-π* electronic transition energy bandgaps, named E_g. As the polymers undergo an oxidation or a reduction, electrons are removed or added to their neutral polymeric systems and a counter ion movement from the electrolyte is created to balance the charges. Polymers are thus doped either by a *p*-doping or a *n*-doping process respectively. A modification of the structure of the polymer backbone occurs through the removal or the addition of the electrons. The original aromatic form is converted to the quinoidal one which is positively charged (*p*-doping) or negatively charged (*n*-doping) by polarons and bipolarons. New energy levels are created and become filled or vacant, leading to the creation of new absorption bands and hence corresponding to a color change.

1.5.3 Small molecules

Aside from conjugated polymers, small electrochromic organic molecules have been extensively studied in the past decades. They show an electrochromic behavior either in their monomeric form or when functionalized with side chains or aromatic compounds. Functionalization of such small molecules offers the advantage of a facile hue tuning. Among the most studied compounds we can name but a few : thiophenes,[174, 175] carbazoles,[176] quinones and triphenylamines (TPA).[177-179] TPA in particular is a very attractive moiety thanks to its trigonal backbone. A triphenylamine consists of a central nitrogen atom linked to three sp^2-hybridized carbon atoms. The angle formed by this C-N-C bond is 120°.[180] This planar conformation serves as an anchor point for three phenyls oriented to form a helix. This provides TPA a low ionization potential of 6.80 eV which makes them suitable for electrochromic applications.[181] Indeed, this potential is smaller than many inorganic and organic compounds and means that TPAs are very good electron donors in addition to being good hole conductors due to their low ionization potential. Their non-planar structure also prevents aggregation and therefore avoids hindering charge transport in addition to giving rise to amorphous materials forming homogeneous films.[182]

1.6 Electrochromic devices

Electrochromic properties of materials are being exploited under the form of cells called electrochromic devices. Solid, flexible or even stretchable,[183] these devices exploit the reversing optical properties of their component to find applications in smart windows,[184] displays[185] or

even camouflage.[186] The device architecture is generally based on the stacking of five layers : two electrodes, the electrochrome, the electrolyte and an ion storage material (**Figure 2-7**).[187] Very recently, Y.Kim et al., developed a stretchable PEDOT:PSS based electrode and a three layered stretchable electrochromic device was demonstrated.[183] In this case, the two electrodes and the electrochrome were mixed to form two layers and the electrolyte makes up the third layer. In this setup, the PEDOT:PSS acts as both the conductive layer and the ion storage material. ECD are classified in two major types, depending on their operation mode: transmission or reflectance. The former concerns devices were the electrodes are fully transparent and the light intensity passing through them is modulated.[29, 188, 189] On the other hand, reflective devices possess one electrode covered with a metallic coating in order to control the reflective light intensity.[190, 191]

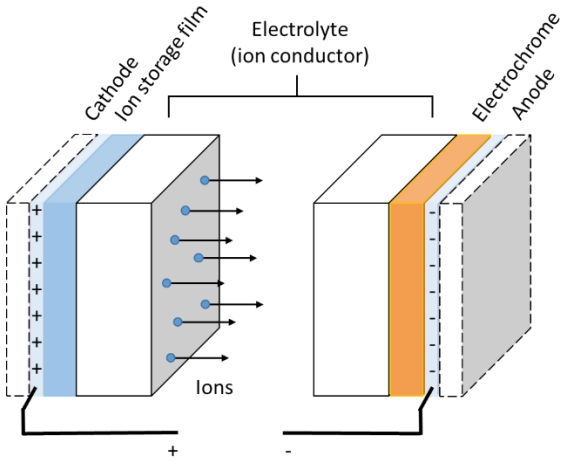

Figure 2-7. Scheme of a generic five-layer electrochromic device design.

1.6.1 Figure of merits

An ideal EC device should possess properties like, high contrast, fast switching and electrochemical stability.

Optical contrast

The degree of optical change between two redox states of an electrochromic material is quantified by its optical contrast (Δ%T). The higher is this value, the more discernible are the colors between the neutral and the oxidized (or reduced) state of the material. The optical contrast is defined as the

percentage difference in transmittance between two redox states: fully oxidized (T_{ox}) and fully reduced (T_{red}) and is expressed by the following relation:

$$\Delta\%\mathrm{T} = T_{ox} - T_{red}$$

Coloration efficiency

Power consumption of electronic devices is a major concern for developing a greener and a more earth-friendly technology. The coloration efficiency (CE) of an electrochrome or an electrochromic device is defined to assess this purpose. This parameter represents the variation of the optical density per unit of charge injected or ejected and is given by the following equation:

$$CE, \eta = \frac{log \frac{T_{ox}}{T_{red}}}{\frac{q}{A}}$$

Where, T_{ox} and T_{red} represent to the percent transmittance (%T) of the bleached and colored states respectively, q the charge consumed during the redox reaction in Coulombs (C) and A is the active area of the electrochrome in cm^2. The higher the value of CE is, the lower is the power consumption for a high optical change.

Switching Time

An efficient electrochromic device is characterized by a fast switching between its redox states in response to an applied voltage. The switching time hence measures how fast the electrochromic device switches from its bleached to colored states and *vice versa*. Although there is not a consensus on how to define the switching time, it is predominantly admitted to consider it as the time needed to reach 90% of the full switch. For these means, the variation of the transmittance during redox cycles between neutral and colored states is recorded over the time. The time taken to reach 90% of the fully colored state is considered as the switching time. The 10 last percent are neglected, based on the consideration that human eyes cannot detect such a finest color change.[192]

Stability

The stability of an electrochromic device is measured by its capacity to sustain a high optical contrast under repeated redox cycling of doping-undoping process. The common approach to determine the stability of an electrochrome or a device consists of recording the number of redox

cycles it can undergo before the apparition of a significant degradation or a certain percentage drop in the optical contrast. Parameters like the applied voltage and the cycle duration significantly impact the performances of the electrochromic behavior. The stability of electrochromic devices is therefore quite challenging to evaluate and compare since this measurement differs from research groups. Recently, Reynolds proposed a standard method to calculate the switching time, offering a way to homogenize the stability measurements and hence opening the door for the creation of an electrochromic device benchmark.[193]

1.6.2 Stretchable electrochromic devices

Stretchable Transparent Conductive Electrodes

ITO is a very brittle material with a high Young modulus of 116 GPa [194] and a very low elongation at break of only 4% strain.[195] Its use in stretchable devices as a transparent conductive electrode (TCE) is hence impossible. On the other hands, it is often used in prototypes of flexible device as a coating on a PET sheet.[196-200] The literature offers a vast range of technics to produce stretchable TCEs, most of them, however, involve the use of inorganic materials. Different strategies were studied like shape memory metal alloys,[201] metallic nanowire networks,[97, 202, 203] core-shell nanowires embedded in PDMS,[204] and metallic grids on stretchable substrates.[205, 206] As previously mentioned, such inorganic materials have the drawback of being more expensive, less processable and with a limited scale up ability compared to their organic counterparts. PEDOT:PSS based stretchable transparent electrodes offer a promising alternative, mainly due to the solution processability and the low-cost of PEDOT:PSS mixtures. J.S.Ha et al. developed a highly stable TCE under strain by a simple mixing of a commercially available solution of PEDOT:PSS with a triblock copolymer followed by an acidic treatment.[207] The copolymer acts as a plasticizer by decreasing the tensile strength and increasing the fracture at break up to 35% while the acidic treatment induced the formation of bigger and more numerous PEDOT domains. As a result, the TCE showed a slight resistance variation upon stretching of only 4% when stretched at 40% strain and a great stability over 10 000 cycles of stretching/releasing. Similarly, Zhennan Bao and coworkers took advantage of mixing ionic liquids with a mixture of PEDOT:PSS to produce a highly stretchable, conductive and transparent polymer.[208] They showed that ionic liquids exhibiting a good solubility in water and in the PEDOT:PSS solution and having an acidic anion can successfully act as dopants to increase both the stretchability and the

conductivity. (**Figure 2-8**) The as-prepared polymers showed a stretchability up to 800% strain and a monotically decrease of the conductivity from 5000 S/cm to 90 S/cm upon stretching. Many recent examples from the literature prove that tuning the stretchability and conductivity of PEDOT:PSS by addition of secondary dopants is a hot topic.[11, 46, 47, 209-212]

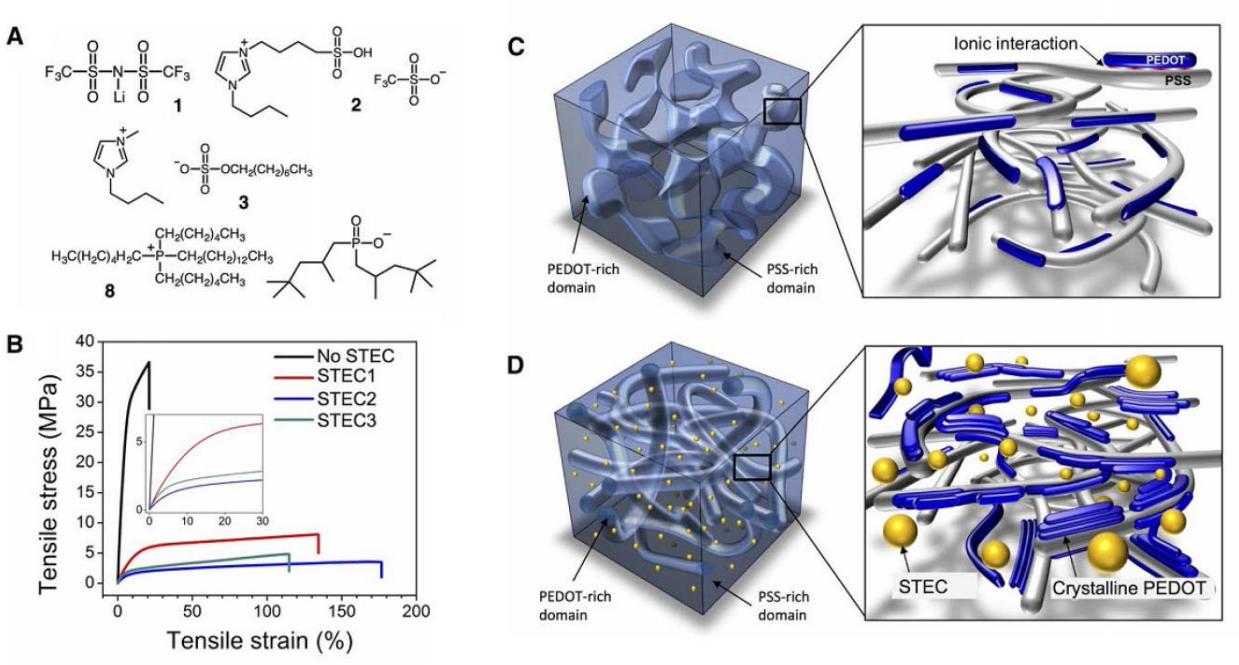

Figure 2-8. Chemical structures and schematic representation. (A) Representative stretchability and electrical conductivity enhancers. (B) Strain-stress curves of PEDOT:PSS with and without stretchability and electrical conductivity (STEC) enhancers. (C and D) Schematic diagram representing the morphology of (C) a typical PEDOT:PSS film versus that of (D) a stretchable PEDOT film with STEC enhancers[208]. Reprinted with permission.

Stretchable organic electrochromic devices

In 2017, a first stretchable all organic electrochromic device was prepared by mixing PEDOT:Tos in PU.[213] A mixture of EDOT, iron tosylate and PU in THF was spincoated on a PU substrate and led to the in situ polymerization of PEDOT:Tos embedded into the PU matrix. The as prepared stretchable and conductive material was further used as an electrochrome in a stretchable electrochromic device, exploiting the coloured and bleached states of the PEDOT upon its reduction and oxidation respectively. The device can work under a strain of 50% and be bent on a glass rod. More recently, an intrinsically stretchable ECD made of PEDOT:PSS deposited on a

stretchable elastomeric substrate has been prepared.[183] PEDOT:PSS stretchability was improved by the addition of PEG, which reacted with PSS to create semi-interpenetrating networks. The networks included bulky structures and dynamic hydrogen bonds as stretchability enhancers. As prepared ECDs can be stretched up to 200% but a clear degradation of the electrochromic contrast was noticed. Ulrika et al. used commercially available PEDOT:PSS inks to develop a scalable screen printing process to produce stretchable ECDs on PU substrates.[214] The devices were functional up to 50% strain and shown a great stability over 500 cyclic stretching at 30% strain. Unfortunately, all the above mentioned electrochromic devices are limited to the use of PEDOT as the electrochrome, displaying only a color switch from deep to sky blue. While electrochromic organic materials offer a large hue of colors, it seems necessary to use PEDOT as a TCE only and to take advantage of electrochromic molecules to display distinct colors.

CHAPTER 3 MATERIAL AND APPROACHES

1.1 Preparation of electrospinning mixtures

In order to produce PEDOT:Tos fibers, iron tosylate in butanol was used as the main solvent and varying amounts of carrying polymer were investigated. Poly(ethylene oxide) (PEO, $M_n = 1x10^6$ g/mol or $5x10^6$ g/mol) or poly(vinylpyrrolidone) (PVP, $M_n = 1x10^6$ g/mol) were dissolved in the range of 4 to 9.7 w% as per the molecular weight and the nature of the carrying polymer. Dichloromethane was chosen as a cosolvent in order to decrease the viscosity of the mixture, leading to the production of thinner fibers. Final composition of the electrospinning mixtures was experimentally determined in order to produce defect-free fibers. As-prepared iron tosylate fiber mats were then exposed to EDOT vapor under reduced pressure to allow the polymerization reaction of PEDOT around the fiber, leading to the formation of PEDOT:Tos fibers. The carrying polymer is then removed through a rinsing step consisting of an immersion in ethanol for 10 minutes followed by a rinse with ethanol to remove physisorbed impurities.

PEDOT:PSS fibers were produced from commercially available mixture (Clevios PH1000). Similarly to PEDOT:tos fibers protocol, different amounts of PEO ranging from 0.7 to 1.7 w% were investigated in order to minimize the diameter of the fiber and the loss of conductivity. The addition of PEG-PPG-PEG as a plasticizer was also studied. Dimethylformamide (DMF) was used as a cosolvent to decrease the surface tension of the Taylor cone and hence reducing the fibers' diameter. A rinse step was also performed as described above to remove the carrying polymer.

1.2 Conductivity and sheet resistance measurements

The conductivity of spin coated films and the sheet resistance of fiber mats were determined with a four-point probe station (Ossila). Due to the heterogeneous nature of fiber mats samples, measuring the conductivity is not accurate and the sheet resistance is used as a benchmark to quantify the conductive nature of the as-prepared samples. By definition, the sheet resistance corresponds to the resistance of a material per unit area and is independent of its size, which is a convenient technique to compare heterogeneous samples.[215] On the other hands, conductivity measurements were performed on homogeneous spincoated samples made from the same

electrospinning mixture to be qualitatively compared with other PEDOT based mixtures from the literature.

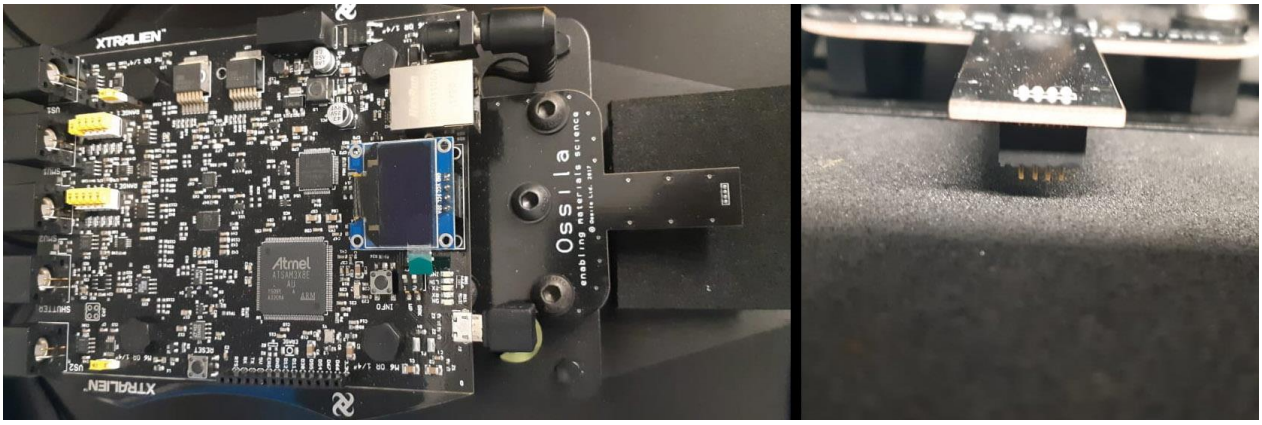

Figure 3-1. Image of the four-point probe station. (right panel: top view of the instrument, left panel: front view with focus on the four probe).

The thickness of the spincoated films were measured with a stilus profilometer (DektakXT, Brucker).

1.3 Electromechanical characterization

1.3.1 Preparation of the elastomeric substrate

PDMS was used as elastomeric substrates for both stretchable OECTs and electrochromic devices. A blend consisting of the elastomer base and the curing agent in 10:1 w/w (Sylgard^{TM} 184, Dow Corning) is stirred with a planetary mixer for 2 minutes at 2000 rpm. The PDMS mixture is then spincoated onto glass substrates of 2" by 3", previously cleaned (with acetone, DI water and ethanol for 30 seconds) at 1000 rpm and heated on a hot plate at 90° for 30 minutes. PDMS films were peeled-off the glass substrates and cut to the desired dimensions for further use in OECTs or electrochromic devices.

1.3.2 Electromechanical test

Electromechanical tests were performed on a stretcher controlled by a homemade LabVIEW software. The stretching program is defined as 5 successive stretching-releasing cycles at given strains and at 0.1 cm/s. The samples were kept under strain for 1 minute and allowed to rest for another minute before the beginning of the second cycle. Strains were increased by steps of 20%,

from 20% to 200% strain. Stretcher's clamps are connected to an Agilent system allowing to record the current flowing through the sample under a 0.2 V potential while being stretched. Cycling tests were also done with this system. To this means, 1000 stretching-releasing cycles at 50% strain were performed with only 5 seconds between two consecutive cycles.

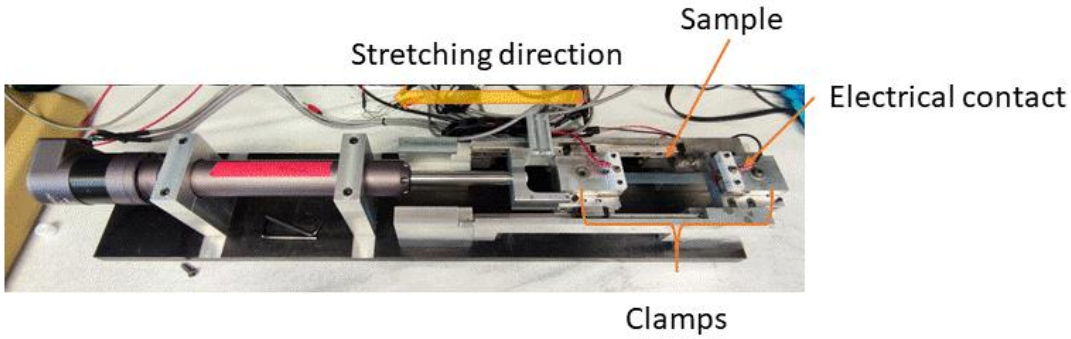

Figure 3-2. Image of the stretcher used for the electromechanical measurements.

1.4 OECT fabrication and characterization

1.4.1 Fabrication

PEDOT:Tos or PEDOT:PSS fibers were obtained on PDMS substrates or on stretchable tape (VHB^{TM}, 3M) as previously described in section 3.1. (**Figure 3-3**) Fibers were covered with a PET stencil mask for plasma etching to form 12 PEDOT patterns. The PET stencil masks were fabricated using a ScanNcut SDX 1200 Brother cutting machine. The patterns were 2 mm wide and 15 mm long. The samples were etched for 1 h at 100 W and 50 sccm of oxygen (O_2) (Plasmionique FLR 300H). Silver electrodes of 3 mm^2 were printed with a Voltera Circuit Printer on each as-formed patterns, resulting in the channel and the source-drain electrodes. Glass cloning cylinders (non-stretchable OECTs) or PDMS wells (stretchable OECTs) were glued on the PEDOT channels or a stretchable encapsulation layer was used to form the gate wells (stretchable OECTs) to complete the OECT fabrication. Glass or PDMS wells were filled with a 0.1 M NaCl aqueous solution as the gate electrolyte and activated carbon (PICACHEM BP9) on carbon fiber (Pectracorp 2050, 10 mils) was used as gate electrode. Liquid metal EgaIn (Sigma Aldrich) were applied at the source and drain electrodes to ensure a good electric contact between the OECT and the probes.

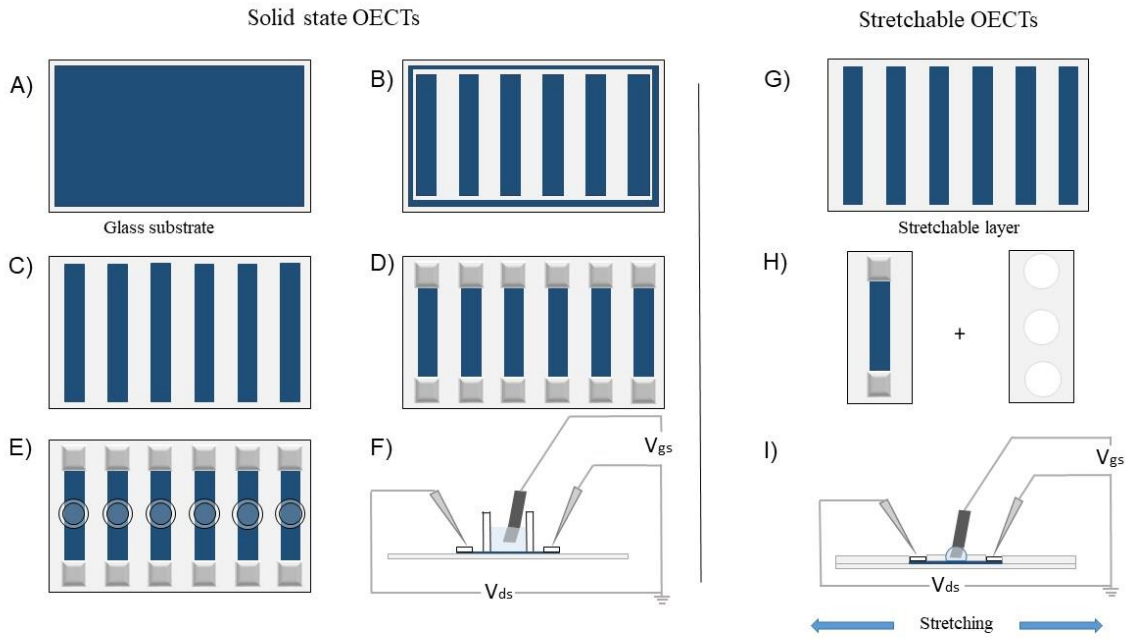

Figure 3-3. Schematic representation of OECT fabrication on glass substrates (left panel) and stretchable substrates (right panel). Left panel: deposition of fibers on the substrate (A), plasma etching (B), resulting fiber channels (C), electrodes printed on the channels (D), cloning cylinders glued on the channels to complete the OECTs (E), and electrical schematic of the final OECT (F). Right panel: electrospun fiber channels produced on a stretchable substrate by plasma etching (G), each channel isolated and the OECT is encapsulated with a top layer (H), and electrical schematic of the final OECT (I).

1.4.2 Characterization

The transistor electrical characteristics are measured with an Agilent B2900A source measure unit controlled with Quick IV Measurement software (**Figure 3-4**). For stretchable OECTs, the strain is applied in situ with a LabVIEW software-controlled tensile tester.

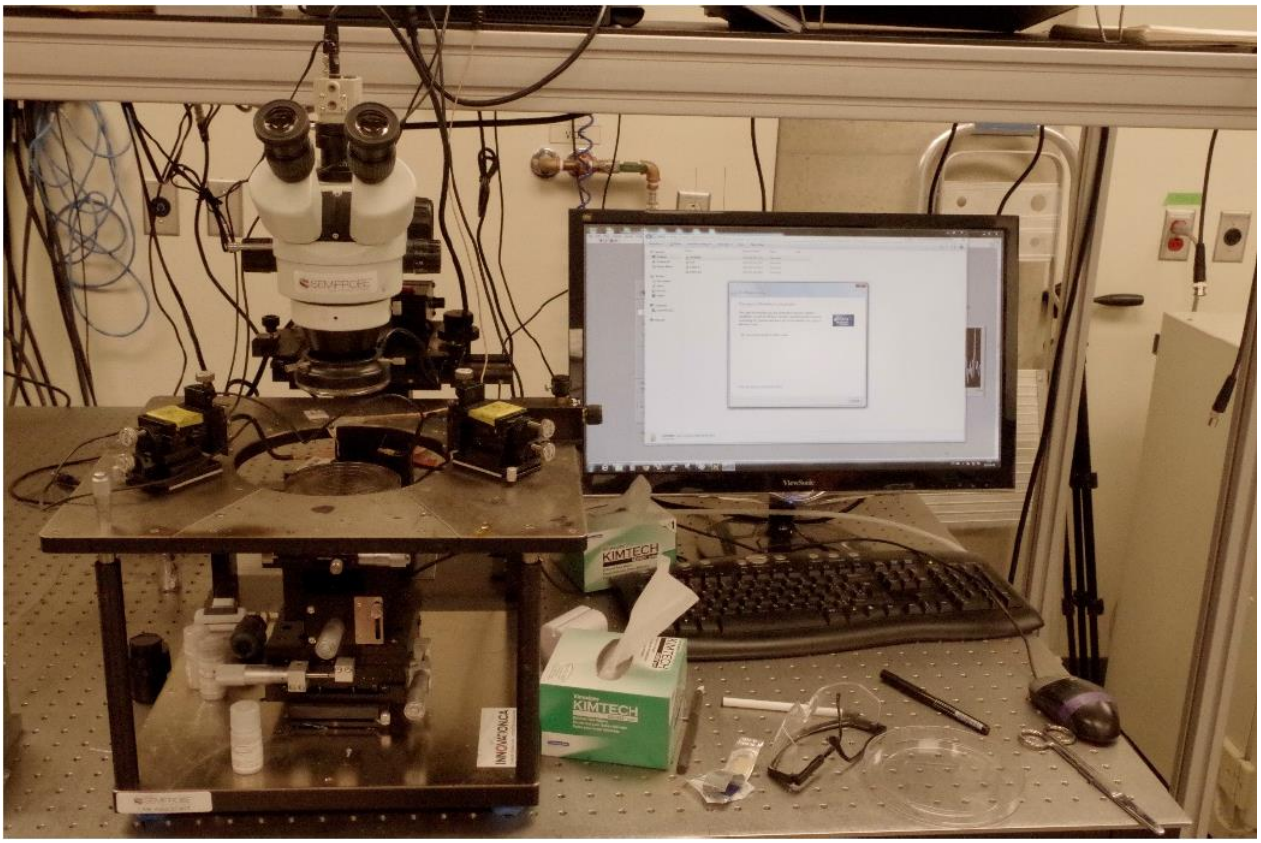

Figure 3-4. The probing system used to measure the transistors

1.5 Cyclic voltammetry

All electrochemical measurements presented in this thesis were performed with a SP300 Biologic potentiostat. Cyclic voltammetry is a widely used technique to analyze the electrochemical redox properties of samples. Generally, the measurement is in a 3-electrode configuration (working, counter and reference electrode). The sample of interest is placed as a working electrode, a reference electrode is used to measure the potential difference between the changing potential at the working electrode and the constant potential of the reference electrode, recorded by the potentiostat. The counter electrode is placed to complete the circuit so that the current flows between working and counter electrode. This current is recorded with the potentiostat. All the electrodes are immersed in an electrolyte solution during the measurements. Cyclic voltammetry experiments can also work in two electrode configuration, adapted from the 3-electrode system, in which the counter electrode also acts as a reference electrode by maintaining constant potential.

This is notably the case of electrochromic devices were the anode acts as both the counter and the reference electrodes.

In cyclic voltammetry, the potential between the working and reference electrode is linearly scanned between the known potential window of the sample, in forward and reverse directions at a defined scan rate and for a desired number of cycles. During the forward and reverse scan, the electrochemically active material in the working electrode undergoes oxidation (loss of electrons) and reduction (gain of electrons). The processes are recorded as current versus voltage plot. The oxidation and reduction potentials measured by cyclic voltammetry is of great interest for electrochromic device characterization as these represent the voltages to apply to the device to allow it to switch between its ON and OFF states.

1.6 Electrochromic device fabrication

Electrochromic devices were fabricated from 2 transparent electrodes, either ITO or PDMS coated with PEDOT:PSS fibers. A copper tape strip was fixed on one edge of each electrode to facilitate the external electrical connection with the potentiostat. A window was created on the surface of one of the two electrode with double-side tape for rigid devices or with PDMS in the case of stretchable devices. An electrolyte gel was placed in the as-formed window and an electrochrome was deposited on the other electrode by spraycoating from a tetrahydrofuran (THF) solution. The two electrodes were then assembled and sealed with PDMS to prevent the electrolyte from leaking out the device and to create a barrier against oxygen and moisture.(**Figure 3-5**)

The electrolyte gel was prepared as follows: a chitosan solution is first prepared by dissolving 1 g of low molecular weight chitosan in 50 mL of acetic acid (1w%) solution for 4 hours, followed by the addition of 40 w% of magnesium sulfate salt. This mixture was allowed to stir for one hour, up to complete homogenization. Finally, 42 w% of glycerol was added and the mixture was stirred for another two hours.

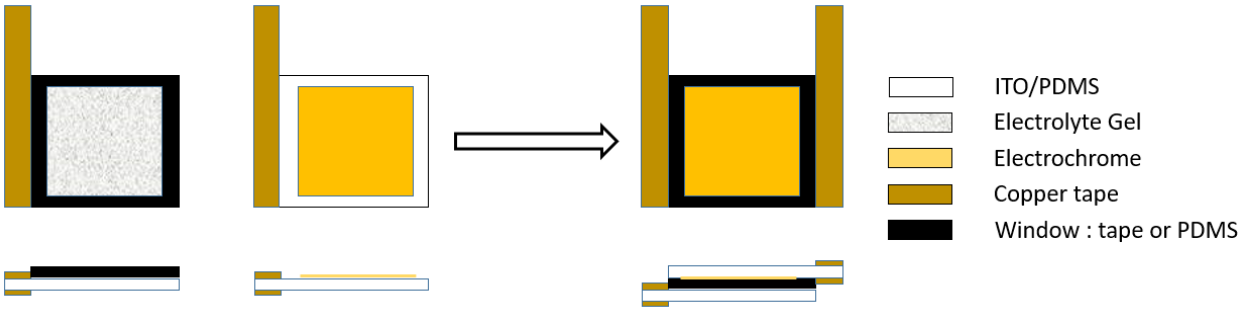

Figure 3-5. Schematic representation of electrochromic device fabrication.

1.7 Spectrophotometric characterization

Spectrophotometric characterizations were performed with a cary 700 from Agilent. The absorption wavelengths of the electrochromic material and the devices were measured in their neutral, oxidized and reduced states, prior to being characterized by spectroelectrophotometry. The electrochromic material wavelengths were recorded in an electrolyte solution and using a blank electrolyte solution as a baseline. Similarly, a blank device was assembled, containing only the electrolytic gel and was used during the wavelengths measurement of the electrochromic devices. Both the electrochrome and the devices were oxidized and reduced while characterized, leading to three absorption spectra in their neutral, oxidized and reduced states. In our case, during the oxidation of the electrochrome, also called ON state, only one peak appeared at 805 nm, while during its subsequent reduction (OFF state), this one disappeared. The kinetic of the absorption at 805 nm was then studied by spectroelectrophotometry.

1.8 Spectroelectrophotometric characterization

The goal of this technique is to study the kinetic of a color change upon a redox reaction. A Cary 700 spectrophotometer (Agilent) was used in combination with a Biologic SP 300 potensiotat in order to record the variation of a given wavelength during the oxidation (or the reduction) of an electrochromic material or device. The spectrophotometer was set up to record the apparition/vanish of the peak at 805 nm upon the oxidation and the subsequent reduction, respectively, over time. The recorded transmittance has been normalized to 100% in the OFF state (reduction) in order to get a relative measurement of the color switch induced by the redox reaction. As a result, the color switch toward the ON state appeared as a decay of the transmittance, while

the OFF state induced an increase of the transmittance. The recorded spectrum provides information about the contrast of the color switch (in percentage between the ON and OFF states), the lifetime of the device (stability of the switch intensity over time) and the kinetic of the color switch between its ON and OFF states.

CHAPTER 4 ARTICLE 1: COMBINING ELECTROSPINNING AND ELECTRODE PRINTING FOR THE FABRICATION OF STRETCHABLE ORGANIC ELECTROCHEMICAL TRANSISTORS

This article has been published in the journal “Frontiers in Physics” on 2021-08-04. This article reports the fabrication of stretchable OECTs from fiber mats of PEDOT:tos. The fibers were produced by a combination of the electrospinning of a mixture containing an oxidizing agent (iron tosylate) and the chemical polymerization of EDOT by a vapor phase polymerization technique. The OECTs fabricated on elastomer substrates based on PEDOT:tosylate fibers were able to work under stretch up to 50% strain. The supporting information for this article is reprinted in Appendix A of this thesis.

1.1 Authors

Michael Lerond[1], Arunprabaharan Subramanian[1], W. G. Skene[2*], Fabio Cicoira[1*]

[1] Department of Chemical Engineering, Polytechnique Montréal, Montréal, QC, Canada

[2] Faculté des arts et des sciences - Département de chimie, Complexe des sciences, Montréal, QC, Canada

***Correspondance :**

Fabio Cicoira : fabio.cicoira@polymtl.ca

William Skene : w.skene@umontreal.ca

1.2 Abstract

Stretchable conductors and organic electrochemical transistors (OECT) were fabricated from PEDOT:Tos (poly(3,4-ethylenedioxythiophene):iron tosylate) nanofibers. The devices were prepared by a combination of electrospinning and electrode printing followed by vapor phase polymerization (VPP). The impact of both the processing time and the composition of three electrospinning mixtures on the electrospun fiber mats was evaluated by scanning electron microscopy and cyclic voltammetry. Fibrillar mats prepared from the different mixtures maintain their electrical properties were stretched to 140% of their original length. Stretchable OECTs were

fabricated by printing silver drain and source electrodes directly on the conductive spun fibers. The fabricated devices showed transistor behavior up to ~50% strain.

1.3 Introduction

Interest in plastic electronics has been spurred on by the development of new synthetic methods for preparing conjugated organic materials, that enable organic electronics such as OLEDs, OPVDs, and OFETs.[216-218] Research in this field has further been motivated to bring the intrinsic properties of plastic electronics to fruition. Towards this end, efforts have focused on exploiting the environmental advantages of devices. For example, the efficiency of clean electricity production from sustainable resources using OPVDs continues to improve.[219] Similarly, advances in OLEDs materials result in reduced power consumption and increased efficacy.[22]

The virtues of plastic electronics also include their processability. They can be cast from inks using various deposition methods such as spray and sheet coating along with roll-to-roll printing.[220, 221] The advantages of these processing methods is their upscaling with the potential of production-scale device fabrication. These methods of printing conjugated materials that enable plastic electronics can further be applied to a range of substrates that have various mechanical properties. The inks can be applied to rigid and flexible substrates alike, opening the possibility of fabricating conformal devices whereby they can adopt a gamut of shapes and sizes including curved surfaces, unlike contemporary devices that are fabricated from rigid substrates. Stretchable electronic devices including light-emitting diodes,[222] transistors[223] and solar cells[224] have been successfully developed. The virtues of merging flexibility and stretchability into devices give them mechanical properties that are ideally suited for their use in wearable electronics. Indeed, wearable plastic devices have found uses in a range of consumer electronics and healthcare applications.

Stretchable and flexible substrates cannot exclusively render devices wearable. Rather, each component that is integrated into devices must have a similar stretchable and bendable behavior. This ensures the layers respond to body motions in concert, resulting in a positive experience by the user when wearing the device. Although the stretchability and flexibility of the device components are critical mechanical properties of wearable electronics, their electrical response must be consistent with applied stress and strain. Given that intrinsically conductive electrodes

underpin the electrochemical performance of devices, the conductivity of these conjugated organic materials must not be compromised under the typically mechanical stresses and strains that are encountered when wear electronics. Indeed, this remains the principal challenge of the field, despite the many fabrication[225] and performances[226, 227] improvements of stretchable devices.

Doped poly 3,4 ethylenedioxythiophene (PEDOT), doped with various counterions is ubiquitously used in plastic electronics owing to its high intrinsic conductivity and its processability. Despite these key properties, its rigid conjugated framework affords it a poor capacity to deform. It further suffers from a dramatic loss of electronic conductivity with applied strain and stress. The limited mechanical properties of PEDOT based materials therefore makes it incompatible for use in truly flexible and stretchable devices. Its elongation at break can, however, be improved by blending it with a plasticizer. The latter inserts between the macromolecular chains and it absorbs the external strain.[47, 228] Different fabrication processes have also been developed to make the mechanical properties of PEDOT compatible for its use in wearable electronics, while preserving its intrinsic conductivity. Strategies towards this end include depositing on a pre-strained elastomeric substrate,[135] the Kirigami method,[17, 229] and electrospinning.[21, 230, 231] In the latter, non-woven fibers are formed by applying a high voltage bias between a given collecting surface and a polymer solution. The continuous collection of the fibers on the substrate forms a film consisting of highly entangled fibers. The degree of entanglement and hence the thickness of the polymer film on the surface is contingent on the deposition time. The virtue of electrospun coatings is the stretchability of otherwise rigid polymers that is governed by the polymer chain entanglement.

The collective flexibility and stretchability of the electrospun coating along with the straightforward fabrication make electrospinning an ideal process for preparing stretchable conjugated polymers. Indeed, a range of conjugated polymers have been electrospun including polyaniline,[232] P3HT,[233] polypyrrole[234, 235] and PEDOT.[236-238] Extensive investigation have correlated the impact of the electrospinning solution viscosity on both the conductivity of the electronpun fiber and the fiber's morphology.[239] It is further known that the diameter of the electrospun fiber can be modulated by modifying the viscosity of the electrospinning solution.[239] Similarly, the morphology of the fibers can be varied with the use of cosolvents and their orientation can be adjusted by the combination of different electrodes and applied voltages.[240] Since the morphology of the fibrillar conductive mat significantly impacts

its electronic properties, their conductivity can be optimized by adjusting the electrospinning solution.

Despite being a viable method for preparing conductive surfaces, electrospinning is incompatible for directly preparing fibers of doped and undoped PEDOT. This is a result of these conjugated polymers being insoluble in the solvents that are compatible with electrospinning.[241] The spinnability of conjugated polymers can be improved by using carrier polymers such as poly(vinylpyrrolidone) (PVP),[242] poly(vinyl alcohol) (PVA)[243] and poly(ethylene oxide) (PEO)[244]. However, blending these insulating polymers in the electrospinning mixture generally reduces the overall conductivity of the resulting non-woven electrospun mat. While electrospun conductive fibers are possible with carrier polymers,[21, 230] the correlation between the composition of the electrospinning solution and the resulting conductivity of the electrospun fiber mats remains relatively undefined.

In light of the critical role that PEDOT plays in enabling electronic devices, there is a need to understand the influence of the electrospinning solution composition on the fibers' conductivity. More importantly, the interplay of the electrospinning mixture composition on the conductivity behavior of PEDOT fibers as a function of fiber stretching and bending needs to be established. This knowledge is of importance for spinning conductive fibers that meet the electronic and mechanical performance requirements for their use in wearable electronic devices. We were therefore motivated to prepare conductive PEDOT:Tos fiber mats by first electrospinning fibers followed by vapor phase polymerization. Three electrospinning mixtures, composed of carrying polymers (PEO and PVP) and varying amounts of oxidant (iron tosylate), along with different spinning times were investigated towards understanding the effect of electrospinning composition on electronic properties and the stretching behavior of the resulting conductive fibers obtained by vapor phase polymerization. Conductive fibers were obtained by chemically polymerizing the monomer directly on the electrospun carrier polymer after evaporating it under vacuum. To validate the method developed for preparing fibers having suitable conductive and mechanical properties for their use in wearable electronics, the conductive mat was used in a stretchable organic electrochemical transistor (OECT). The conductivity and morphological dependency of PEDOT fibers on the electrospinning mixture composition, their stress/strain dependent conductivity and their use in a proof-of-concept stretchable transistor are herein described.

1.4 Materials and methods

1.4.1 Reagents and materials

All reagents and materials were used as received. Polyethylene oxide (PEO) (1×10^6 Da and 5×10^6 Da), imidazole, PVP (1.3×10^6 Da), 3,4-ethylenedioxythiophene (EDOT), ethanol (100%), methylene chloride (DCM), dimethyl sulfoxide (DMSO), activated carbon (Norit, chemically activated), Nafion, isopropanol and the liquid metal gallium–indium eutectic (EGaIn) were purchased from Millipore Sigma. Fe(III) tosylate in butanol (CLEVIOS C-B 54 V3) was purchased from Heraeus Electronic Materials GmbH. Polyethylene terephthalate (PET) sheets (antistatic coating on both sides, thickness ~ 175 µm) were purchased from Policrom Inc (Bensalem, PA, USA). Polydimethylsiloxane (PDMS, SylgardVR 184 Silicone Elastomer kit) was purchased from Dow Corning and processed according to a previously reported method. [145] Glass slides and cloning cylinders were purchased from Corning. Carbon paper (Spectracarb 2050A) was obtained from Fuel Cell Store, USA and the silver ink (Conductor 2, containing metallic silver, ethyl diglycol acetate and mineral salts) from Voltera.

1.4.2 Preparation of electrospinning solutions

Three different electrospinning mixtures (A, B and C) were prepared as per below. Before adding CB54 v3, all mixtures were stirred with a magnetic stirrer until the polymer was completed dissolved.

A) A 4 wt % of PEO (400 mg, 1×10^6 Da) was dissolved in DCM (7.22 mL). Afterwards, an aliquot (2.5 g) was mixed with Clevios CB54 v3 (10 g) and imidazole (271 mg).
B) A 9.4 w% PVP (230 mg, 1.3×10^6 Da) solution was prepared by dissolving the polymer in a mixture of EtOH (74 w%, 1.81 g) and DMSO (16.6 w%, 402 mg). Then Clevios CB54 v3 (20.34 g) and imidazole (552 mg) were added to the mixture.
C) As for mixture A, a 4 wt % PEO (400 mg, 5×10^6 Da) solution in DCM (7.22 mL) was prepared. An aliquot (1.5 g) of the solution was mixed with Clevios CB54 v3 (17 g), DCM (4 g), and imidazole (461 mg).

The solutions were stirred with a magnetic stirrer during 10 h at room temperature to ensure the complete dissolution of the polymer carriers (PEO and PVP).

1.4.3 Electrospinning

The electrospinning setup includes a RT-collector (Linari Engineering) equipped with a cylindrical collector connected to a high voltage power supply. The electrospinning solution was injected through a 10 mL syringe equipped with a 0.8 mm diameter needle (Linari Engineering) and the injection flux was ensured by a computer-driven pump (Spraybase) at 0.1 mL/h. The relative humidity in the electrospinning hood was maintained between 18 and 23 %. All fibers were electrospun at a 10 kV voltage with a distance of 22 cm between the needle and the collector. The collector translation speed was fixed to 20 mm/second and at 500 RPM. The spinning parameters were chosen such that fibers would exclusively be produced without any visible spray and droplets.

The process resulted in a non-woven mat of microfibers composed of the carrying polymer, imidazole, and iron tosylate. Three electrospinning times (700, 1000 and 1500 sec) were chosen to study the effect of the fiber density on the electronic properties. The fibers were spun on different substrates depending on the required measurement: poly(ethyleneterephtalate) (PET) sheets for sheet resistance and transistors measurements, carbon paper for the electrochemical characterization and poly(dimethylsiloxane) (PDMS) for the stretching tests.

1.4.4 Spin coating

Spin coating was performed with an Ossila Spincoater. The polymer mixtures used for electrospinning were diluted by a factor of 2 to allow spincoating of thin films (200 to 300 nm). Homogenous films for conductivity measurements were obtained on 25 mm^2 glass slides. For the stretching tests, the films were deposited on PDMS substrates.

1.4.5 Vapor phase polymerization

The fibers and spin coated films were subsequently transferred to a vapor phase polymerization (VPP) chamber for polymerization.

VPP of EDOT was carried out in a vacuum oven at 45 mBar and 50°C for 24 h. A petri dish containing EDOT (1 mL) was placed in the lower part of the oven and the samples to polymerize were placed on top. A color change from yellow to light blue confirmed the formation of PEDOT around the fibers and on the spincoated films (Appendix A, Figure 1). After VPP, the carrying

polymer, unreacted species, and the undesired side products were removed by soaking the polymerized fibers (or films) in a deionized water (DI) bath for 10 minutes followed by a short rinsing step with EtOH and then water. These are referred to herein as the electrospun fibers (or spincoated films).

1.4.6 Characterization of fibers and films

Optical images of the fibers were obtained with a Zeiss Imager M1 microscope equipped with an AxioCam MRm camera (Carl Zeiss). Scanning electron microscopy images were obtained after a metallization of the sample with gold for 50 seconds and using a scanning electron microscope fitted with a field emission gun (JEOL JSM7600F). Distributions of the fiber's diameters were calculated using the software ImageJ, based on SEM pictures. The thickness of the spincoated films was measured with a stylus profilometer (DektakXT Brucker). The sheet resistance was measured with a 4-point probe system (Ossila). The average value of the sheet resistance for each mixture was calculated from 5 arbitrary chosen regions per sample from 5 individual samples. Electrochemical measurements were carried out with a potentiostat (Biologic SP 300) and the data were recorded with Ec-lab software. Cyclic voltammetry was performed after bubbling N_2 in the electrolyte solution. Potentials were measured relative to an Ag wire that was used as a pseudo-reference electrode in a three-electrode setup with a platinum mesh counter electrode. The working electrodes were electrospun fibers deposited on a 25 mm^2 carbon paper. Electrical measurements were performed under ambient conditions with an electrical probe station equipped with a Keysight B2900A source measure unit controlled with a Labview software. The stretchability tests were done with a LabVIEW software-controlled tensile tester.

1.4.7 Transistor fabrication

Organic Electrochemical Transistors (OECTs) were prepared from either electrospun fibers on PET substrates or spincoated films on glass substrates. The fabrication process is schematically represented in **Figure 4-1**. Fibers or films were covered with a PET stencil mask for plasma etching to form 12 PEDOT patterns. The PET stencil masks were fabricated using a ScanNcut SDX 1200 Brother cutting machine. The patterns were 2 mm wide and 15 mm long. The samples were etched for 1 h at 100 W and 50 sccm of O_2 (Plasmionique FLR 300H). Silver electrodes 11 mm long and 2 mm wide were printed with a Voltera Circuit Printer. The activated carbon gate electrode for

aqueous gating medium was prepared using a carbon ink containing activated carbon (28mg mL^{-1}) and Nafion (1.4 mg mL^{-1}) in isopropyl alcohol. The carbon ink was drop-casted on the carbon paper (Spectracarb 2050) and subsequently heated at 60˚C for 5 h to remove solvent traces. The electrode was then confined in a glass cylinder (Φ 7 mm) that was filled with a NaCl solution (0.1 M) as the electrolyte and connected to the gate of the instrument.

Stretchable OECTs were prepared as previously reported, using a PDMS layer as the substrate instead of a PET sheet.[135] Glass cloning cylinders were replaced by PDMS wells so the gate electrode could sustain the applied strain without breaking. Similarly, the printed silver drain and source electrodes were replaced by EGaIn to further allow the device to be stretched without breaking the contacts.

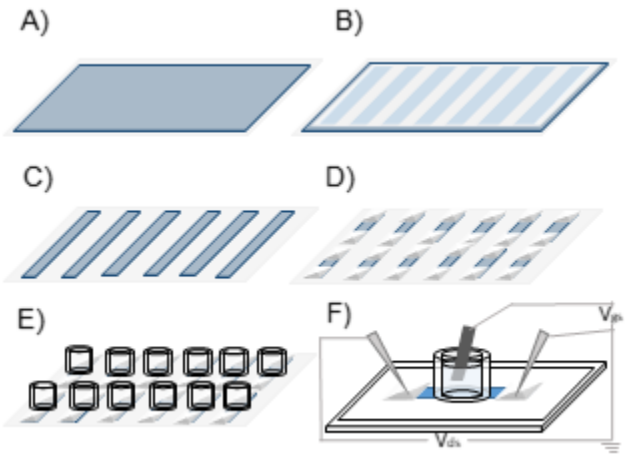

Figure 4-1. Schematic representation of the fabrication process of OECTs. **(A)** PEDOT:Tos either electrospun or spincoated; **(B)** PET stencil mask is used to cover the samples and protect unexposed areas; **(C)** plasma etching is used to remove the unprotected areas; **(D)** silver source-drain electrodes are printed at both extremities of the patterns; **(E)** cloning cylinder are used to confine the electrolyte at the center of the device; **(F)** activated carbon gate electrode is inserted into the glass cylinder and tungsten probes are used to connect the source and drain electrodes to the measuring unit.

1.5 Results and discussion

1.5.1 Morphology of Electrospun Fibers

Fibers were prepared by electrospinning either the PEO or the PVP solutions, as per Table 1. These polymers were chosen because they are ideal carriers for combined electrospinning and vapor phase polymerization of PEDOT. [145, 245] The concentration of the polymers was kept below 1 wt% because a low concentration permits to obtain fibers with a smaller diameter, which are expected to ensure consistent conductivity upon an applied strain. In contrast, fibers with larger diameters were expected to suffer from an undesired decrease in conductivity with applied stress/strain. Clevios CB54-V3 was used as the main component of the mixture to enrich the carrier polymer in the oxidant, thus providing a sufficient number of polymerization sites during VPP. Imidazole was added with a ratio of 0.5% mole relative to the iron tosylate to prevent acidic side-reactions that can arise from the two protons that are formed per degree of polymerization.[246] Two molecular weights of PEO were chosen in part because of their commercial availability. The two chosen molecular weights of PEO are known to form continuous fibers, while being consistent with the molecular weight of the extremely hygroscopic PVP that was also used in the study. The benefit of PEO is that it can be dissolved in minimal amounts of solvent, unlike PVP, resulting in spinning solutions with low viscosities. With the higher molecular weight of PEO, its amount in the electrospinning mixture could be reduced to 0.3 w% without compromising its spinnability. The solvent viscosity can be adjusted varying either the amount of solvent or polymer content, providing the means to control the diameter of the electrospun fibers.

The SEM images revealed a difference in the fiber morphology contingent on the electrospinning composition. Qualitative differences in the fibers obtained from the two PEO mixtures are evident in **Figure 4-2A**) and **C**). The Mixture B produced homogeneous fibers, whereas those produced from Mixture A are heterogenous. Indeed, both fine needle and bulb-like regions are formed on the same fibers along with the fibers having different thicknesses. Such is the case where multiple fibers of different diameter intersect. The resulting multiple bulb-like crossing points skew the mean average calculated diameter. This aside, randomly orientated fibers that are well-formed on the PET substrate (**Figure 4-2**) were observed regardless of the electrospinning mixture.

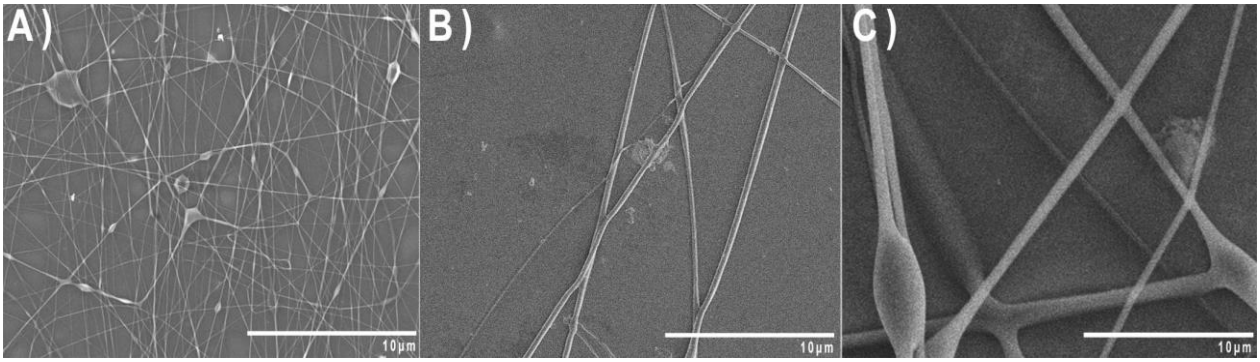

Figure 4-2. SEM pictures of the fibers from the mixtures A **(A)**, B **(B)** and C **(C)** after 700 seconds of electrospinning.

Table 1. Composition of the electrospinning mixtures used to prepare fibrillar mats.

Solutions	Polymer	Carrier Polymer (wt %)	Solvent (wt %)	Clevios CB54-V3 (wt %)	Imidazole (wt %)
A	PEO (1×10^6 Da)	0.8	19.2 (DCM)	77.0	3.0
B	PVP (1.3×10^6 Da)	1.0	9.5 (7.8 EtOH and 1.7 DMSO)	86.5	3.1
C	PEO (5×10^6 Da)	0.3	23.7 (DCM)	74.0	2.0

The different molecular weight of the carrying polymer in mixtures A and C led to distinct fiber's diameters. The diameter of the as-produced fibers was larger with the higher molecular weight of PEO in Mixture C. This is a result of its increased intrinsic viscosity relative to Mixture A, according to the Mark-Houwink relationship.[247] The diameter distribution of the fibers produced from Mixture A was bimodal, centered around 300 with a shoulder at 650 nm. In contrast, the diameter distribution from Mixture C had a typical Gaussian distribution with a maximum diameter around 2000 nm (**Figure 4-3**). The fibers from mixture B were consistent with those from Mixture

A, but with a broader distribution. There was also a difference in the ratio of the two dominant diameter distributions: 2:1 for A and 1:1 for B for the diameters centered at 264 and 616 nm on the one hand and 396 and 748 nm on the other hand.

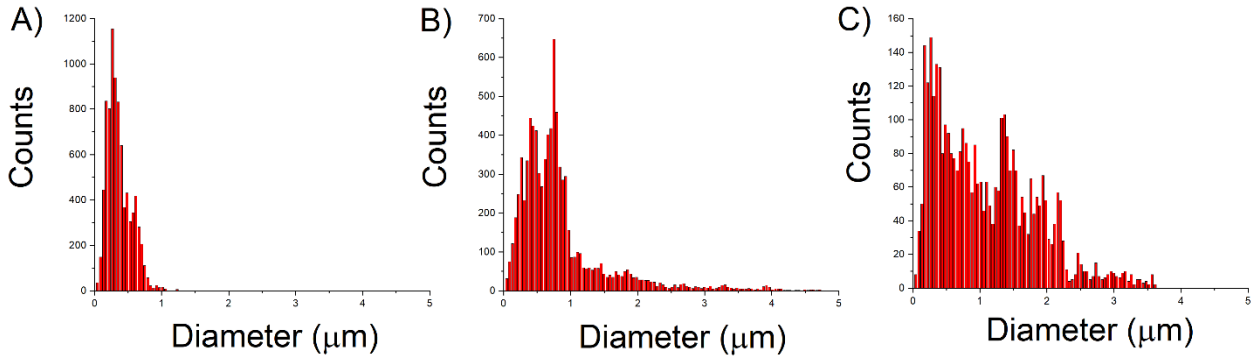

Figure 4-3. Fiber diameter distribution of electrospun mixtures A **(A)**, B **(B)** and C **(C)** using 700 seconds electrospinning time obtained from SEM images.

1.5.2 Electrical properties

The electrical properties of the fibers were evaluated in terms of sheet resistance rather than conductivity, due to the difficulty to define the sample thickness. The effect of electrospinning time along with the composition of the spinning mixtures on the fibers' sheet resistance was evaluated. The sheet resistance was found to decrease with increasing electrospinning time (Table 2). This was expected, due to the higher substrate coverage and the higher number of fiber junctions formed with longer spinning times. There is nearly a twofold decrease in the sheet resistance when increase the spinning time from 700 s to 1000 s, while no improvements were observed increasing the spinning time to 1500 s. This implies the minimum number of junctions that is required to reach the intrinsic conductivity limit of the fibers is formed at 1000 s. These values are consistent with those reported in the literature for different PEDOT electrospun fibers.[238, 248-250] There was no significant difference in the sheet resistance between the longitudinal and transversal electrospinning direction. Assuming the electronic percolation between the chains at their crossing junction is the transport limiting process in the fibers, the consistent conductivity implies a large number of fiber junctions.

Table 2. Sheet resistances of the electrospun randomly oriented fibers non-woven for three different electrospinning times.

	Sheet resistance of electrospun fibers[2] (Ω/sq)		
Electrospinning time (sec)	**Mixture A[1]**	**Mixture B**	**Mixture C**
700	$30.7 \times 10^3 \pm 19$	$124.3 \times 10^3 \pm 11$	$18.6 \times 10^3 \pm 92$
1000	$12.8 \times 10^3 \pm 16$	$83.1 \times 10^3 \pm 17$	$17.0 \times 10^3 \pm 45$
1500	$10.2 \times 10^3 \pm 56$	$38.3 \times 10^3 \pm 43$	$7.9 \times 10^3 \pm 17$

[1]Errors are given from the range and the correction factor used for each measurement and these were averaged for the five sampled areas.

While the sheet resistance of fibers obtained from mixture A and C were similar, that of fibers obtained from mixture B was remarkably larger. This can in part be attributed to the morphological differences of the fibers. The fibers spun from PEO had fused junctions and they adopted a 2D arrangement, in contrast to the PVP spun fibers that were superimposed. The PVP fibers were stacked and a 3D arrangement was maintained where the fibers intersected. This topology was further expected to enhance the mechanical properties (vide infra).

Conductivity measurements were carried out on samples spincoated from the same mixtures having a similar thickness (ca. 200 nm). As per Table 3, the homogeneously smooth spincoated films have consistent conductivities ranging from ~200 to ~250 Scm^{-1}. The measured sheet resistances were similar to those of the fibers electrospun for 1000 and 15000 sec in the case of the Mixtures A and C. The fibers produced from the Mixture B showed a higher sheet resistance versus the spincoated

films. The great similarity of the sheet resistances in the case of the spincoated samples indicates the typical morphology of the fibers from the Mixture B is responsible of the diminution of the conductivity in the fiber mat.

Table 3. Conductivities and sheet resistances of spincoated films from the three different electrospinning mixtures.

	Mixture A	**Mixture B**	**Mixture C**
Conductivity (S/cm)	268 ± 0.56	246 ±0.31	207 ± 0.32
Sheet Resistance (Ω/sq)	$18.6\times10^3 \pm 56$	$20.3\times10^3 \pm 31$	$24.2\times10^3 \pm 32$

1.5.3 Electrochemistry

The electrospun fibers were further assessed by cyclic voltammetry. This was to evaluate the effect of the spinning time and the polymer carrier on the electrochemical properties of the fibers. More specifically, the quantity of charge transferred with an applied potential, and hence the doping/dedoping capacity of the fiber, can be assessed from the area of a potential vs. current voltammogram. Large areas of the voltammogram are indicative of greater doping/dedoping. Since the spinning time affects the number of fibers that are deposited on the surface along with the number of fiber junctions, the area of the voltammograms depends on the spinning time. The integrated area of the voltammogram for the fibers prepared from the mixture A was indeed greater than the other two mixtures (**Figure 4-4**). The relative order of the integrated areas was further consistent with the measured sheet resistance, confirming the higher density of fibers and the enhanced conductivity of the electrospun mat.

The absence of a well-defined redox process in the cyclic voltammograms confirms the nonexistence of a discrete electron transfer process. It further implies that charge transfer processes

take place over a broad range of potentials. This is consistent with a double-layer capacitance in an electrical double layer, common to the three spinning mixtures.[251, 252] Meanwhile, the symmetry of the voltammograms confirms that the fibers can be reversibly doped and undoped with an applied potential with minimal loss of charge. This is a required behavior for use in OECT.[253] The conjugated organic components of OECTs make them suitable for use in both in vivo and in vitro bioelectronics. Similar to other plastic electronics, the mechanical properties of OECTs can be tailored by the judicious choice of the substrate that is used for their fabrication.

A key electrochemical parameter for assessing the suitability of the fibers for used in OECT is their specific capacitance. This can be calculated by integrating the voltammogram, providing the weight of active material is accurately known. Unfortunately, variabilities in the fabrication preclude accurately quantifying the amount of the deposited spun fibers. However, we can calculate an estimated amount of PEDOT:Tos fiber deposited on the carbon paper using the electrospinning flow rate, the density of the PEDOT and the surface of the carbon paper used for electrochemical measurements. Given the conductive mats were prepared using similar parameters, the quantity of the fibers deposited for each mixture for the specific electrospinning time is understood to be consistent. The estimated specific capacitance of the samples A, B and C is of 38.94, 12.60 and 25.04 F/g respectively Further details on the calculations can be found in the supporting information. The specific capacitance of the fibers from the mixture A is greater than the other mixtures. This behavior can be ascribed to two factors. On one hand, there are more fiber junctions for sample A compared to the other samples. This results in the fiber's better overall conductivity and its smaller sheet resistance. On the other hand, the fibers from Sample A have the smallest diameter relative to the other samples. This affords them a higher specific area and hence a greater electroactive surface area, collectively contributing to its greater capacitance.

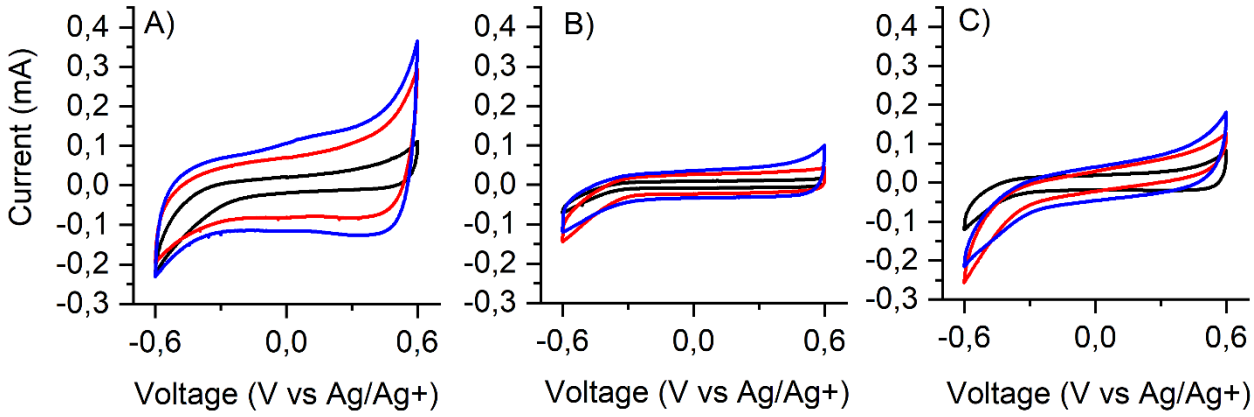

Figure 4-4. Cyclic voltammograms of Mixtures A, B and C in aqueous NaCl (0.1 M) at a scan rate of 20 mV/s for different electrospinning times: 700 (—), 1000 (—) and 1500 sec (—).

1.5.4 Electromechanical testing

Our electrospun fibers were evaluated to see whether they had a similar behavior, which would make them suitable for stretchable transistors. This was done by monitoring their current during consecutive stretching cycles. The current as a function of applied strain for the three mixtures and for the three electrospinning times were measured. The fibers obtained from 1500 s of electrospinning showed the highest current, consistent with the sheet resistance measurements. All the three samples could undergo at least 80% of strain without significant changes in their sheet resistance. Remarkably, the fibers prepared from Mixture B could be stretched upwards of 140% strain, courtesy of its nodeless morphology. This allows most of the fibers to freely glide upon applied strain without breaking. At this stretching level, the sheet resistance decreased by only ~15%. (**Figure 4-5B**). The limited current loss of this sample with strain nonetheless makes it a promising candidate for use in stretchable electronic devices. We previously reported a similar mixture to afford fibers that could be stretched beyond the stretching limit of PDMS (160%) while retaining 15-20% of the initial current.[145] Cycling tests of stretching and destretching also showed a current retention about 50% of the initial current and a stabilization of the signal after only 30 cycles. Also, Shaker et al. reported a high current retention at 40% strain of PEDOT:PSS fibers that were prepared by wet electrospinning on a polyurethane matrix.[254]

The capacity of the fibers to rearrange and dissipate the strain when stretched were qualitatively evaluated from the pictures that were taken with different applied strains (Figure S2 (A) to (C)). The images show the fibers are progressively damaged (Figure S2 (D) to (G)) when stretched. The onset of the fiber damage for Mixture B occurred at ~40% strain at which point the fibers lost their linear shape and they curled. No cracks were observed within the fibers from the mixture B, even with ~120% strain. This is in contrast with the samples that spincoated on PDMS, which cracked at lower applied strains (white clusters Figure S2 (F)).

To validate the enhanced stretching capacity of the electrospun samples, their performance was compared to the three mixtures that were spincoated on PDMS. For this, the PDMS was pre-strained to 30% and the samples were then subsequently spincoated. [16] These films adopted a wavy shape when the substrate returned to its normal shape after the applied strain. The spincoated films on PDMS that were not pre-strained broke below 10% strain (Figure S3), mainly due to the rigid structure of the PEDOT chains that prevents them from reorganizing and absorbing the strain when stretched. In contrast, the samples that were prepared on pre-strained PDMS could sustain the five stretching cycles at 20% strain but broke at 30% strain, owing to their buckling.

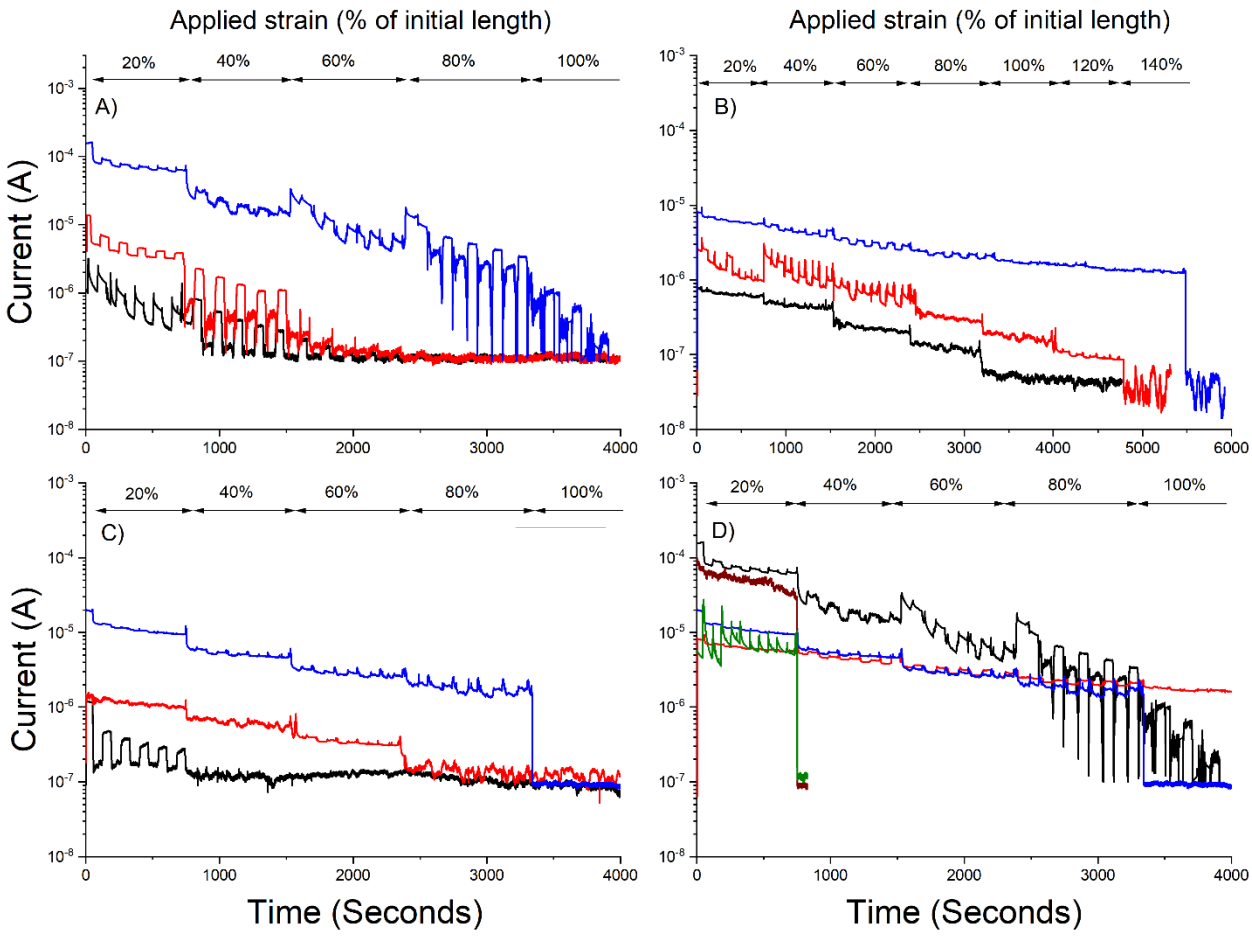

Figure 4-5. Current as a function of time for PEDOT:Tos fibers : Mixtures A **(A)**, B **(B)** and C **(C)** on PDMS with different electrospinning times: 700 (—), 1000 (—) and 1500 sec (—).**(D)** Current vs time for electrosposun samples: Mixtures A (—), B (—) and C (—) for 1500 sec and spincoated samples on pre-strained PDMS : Mixtures A (—) and B (—). The samples were stretched between 20% and 100% strain at 0.1 cm/s. Five consecutive stretching/release cycles were done for each strain between 20% and 100%. The samples were kept in each state (stretched or released) for a resting time of 1 minute.

This aside, the PEDOT fibers produced from the three Mixtures could be stretched up to a minimum of 60% strain. The consistent current between the electrospun (1500 s of electrospinning) and spincoated samples (**Figure 4-5D**) confirms that the fiber shape, which is underpinned by the electrospinning process, does not affect the intrinsic electronic properties of PEDOT. The fibers

can sustain mechanical deformation under strain because they can reorganize their structure with strain, unlike spincoated films. More importantly, both the mechanical and electronic properties of the final material can be tuned by adjusting the number of fused junctions in a fiber mat.

1.5.5 Organic Electrochemical Transistors (OECTs)

OECTs were fabricated from both electrospun (**Figure 4-6**) and spincoated samples (**Figure 4-7**). The output and transfer characteristics of the as-prepared OECTs showed the typical p-type behavior of PEDOT OECTs operating in depletion mode. Electrospun OECTs prepared from the mixture A showed the best performances. Transistors prepared from spincoated PEDOT showed similar performances to the electrospun fibers, but with higher ON/OFF ratios (~ 45). This is consistent with a uniform and similar film morphology that is adopted over the entire surface of the device. In contrast, the fibers adopted unique morphologies that were highly dependent on the composition of the spinning solution and the spinning time. The larger ON/OFF ratios that were observed for the thin spincoated films can be ascribed to the larger contact area of the polymer with the gating medium between the source and the drain terminals compared to the fibers. However, as shown below, the spin coated devices have limited strain performance with respect to fibers.

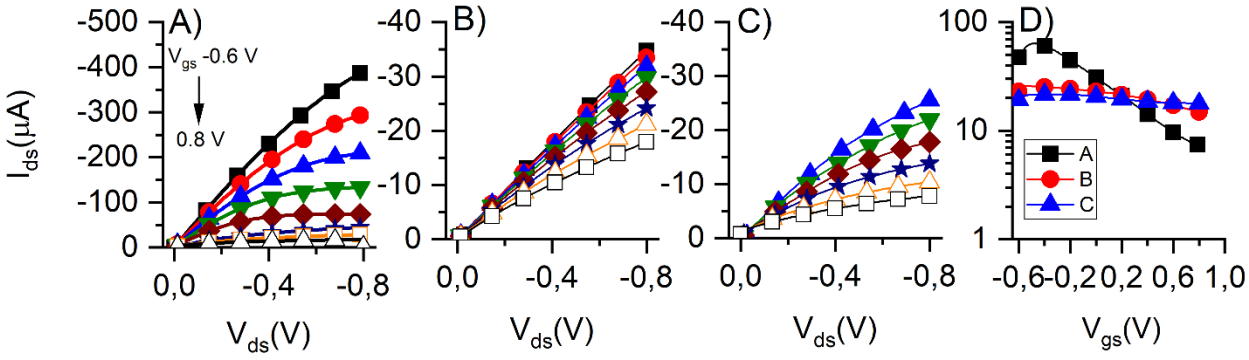

Figure 4-6. Output curves of transistors of Mixtures A **(A)**, B **(B)** and C **(C)** prepared by 1500 sec electrospinning and an applied gate voltage: -0.6 (■), -0.4 (●), -0.2 (▲), 0 (▼), 0.2 (◆), 0.4 (★), 0.6 (□), and 0.8 (△) V, at a sweep rate of 60 sec. **(D)** Transfer curves of transistors of Mixtures A (■), B (●) C (▲) prepared by 1500 sec electrospinning at a V_{DS} of -0.6 V. For visual acuity: the solid lines connect every measured data point and the symbols are drawn at every fifth data point.

Fibers produced from the mixture B showed the best results during the stretching tests while the ones produced from A led to higher currents, making both of them promising for use in stretchable transistors. Transistors were successively strained in 10% increments and both their transfer characteristics were subsequently recorded (**Figure 4-8**).

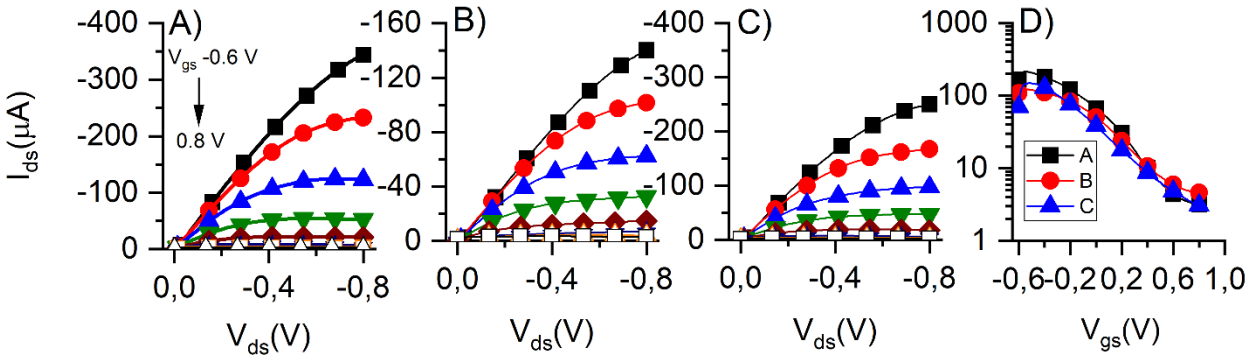

Figure 4-7. Output curves of the transistors of Mixtures A **(A)**, B **(B)** and C **(C)** prepared by spincoating and an applied gate voltage: -0.6 (■), -0.4 (●), -0.2 (▲), 0 (▼), 0.2 (◆), 0.4 (★), 0.6 (□), and 0.8 (△) V, at a sweep rate of 60 sec. **(D)** Transfer curves of the transistors of Mixtures A (■), B (●) C (▲) prepared by spincoating at a V_{DS} of -0.6 V. For visual acuity: the solid lines connect every measured data point and the symbols are drawn at every fifth data point.

The transistors prepared from the mixture A ceased to work beyond 30% strain, while those from Mixture B functioned up to 50% strain. The OECTs fabricated from Mixture A had ON/OFF ratios that were about 10-fold greater than the devices prepared from Mixture B. Overall, the performance of the transistors prepared from Mixture B was less sensitive to the strain. This is a result of the greater degree of freedom of the fibers and the reduced number of fiber junctions for B relative to A. These distinct features stem from the different fiber morphology that is adopted by the two carrier polymers and from the different density and the number of fused junctions. Indeed, the conductivity of the resulting mat correlates with the number of fused fibers, which in turn, affords more electronic pathways. The tradeoff to this morphology is a reduced elongation at break because the fibers cannot contiguously slide and rearrange without breaking an electronic junction.

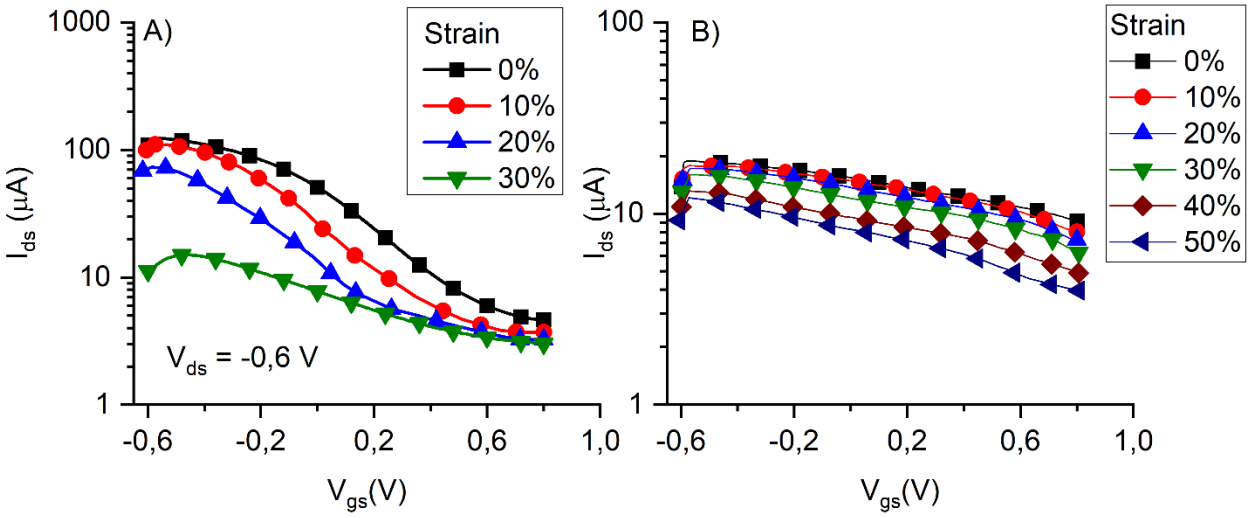

Figure 4-8. Transfer curves of a transistor of Mixtures A **(A)** and B **(B)** prepared by electrospinning under different strain : 0% (—), 10% (—), 20% (—), 30% (—), 40% (—) and 50% (—), at a V_{DS} of -0.6 V.

1.6 Conclusions and perspectives

Three electrospinning mixtures were prepared to investigate the impact of their composition on the morphology and the electrical properties of the resulting conductive PEDOT:Tos fibers. Conductive fibers were successfully prepared by the vapor phase polymerization of EDOT on the electrospun carrier fibers. The composition of the electrospinning solution and the spinning time led to distinct differences in both the distribution of the diameter and the number of junctions of the conductive fibers. Fibers with a smaller diameter distribution and a greater number of fused fiber junctions were the most conductive. A conjugated polymer can be considered as a blend of metallic-like grains embedded in a disordered and non-conductive environment. A smaller fiber diameter implies a more densely packed polymer and a higher degree of order of the polymer chains, leading to a diminution of probability of occurrence of defaults compared to a larger diameter.[255] Hence electrons are less trapped and can contribute to the conductivity. These fibers also had the greatest specific capacitance owing to their larger specific electroactive area. The electrospun conductive fibers had enhanced stretchable and conductive properties compared to spin coated thin films of PEDOT:Tos. Indeed, the conductivity of the fibers decreased by only 16%

when stretched to 140% in length. This is due to their capacity to reorganize their structure with strain. The fibers could also be used in stretchable OECTs. Devices prepared from the fibers acted as OECTs under successive strains from 0 to 50%. Our results illustrate that conductive wires for use in stretchable electronics can be prepared from straightforward methods. By controlling the fiber morphology and their junction density, possible by readily tuning parameters such as polymer carrier and spinning time, stretchable electrodes having consistent conductivities when stretched can potentially be fabricated.

1.6.1 Conflict of interest

The authors declare that the research was conducted in the absence of any commercial or financial relationships that could be construed as a potential conflict of interest.

1.6.2 Acknowledgements

The Natural Science and Engineering Council Canada (NSERC) is acknowledged for Discovery Grants awarded to FC and WS that enabled this collaborative research. Equipment and infrastructure used for this research were acquired and maintained by the Canada Foundation for Innovation and Quebec Strategic Networks (CQMF-QCAM, RQMP, and GCM). This work is supported by Defence Research and Development Canada through an IDEaS Micronet (CFPMN1-008) grant awarded to F.C.

CHAPTER 5 ARTICLE 2: AN INTRINSICALLY STRETCHABLE AND BENDABLE ELECTROCHROMIC DEVICE

This article was submitted to the journal "IOP Nanotechnology" on 2021-12-07. This article reports the fabrication of stretchable ECDs from fiber mats of PEDOT:PSS. The fibers were produced from a commercially available PEDOT:PSS dispersion in water with PEO as a supporting polymer. PEDOT:PSS fiber mats were used as transparent and stretchable electrodes in the electrochromic device fabrication. As-prepared devices were shown to be able to be stretched up to 150% strain while being reversibly switched between their ON and OFF states. The supporting information for this article is reprinted in Appendix B of this thesis.

1.1 Authors

Michael Lerond[1], Anthony Raj Mohan Raj[2], Veronica Wu[2], W. G. Skene[2]*, Fabio Cicoira,[1]*

1 Department of Chemical Engineering, Polytechnique Montréal, Montréal, QC, Canada

2 Département de chimie, Université de Montréal, Montréal, QC, Canada

E-mail: fabio.cicoira@polymtl.ca

w.skene@umontreal.ca

Submitted : 2021-12-16

1.2 Abstract

Stretchable electrochromic devices were fabricated from electrospun PEDOT:PSS (poly(3,4-ethylenedioxythiophene):polystyrene sulfonate) fibers. Stretchable and transparent electrodes with a sheet resistance of 1200 Ω/sq were prepared by depositing the conductive fibers on elastomeric substrates that were prepared from polydimethylsiloxane. The conductive substrates replaced the ITO coated glass electrodes that are typically used in electrochromic devices. The functioning device was prepared from a flexible chitosan electrolytic gel and a 4,7-bis(4-diphenylaminophenyl)-2,1,3-benzothiaziazole (TPA-BZT-TPA) electrochrome that were

deposited on the stretchable transparent electrodes. The assembled device could be stretched to 150% its original length and bent to a curvature of 0.1. The device could be operated and switched between its yellow (off) and blue (on) states while being stretched and bent with a maximum contrast $\Delta T \approx 30\%$ at 805 nm and a coloration efficiency of 168 cm^2/C. The stretchable device had an electrochromic contrast that was 30% greater than its counterpart that was prepared from conventional ITO-glass electrodes. The critical composition required for making devices truly stretchable was possible by evaluating the performance of five types of devices consisting of different layers.

Keywords: Stretchable transparent electrodes, Stretchable electronics, Stretchable electrochromic device, Electrospinning, Poly(ethylenedioxythiophene) (PEDOT)

1.3 Introduction

The first electrochromic device (ECD) was reported in 1969, when it was discovered that thin films of WO_3 reversibly changed color.[162] Since the original transparent-to-blue color switching discovery, ECDs have morphed to span the entire visible spectrum and extend to the NIR region. The extended palette of colors and the visible tunability is curtesy of conjugated organic polymers whose energy gap can be tailored.[256] ECDs also have low power consumption requirements with the added benefit of using low cost components for their fabrication.[257] The visible color changes with applied potential have found uses in smart windows,[184] optical shutters, and optical display technology.[185]

ECDs require transparent electrodes. These are typically enabled by ITO that is coated on rigid substrates. While this transparent metallic oxide meets the electrical conductance requirement for its use in devices, it represents a significant portion of the fabrication cost of ECDs. Moreover, the limited flexibility of ITO precludes its use in truly stretchable applications. In fact, ITO is restricted to low radii of curvature that are possible with rollable substrates such as polyethylene terephthalate (PET).[36, 258] The mechanical properties of conductive coatings must mimic those of the substrates on which they are coated for their use as stretchable electrodes. The conductivity of the coating also must not be affected with mechanical deformation with stress and strain forces that occur when the electrode is stretched. Nanoscale and fibrillar wires are suitable morphologies for enabling stretchable electrodes. This is owing to their interchain slippage that can absorb applied

stresses and strains without breaking the contiguous contacts that are required for electronic mobility. The scalable processing of organic polymers makes them ideal choices for preparing conductive fibers. This attribute further contributes to lowering the fabrication cost of electronic devices compared to their ITO counterparts. Indeed, transparent polymeric electrodes were originally prepared from polyaniline and used in OLEDs.[259] This conductive material in transparent electrodes has been surpassed by PEDOT:PSS owing to its higher conductivity,[260-264] greater chemical stability,[265] and its biocompatibility compared to polyaniline.[266] This is evidenced in solar cells that take advantage of the transparent conductive electrode.[267-270] The added benefit of fabricating electronic devices exclusively from organic materials might be their straightforward disposal by pyrolysis. This contrasts with their metal containing counterparts that require additional care when discarded to ensure the ecologically deleterious metals are not released into the environment.

An electrochromic device fabricated exclusively from polymers was first developed by Reynolds et al.[271] Despite this advancement, the field has remained reliant on ITO electrodes to enable electrochromic devices. Therefore, truly stretchable and bendable electrochromic devices remain elusive. Recently, both electrodes of a functioning electrochromic device were prepared from PEDOT:PSS spincoated on a plastic substrate. Furthermore, a stretchable all-polymer electrochromic device was fabricated by Kim *et al*,[183] who used interlaced networks of poly(ethylene glycol) and PEDOT:PSS. In this example, the conjugated polymer served as both the electrode and color switching material. This device had a strong mechanical cycling stability and it could be stretched upwards of 200% from its resting state. However, it was limited to monochromatic changes, switching exclusivley between dark and light shades of blue.

The demand for stretchable electronic devices has increased over the years[272] because of their use in wearable electronics,[273, 274] robotic skins,[275, 276] and healthcare devices.[277, 278] Stretchable organic electronics offer the advantage of being biocompatible, easily processed, and less expensive compared to their inorganic counterparts. While LEDs are the most used technology for displays in wearable devices, their operation consumes constant power. In contrast, an ECD requires an applied bias to switch between its on and off states. It therefore consumes less power than LEDs. The use of complementary ion storage layers further reduces the power consumption,

since an applied potential is required only to switch the device between the on and off states. The color of the on state once it is switched is maintained by the ion storage layer.

The electrospinning of PEDOT:PSS fibers has been extensively studied.[245, 249, 279-281] It is now a mature field where the upscaling of PEDOT:PSS fibers and the preparation of large area conductive surfaces are common knowledge. The advantage of electrospun PEDOT:PSS fibers relative to their contiguous thin film counterparts that are prepared by spin coating is the consistent conductivity of surfaces with stretching and bending. Indeed, conductive PEDOT:tosylate fibers that can reorganize their structure with applied strain have enabled stretchable organic electrochemical transistors (OECTs).[282]

Herein, we demonstrate that the rearrangement of electrospun conductive fibers under applied strain and stress without breaking can be exploited to prepare stretchable electrodes for use in electrochromic devices. These electrodes have the advantage of overcoming the monochromatic limitation of stretchable ECDs by expanding the perceived color change when used with a conjugated colored electrochorme. The functioning ECDs fabricated exclusively from organic materials have the benefit of undergoing reversible color changes that are perceivable by the user. Towards developing truly stretchable and bendable electrochromic devices, electrodes that maintain their intrinsic conductivity with mechanical deformation were prepared from inexpensive polydimethylsiloxane (PDMS) substrates. The stretchable and biocompatible supports were rendered conductive by electrospinning PEDOT:PSS fibers. The electrolyte required for electrochromic device operation, was additionally prepared from stretchable chitosan.[283] Complementary mechanical deformation of the electrolyte layer with applied stress and strain when sandwiched between the two electrodes is key to ensuring the continuous operation of the device when it is reversibly stretched. This behavior prevents irreversible sheering between the different device layers. The added benefits of the chitosan electrolyte film are its biocompatibility and sustainable resourcing. Its use in electrochromic devices therefore improves the ecological fabrication footprint of the plastic electronics. Meanwhile, a conjugated molecular electrochrome (TPA-BZT-TPA; Figure S1) was chosen for its mechanical compatibility with the flexible surfaces, while its intrinsic color is visually different than that of the PEDOT:PSS electrodes. When the device is operating, the yellow to blue color changes originating from the electrochrome can readily be distinguished from those of the stretchable electrodes. The intrinsic color of the stretchable

electrodes was used to evaluate both their mechanical and their electronic performance with applied stress/strain. The overall performance of the electrochromic device upon stretching and bending are herein presented. This proof-of-concept device demonstrates that inexpensive materials can be used to replace otherwise costly transparent ITO electrodes in electrochromic devices, while also making the color switching devices truly stretchable and bendable.

1.4 Experimental

1.4.1 Reagents and materials

All reagents and materials were used as received. Polyethylene oxide (PEO) (1×10^6 Da), 4,7-dibromobenzo[c][1,2,5]thiadiazole, 4-(diphenylamino)-phenyl boronic acid, K2CO3, Pd(PPh3)4, chitosan (low molecular weight), acetic acid, magnesium acetate, glycerol, ethanol (100%), tetrahydrofuran (THF), and dimethyl formamide (DMF) were purchased from Millipore Sigma. The PEDOT:PSS aqueous suspension (CLEVIOS PH 1000 S) was purchased from Heraeus Electronic Materials GmbH. Poly(dimethylsiloxane) (PDMS, SylgardVR 184 Silicone Elastomer kit) was purchased from Dow Corning and it was processed according to a previously reported method.[145] 4,7-Bis(4-diphenylaminophenyl)-2,1,3-benzothiaziazole (TPA-BZT-TPA) was synthesized according to known means.[284]

1.4.2 Electrospinning

The electrospinning solution was prepared by dissolving PEO (167 mg) in a mixture of Clevios PH1000 (9.30 g) and DMF (533 mg) by magnetic stirring for 24h. The critical chain overlap concentration of 0.167% of PEO was calculated according to Equations S1 and S2. The chain entanglement concentration (Ce) of PEO to produce fibers by electrospinning can be estimated by [C]x[η]>10.[285] The PEO electrospinning concentration was set to Ce = 10 x C = 1.67 w%. DMF was chosen as a co-solvent because it increases the charge density and it reduces the surface tension in the polymer mixture. These effects collectively give thinner electrospun fibers.[285] The amount of carrying polymer was minimized to have the smallest diameter possible of the electrospun fibers, according to the Mark-Houwink-Sakurada equation.[286] The electrospinning setup included a RT-collector (Linari Engineering) equipped with a cylindrical collector that was connected to a

high voltage power supply. The electrospinning solution was injected through a 10 mL syringe that was equipped with a 0.8 mm diameter needle. The injection flow was regulated and maintained at 1.0 mL/h by a computer-driven pump (Spraybase). The relative humidity in the electrospinning hood was maintained between 20 and 26 %. All fibers were electrospun with a 9 kV voltage with a 10 cm separation between the needle and the collector. The collector translation speed was fixed at 20 mm/second and 300 RPM. These parameters produced exclusively fibers with no visible droplets. The process resulted in a non-woven mat of microfibers that were composed of the carrying polymer and PEDOT:PSS on the given substrates.

1.4.3 Device fabrication

The PDMS substrates were prepared with a commercial kit that was added to a Teflon mold and cured at 90° C for 30 minutes. PEDOT:PSS fibers were electrospun for 4000 seconds on a large area PDMS film (10 cm x 14 cm x 300 μm). The fiber mat was soaked in ethanol for 10 min to remove the carrying polymer. The substrate was then cut with a razor blade to the desired dimensions: 2.5 cm x 2.5 cm for the spectroscopic and spectroelectrochemical studies, and 3 cm x 2.5 cm for bending/stretching tests. A piece of copper tape was fixed to each PDMS substrate to which were affixed the electrical alligator connections for electrochemical measurements.

The electrolyte gel was prepared from 1 wt% chitosan solution in acetic acid, glycerol, and magnesium acetate (42:30:28 wt %) according to a previous method.[283] The salt preserves electroneutrality of the elecrochrome device during operation, while the gel contributes to the structural integrity of the solid state device. A volume (500 μL) of the electrolyte solution was dropcasted on the electrospun PEDOT:PSS layer on a PDMS substrate and was gelled by evaporating the solvent at 80°C for 2h to afford the counter electrode (CE). The working electrode (WE) was prepared by spray coating (Aztec Airbrush) a THF solution (10 mg/mL) of TPA-BZT-TPA. Spraycoating was chosen instead of spincoating because this coating method is amenable to upscaling large area ECD devices. The ECD was fabricated by sandwiching the CE and WE together (**Figure 5-1**). The device was then sealed with PDMS to ensure its mechanical integrity and prevent the electrodes from separating under applied strain and stress. Copper tape was fixed to the electrodes for the easy connection of the device to the potentiostat via alligator clips. The applied potential used to drive the devices was relative to the CE. Five devices consisting of

different layers were fabricated according to the following: (D1) ITO/CEG/PPF/PDMS (reference device); (D2) ITO/CEG/TPA-BZT-TPA/PPF/PDMS (semi-flexible device); (D3) PDMS/PPF/CEG/TPA-BZT-TPA/PPF/PDMS (fully stretchable device); (D4) ITO/CEG/TPA-BZT-TPA/ITO (rigid device), and (D5) PDMS/PPF/CEG/PPF/PDMS (stretchable reference device). CEG is the chitosan electrolytic gel and PPF is the PEDOT:PSS conductive fibers. The schematic representation of the devices is given in Figure S1.

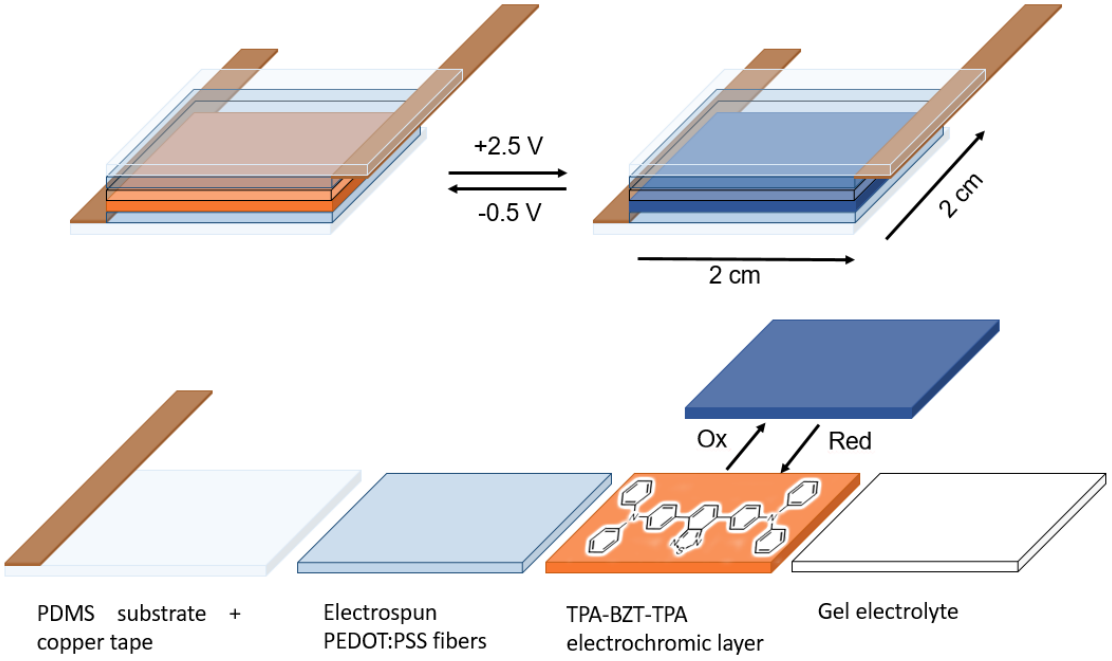

Figure 5-1. Schematic representation of the fabrication of a fully stretchable electrochromic device.

1.4.4 Characterization of fibers and films

Scanning electron microscopy images were obtained after metallization of the samples with gold using a scanning electron microscope fitted with a field emission gun (JEOL JSM7600F). Distribution of the fiber's diameters from the SEM pictures was evaluated using the software ImageJ (National Institute of Health). The sheet resistance was measured with a 4-point probe system (Ossila). Absorption spectra were measured with a UV-vis-NIR spectrometer (Cary 5000 Varian). For the spectroelectrochemical measurements, the electrochromic device was placed in the spectrometer and its electrodes were connected to the potentiostat (Biologic SP300). The

change in the absorption spectra was monitored as function of applied potential. The change in transmittance percent at a given wavelength when switching the applied potential overtime was also monitored. The potentials were switched between +2.5 and -0.5 V at 40 second intervals. The baseline of 100% transmittance at the redox state's absorption wavelength (952 nm for the reference device and 805 nm for the fully stretchable device) was mathematically adjusted to be consistent over extended times. The mathematical correction adjusted the baseline of the switching data, while the relative transmittance difference between the neutral and oxidized states was unaltered. Chronoamperometric response measurements were carried out with a potentiostat (Biologic SP 150) during the coloration/bleaching processes of the devices under mechanical deformation. The data were recorded with Ec-lab software. Bending of the devices was done using 10 and 20 mm radii curved gauges. Defining the curvature as the reciprocal of its radius, the 10 and 20 mm gauges correspond to be of 0.1 and 0.05 curvatures, respectively. The colour forming/bleaching cycles were done by applying either a constant positive or negative voltage bias when the devices were bent. Device stretching was done by immobilizing one side of the device with tape and by manually pulling on the other side to reach the desired strain percentage. A constant bias was applied to bleach the color while the devices were stretched and their chronoamperometric responses under different strains were recorded.

1.5 Results and Discussion:

1.5.1 Conductive fibers

Both the morphology of the electrospun fibers on the substrate and their diameter underpin the overall conductivity of the electrode. The diameter also affects the conductivity when the substrate is stressed. Highly entangled and thick fibers have high conductivities. However, the high degree of chain entanglement of the fibers limits their mobility. They cannot absorb the strain and the junctions between the fibers disconnect when stretched. This results in an irreversible decrease in the conductivity. In contrast, the electronic percolation network is maintained in small diameter fibers, even when stretched. This results in consistent conductivity with stretching and bending. Relatively thin diameter PEDOT:PSS fibers are therefore desired to ensure that electrodes maintain their electrical conductivity with the applied strain. Thin PEDOT:PSS fibers are also desired when

they are used as the electrode material in electrochromic devices. This is to minimize their contribution to the perceived color when the device is operating owing to their intrinsically high absorption that spans the entire visible and NIR spectrum (vide infra).

To limit the electrochromic device color contamination by the electrodes, both the diameter and thickness of the fibers deposited on the flexible substrate were minimized. This was done by both controlling the electrospinning parameters and adjusting the composition of the spinning solution. Selective removal of the PEO carrier polymer post electrospinning was done by soaking the coated mats in ethanol for 10 minutes. This treatment increases the conductivity of the isolated fibers. This is a result of an elongation of the PEDOT grains upon doping with either a polar or a high boiling point solvent.[287] While the carrier polymer is required for fiber formation on the surface, its semicrystalline state is an intrinsic light scatterer. This makes the surface spectroscopically opaque,[249] while electrochromic devices require spectroscopically transparent electrodes. Desired transparent electrodes are possible by post-deposition rinsing that removes the light scattering PEO. PEO was chosen as the carrier polymer because of its solubility in green solvents, such as water and ethanol for example. The post-deposition processing solvent was once again chosen to remove the carrier polymer using environmentally benign conditions. Sustainable practices for conductive fiber electrospinning can therefore be implemented to move towards making electrochromic device fabrication more environmentally friendly.

The improved conductivity and spectroscopic benefit afforded by the post-electrospinning treatment were assessed by spincoating the electrospinning mixture on glass substrates. The sheet resistance decreased by more than one order of magnitude, from 3988 ± 40 Ohm/sq to 126 ± 2 Ohm/sq after removing the carrier polymer. The transparency also increased once the PEO was removed. Haze measurements, defined as the ratio between the diffuse transmittance and total transmittance, showed a decrease of roughly 40% after the removal of the PEO (Figure S1).[249]

The thinnest possible PEDOT:PSS fibers were electrospun by lowering the PEO concentration in the electrospinning solution and by diluting the mixture with DMF as a highly dielectric co-solvent. The quality and the diameter distribution of the resulting fibers were evaluated by SEM. It can be clearly seen that the fiber mats are defect-free (**Figure 5-2A**). In fact, the fibers, are randomly aligned and they have multiple junctions. This morphology is ideal for maintaining a consistent conductivity when stress and strain are applied to the substrate. The distribution of the fibers'

diameter was centered at ca. 100 nm with a mean of 108 nm. Their porosity was ~ 9% of the surface area and it was centered at ca. 200 nm (**Figure 5-2B** and S3, respectively). The fibers were expected to be sufficiently strong to neither break nor crack with applied strain. Meanwhile, the collective morphology, density, and low degree of entanglement were expected to confer a high degree of mobility to the fibers. These attributes were also expected to prevent the irreversible damage of the fibers when either stretching or bending the substrate. It was experimentally demonstrated that decreasing the fiber diameter increased the elastic modulus.[288] This was attributed to the orientation of the fibrillar polymer inside the nanofibers, arising from the strong strain forces in the polymer jets during electrospinning. Previously, we also observed a similar relationship between the fiber diameter and the elastic modulus for PEDOT:tosylate fiber mats.[282] Mats with small diameter fibers could be stretched to a higher strain than thicker fibers. The intrinsic conductivity of the small diameter fibers decreased less abruptly during testing compared to thick fibers. This confirms the thin fibers are less damaged when stretched.

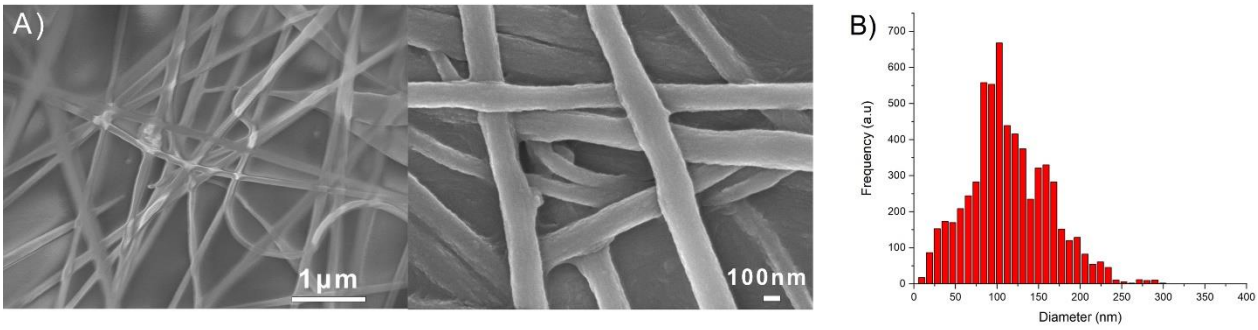

Figure 5-2. A) SEM pictures of the electrospun PEDOT:PSS fibers after removal of the carrying polymer. B) The diameter distribution of the fibers obtained from SEM images.

1.5.2 Electrochromic Performance

The quintessential property of electrochromic devices is their reversible color change in the visible spectrum with applied potential. The collective components of the device must therefore sustain charge transport between the two electrodes to promote the reversible electrochemical redox process of the color changing layer. TPA-BZT-TPA was chosen as the electrochrome for investigating the stretchable electrochromic device because it undergoes a reversible oxidation at the triphenylamine moieties, [289, 290] resulting in a color change from orange to blue.[291]

Moreover, the radical cation of the triphenyl can sustain multiple cycles of switching between its neutral state with applied potential. This leads to consistent color changes when it is used as an electrochrome in functioning devices, a key performance metric of ECDs. The performance of the electrodes was first evaluated in the absence of the electrochrome. This was to benchmark the unique spectral contribution of the fibers to the color of the operating device. This was important because of the overlapping spectral absorption of the oxidized states of both the PEDOT:PSS fibers and the TPA-BZT-TPA electrochrome. Five types of devices were fabricated to benchmark the performance of the different layers towards fabricating a truly stretchable working electrochromic device. The devices differed in the type of substrate and the active layers used for their assembly. The color change of the PEDOT:PSS fibers and their background contribution when operating under device-like conditions was assessed with the reference device (D1). This device consisted of a ITO-coated glass cathode, electrolytic gel, and an anode prepared from PEDOT:PSS fibers electrospun on PDMS. The intrinsic color of the fibers in this configuration was light blue. Indeed, the fibers absorbed broadly from 600 to 1200 nm when electrochemically oxidized (black line **Figure 5-3A**). The blue hue decreased when the fibers were further oxidized with 0.5 V bias, concomitant with an increased absorption in the NIR. The fibers were colored deep blue when they were fully reduced at -2.5 V. While two distinct absorption maxima were observed at 653 and 952 nm, the reduced state of the fibers absorbed broadly in the visible spectrum. The color change with applied potential was reversible with an applied bias of 0.5 V. This indicates that a blue color would be perceived at the cathode when the electrochromic layer is oxidized at the anode during device operation. In contrast, the anode would not contribute to the perceived color when the device is operating.

The color changing TPA-BZT-TPA layer was incorporated in the reference device by spraycoating it on the conductive fibers prior to assembling the device (D2). As the color of the TPA-BZT-TPA changes upon oxidation, the flexible electrode was used as the device anode. A change in absorption of this device was observed when it was operated at between +2.5 and -0.5 V. The absorption at 460 nm arising from the conjugated framework between the terminal electronic donating triphenylamines and the electron deficient core decreased upon electrochemical oxidization concomitant with a new absorption at 805 nm (**Figure 5-3B**). The device (D2) could hence be switched between an orange/yellow color in its neutral/resting state and a green/blue color

in its oxidized state with a coloration efficiency of ca. 300 cm2/C. Both the perceived color and absorption of this semi-flexible device differed from the reference device (D1). The ITO electrode was replaced with the PDMS coated with PEDOT:PSS fibers in order to make the fully stretchable device (D3). The device was assembled and sealed with PDMS after depositing the electrolytic gel and the electrochrome on the cathode and anode, respectively. Both the original resting state and the state formed upon reducing the oxidized state had both the same perceived color and absorption spectrum as the semi-flexible device (D2), albeit with a lower coloration efficiency of ca 170 cm2/C. Rather than a discrete absorption at 805 nm, corresponding to the oxidized electrochrome, the fully stretchable device absorbed broadly over the visible region with an applied positive bias (**Figure 5-3C**). Both the oxidized state of TPA-BZT-TPA and the fibers at the cathode contributed to the absorption spectrum, giving rise to a perceived blue color. To verify this, the absorption of the oxidized state of the electrochrome that was measured with the semi-flexible device (D2) was subtracted from the spectrum of the fully stretchable device (D3) (Figure S4). The spectrum of the oxidized state of the fully stretchable device could also be deconvoluted into four discrete components: the two absorptions from TPA-BZT-TPA and two peaks from the reduced fibers (Appendix 2 Figure 5). The electrochrome contributed ~60% to the absorption spectrum with the cathode contributing to the remainder. The collective spectroelectrochemical device data demonstrate that PEDOT:PSS fibers can be used as electrodes in an operating electrochromic device. Their spectral contribution to the device when in operation can be minimized by preparing small diameter fibers and by the judicious choice of the electrochrome.

The change in color with applied potential demonstrates the suitability of the PEDOT:PSS fibers are indeed conductive and they are suitable for use as the electrodes in an electrochromic device. However, the color change does not provide information about the device performance under continuous switching of the potential. Towards this end, the change in transmittance percent when reversibly generating the oxidized state of TPA-BZT-TPA was evaluated at 805 nm over 60 minutes. The semi-flexible device (D2) showed a transmittance difference of 47% at the onset of device operation. It retained over 20% transmittance difference during 20 minutes before decreasing to 7% after one hour of device operation. The decrease in the contrast ratio between the neutral and the oxidized states with prolonged switching of the applied potential can be assigned to a partial degradation of the electrochrome by oxygen that continuously permeates into the device

during operating.[292] This is based on an oxygen impervious ECD that operated continuously for 5 hours with minimal loss of color contrast of a similar triphenylamine electrochrome.[293] The fully stretchable device (D3) showed a similar trend. It had a maximum contrast of 35%, which decreased to 10% after operating the device for one hour. To frame the contrast performance of the PEDOT:PSS fiber devices, a rigid reference device (D4) was fabricated. The PDMS-PEDOT electrodes of the fully stretchable device were replaced with ITO coated glass electrodes. The percent transmittance difference of the rigid device was more consistent over the 60 min device operation, albeit reduced (10%; Figure S6) compared to the devices fabricated with the PEDOT:PSS fibers (**Figure 5-3E** and **F**). The performance of the reference device (D1) that was prepared uniquely from the PEDOT:PSS fibers was also evaluated. It showed a similar behavior to the other PEDOT:PSS devices; a consistent color change at 952 nm over time, albeit a smaller difference in the transmittance percent between the on and off states. The consistent optical difference of D1 confirms the electrodes maintain their performance over extended periods of switching the applied potential. It further confirms the change in performance of D2 and D3 during the device operation is from the electrochrome (vide supra) and not a change in the electrodes. The enhanced color contrast of the devices that were fabricated using the PEDOT:PSS fibers was attributed to the different specific surface area of the fiber morphology compared to the flat homogenous ITO surface. This is based on the knowledge that redox reactions are favored when the surface area of the counter electrode is greater than that of the working electrode.[294] The switching data confirm PEDOT:PSS fibers can be used as the electroactive material to enable stretchable electrodes for their use in electrochromic devices.

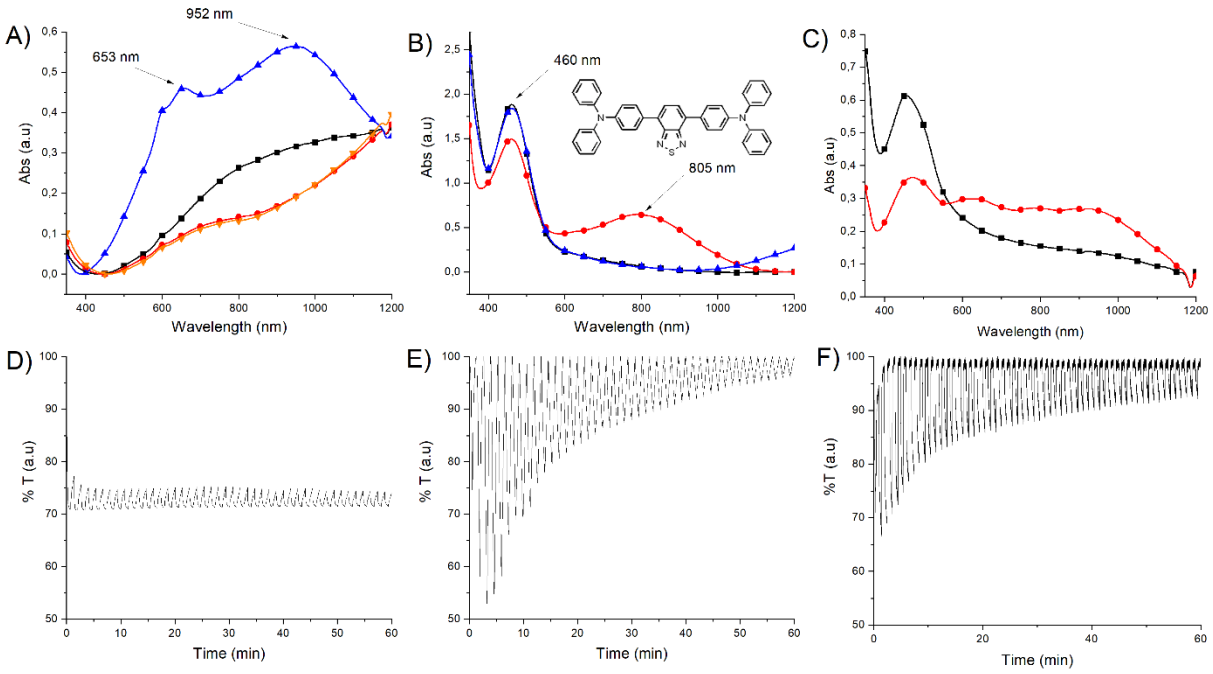

Figure 5-3. Change in absorption spectra between the original state (■) of the various devices and with applied potential of: A) + 0.5 V (●), -2.5 V (▲), followed by + 0.5 V (▼) for the reference device; B) the semi-stretchable device with applied potentials of + 2.5 V (●) and - 0.5 V (▲); C) the fully stretchable device with a + 2.5 V (●) applied potential. Change in transmittance percent with applied potential switched at 30 sec intervals over 60 minutes for: D) the reference device monitored at 952 nm with applied potentials of 0 to -2.5 V; E) the semi-flexible device monitored at 805 nm with applied potentials of 0 to + 2.5 V; and F) the fully stretchable device monitored at 952 nm with applied potentials of 0 to + 2.5 V.

1.5.3 Bending Performance

The fully stretchable device (D3) was subjected to the same switching bias (vide supra) at 40 sec intervals and its performance was monitored when bent to 10 and 20 mm radii of curvature (**Figure 5-4A**). The chosen radii of curvature corresponded to 0.1 and 0.05 curvatures, respectively. The chronoamperometric response was measured during 11 off/on switching cycles for the two radii of curvatures. This was referenced against a similar device that was operated in a flat configuration. The current flowing between the electrodes decreased by ~85% and ~55% for the 10 and 20 mm

radii of curvature, respectively (**Figure 5-4B**). The transmittance difference between the off and on states also decreased inversely with the radius of curvature. The bending induced current change was likely from some of the PEDOT:PSS fibers being displaced within the device. The internal strains with bending also irreversible damaged a small amount of the PEDOT:PSS fibers. It is worthy to note that the current decreased only at the onset of bending. Afterwards, it remained constant during the time when the device was bent: 0.7, 0.6, and 0.4 mA for the flat, 0.05 and 0.1 forms, respectively. This behavior implies that the fibers are damaged only at the onset of bending. No subsequent damage occurred when the device was maintained in its bent form.

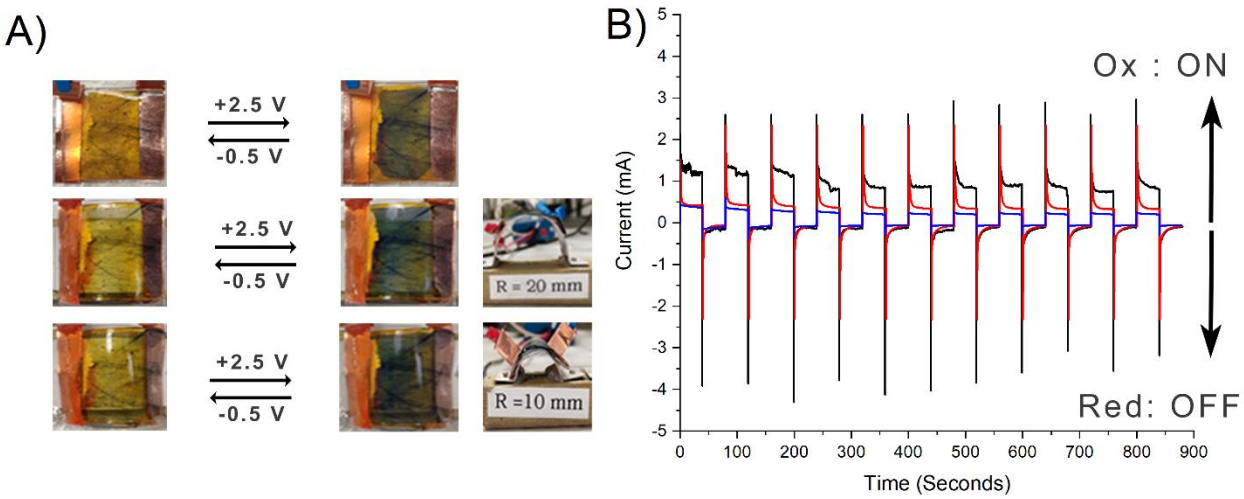

Figure 5-4. A) Pictures of the fully stretchable device switched between its resting (neutral; left) and bleached (oxidized; middle) states when operating on a surface that is: flat (top), 10 (middle), and 20 (bottom) mm curvature of bending (bottom). B) Chronoamperometry of the fully stretchable device when switched between +2.5 and -0.5 V at 40 sec intervals over 11 cycles when bent at a 0 (—), 20 (—), and 10 (—) mm radius of curvature.

A stretchable reference device (D5) was also fabricated to verify exclusively the electronic performance of the PEDOT:PSS fibers when the device was bent (Figure S7). This device consisted of two PDMS electrodes prepared by electrospinning PEDOT:PSS fibers, separated by the electrolyte and sealed with PDMS. The resulting device was fully stretchable and it could be bent without mechanically failing. The chronoamperometric behavior of the fully stretchable device (D3) was identical to the stretchable reference device (D5) under similar operating conditions and

bias regime. The consistent performance of the different electrochromic devices proves PEDOT:PSS fibers can successfully be used to make transparent electrodes.

1.6 Stretching Performance

PEDOT:tosylate fibers are known to remain conductive up to 160 % strain.[145] The use of PEDOT:PSS fibers as electrodes was therefore expected to maintain a certain electric continuity when stretched, allowing the electrochromic device operation under strain. This was tested by evaluating the performance of both the stretchable reference device (D5) (Figure S8) and the fully stretchable device (D3) with applied stress. The change in color with applied potential when the device was stretched upwards of 150% strain can qualitatively be seen in **Figure 5-5A**. The reversible color change with applied stress confirms the PEDOT:PSS fibers retain their conductivity even when the device is stretched. The electrical performance was quantitatively evaluated by monitoring the current during consecutive stretching cycles between 10 and 100% strain in 10% increments. The chronoamperometric response of the fully stretchable device was similar to what was observed with the bending test. The device current decreased from 2.91 to 0.04 mA when stretching from its resting position to 150% strain. This decrease in current (**Figure 5-5B**) is likely due to the reorganization and subsequent breaking of the fibers when they are stretched. The electrochromic contrast also decreased when the conductivity decreased. The overall active area of the working electrode reduces when the electroactive fiber density is decreased from the fibers breaking. Therefore, the electrochrome undergoes fewer redox processes with an applied potential. The current of both the stretchable reference (D5) and the fully stretchable (D3) devices dropped significantly at 10% strain. Afterwards, it decreased quasi linearly up to 90%. The current remained constant from 100 to 150 % strain (**Figure 5-5C**). This behavior is consistent with other electrospun materials that have been used as strain sensors.[295, 296] The initial regime is caused by fibers unaligning at their crossover junctions. The fibers slide apart with continued strain and the conductive network becomes damaged. Finally, between 100 and 150% strain, the fibers elongate and they become aligned. This decreases the number of interfiber junctions, limiting the electronic network and ultimately, the conductivity decreases. The remaining fibers break with subsequent strain, further causing the conductivity to decrease. These correspond to slipping and other motions of the fibers inside the device. To better understand the change in current with

stretching of this device, the properties of a single electrode were also assessed. (Figure S9) This consisted of a single PDMS substrate on which PEDOT:PSS fibers were electrospun. The substrate was not sandwiched as opposed to the other devices and no electrolytic gel was used.

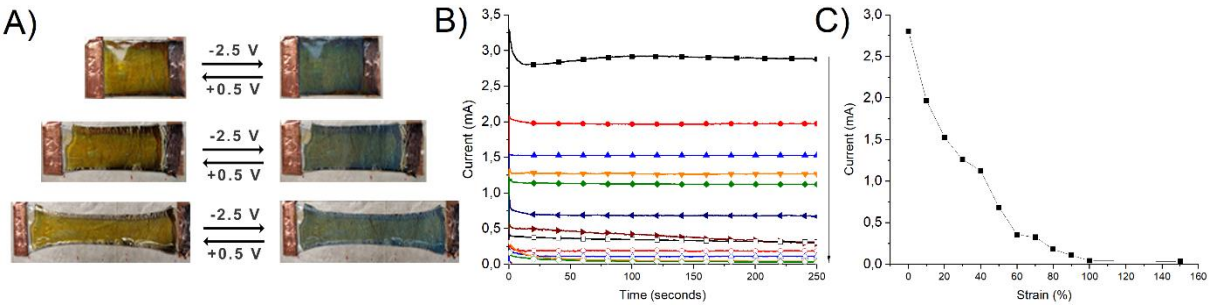

Figure 5-5. A) Pictures the fully stretchable device when switched between its resting (left) and bleached (right) states when stretched to 0% (top), 100% (middle) and 150% (bottom) strain. B) Chronoamperometry of the fully stretchable device when stretched from 0 to 150% and measured at 10% strain intervals: 0%(—■—), 10% (—●—), 20%(—▲—), 30% (—▼—), 40% (—◆—), 50% (—◀—), 60% (—▶—), 70% (—□—), 80% (—○—), 90% (—△—), 100% (—▽—) and 150% (—◇—). C) Evolution of the measured current contingent on the applied strain when the device is operating in the bleached state.

The current flowing through the single electrode was recorded as a function of the applied strain. Contrary to the devices, the current slowly decreased to 20% of its original value at 90% strain. At 100% of strain, the sample was permanently damaged and it was no longer conductive. The different performance of the stretchable reference device and the fiber-only sample can in part be due to the electrolytic gel. The gel could act as a lubricant at the fiber interface and help the fibers reorganize during strain with minimal damage. The gel can also absorb the strain at the interface. As a result, the fibers are exposed directly to the strain only from the substrate on which they are electrospun. This is in contrast with the fiber-only sample where the fibers are exposed to direct strain from both the top and the bottom substrates. A single electrode was subjected to 500 consecutive cycles of stretching to 50% strain followed by releasing the applied strain. (Figure S10). The conductivity of the electrode increased slightly during the initial stretch/release cycles. This is a result of an increased number of electronic contacts that are formed between the conductive fibers when the applied strain forces the fibers to align. After their initial alignment, the

fibers do not further reorganize with subsequent stretching/releasing. This is apparent from the conductivity that remained constant over the course of the 500 cycles. The consistent conductivity further indicates the robustness of the fibers and their structural integrity that is maintained with repetitive stress. This aside, both the visible color changes with applied bias and the measurable conductivity with strain demonstrate the suitability of PEDOT:PSS fibers as electrodes for fabricating stretchable electrochromic devices.

1.7 Conclusions

Functioning electrochromic devices were prepared from conductive PEDOT:PSS fibers that were electrospun on flexible PDMS substrates. The transparent electrodes were used to fabricate truly stretchable and bendable electrochromic devices. The devices were fabricated via a straightforward device architecture, consisting of a stretchable electrolytic gel and an electrochrome that were sandwiched between two stretchable transparent electrodes. The color of the devices could be reversibly bleached with an applied potential even up to 150% of strain. The reversible color switching when stretched and bent demonstrates that otherwise expensive transparent metallic electrodes can be replaced with inexpensive PDMS substrates that can be made conductive with PEDOT:PSS fibers. Truly stretchable electrochromic devices are therefore possible by taking advantage of the intrinsic elastomeric properties of PDMS and by matching its flexibility and stretchability with a complementary electrolytic elastomer. Moreover, stretchable ECDs potentially covering a range of colors are conceivable by replacing the color changing layer with known electrochromes. Stretchable electrodes of various sizes can ultimately be fabricated from inexpensive commodity elastomers given that conductive fibers can be electrospun on a wide range of substrates and dimensions. The universality of electrospinning conductive fibers opens the possibility of greening the fabrication of stretchable electrochromic devices by using sustainable and degradable elastomers along with taking advantage of their greener processing conditions relative to conventional electrode fabrication.

1.7.1 Acknowledgements

The Natural Science and Engineering Council Canada (NSERC) is acknowledged for Discovery Grants awarded to FC and WS that enabled this collaborative research. Equipment and

infrastructure used for this research were acquired and maintained by the Canada Foundation for Innovation and Quebec Strategic Networks (CQMF-QCAM, RQMP, and GCM). V.W. thanks both NSERC and the GCM for undergraduate scholarships. This work was also supported in part by Defense Research and Development Canada through an IDEaS Micronet (CFPMN1-008) grant awarded to F.C.

CHAPTER 6 ARTICLE 3: ENHANCING THE PERFORMANCE OF TRANSPARENT AND HIGHLY STRETCHABLE ORGANIC ELECTROCHEMICAL TRANSISTORS BY ACID TREATMENT AND COPOLYMER BLENDING OF ELECTROSPUN PEDOT:PSS FIBERS

This article was submitted to the journal "Journal of Materials Chemistry C" on 2022-03-18. This article reports the fabrication of stretchable OECTs from fiber mats of PEDOT:PSS. The fibers were produced from a commercially available PEDOT:PSS dispersion in water with PEO as a supporting polymer and PEG-PPG-PEG as a plasticizer. PEDOT:PSS/PEG fiber mats were post treated with sulfuric acid to increase their conductivity. Electromechanical measurements shown an increased stretchability, up to 200% strain and a higher conductivity due to the PEG-PPG-PEG and the acidic post-treatment, respectively. As-prepared OECTS can be stretched up to 100% while exhibiting transistor behaviors and they partially recovered their performances once released from strain. The supporting information for this article is reprinted in Appendix C of this thesis.

1.1 Authors

Michael Lerond,[1] Fabio Cicoira[1*], W. G. Skene.[2*]

[1] Department of Chemical Engineering, Polytechnique Montréal, Montréal, QC, Canada

[2] Département de chimie, Université de Montréal, Montréal, QC, Canada

***Correspondance:**

Fabio Cicoira

fabio.cicoira@polymtl.ca

William Skene

w.skene@umontreal.ca

Keywords: Stretchable electronics, Organic Electrochemical Transistors, Electrospinning, Poly (ethylenedioxythiophene): Poly (styrene sulfonate) (PEDOT:PSS), Printed Electrical Contacts.

1.2 Abstract

Organic electrochemical transistors (OECT) were fabricated to assess the treatment of poly(3,4-ethylenedioxythiophene):poly(styrene sulfonate) (PEDOT:PSS) fibers with sulfuric acid (H_2SO_4) on the electronic performances and the mechanical properties of the devices. The devices were prepared by a combination of electrode printing and electrospinning of PEDOT:PSS nanofibers. Fibrillar mats treated with H_2SO_4 could be stretched to 200% of their initial length with minimal loss (≈20%) of the current. Stretchable OECTs were fabricated by printing silver drain and source electrodes directly on the conductive spun fiber mats. The fabricated devices showed transistor behavior up to 100% strain and their transistor performance was maintained during 100 stretching/release cycles. The overall electronic and mechanical performance of the stretchable OECTs were better, even after stretching, than their counterparts that were prepared from spincoated thin films.

1.3 Introduction

Organic electronic devices have matured to the point where they are now commonly used in consumer applications such as lighting and displays.[216, 297] Such devices are reliant on conductive substrates that are either rigid or have limited flexibility.[298, 299] Replacing the rigid-like substrates with elastomers yields truly flexible and stretchable devices.[300-302] Such mechanically compliant devices have been used in bioelectronics,[303-305] robotics,[306, 307] solar cells,[308, 309] and OECTs.[56, 310-312] An overarching component that enables these devices is poly(3,4-ethylenedioxythiophene):poly(styrene sulfonate) (PEDOT:PSS) courtesy of its intrinsic conductivity, its high degree of transparency in the visible spectrum, and solution processability.[39, 313, 314]

While PEDOT:PSS promotes charge transfer to enable device operation, its pristine films are poorly conductive (0.6 S/cm). Furthermore, pristine PEDOT:PSS films are not mechanically compliant for their use in flexible and stretchable devices. Much effort has focused on overcoming these limitations by improving the flexibility[315], stretchability[47], self-healing,[316] and conductivity of PEDOT:PSS.[317, 318] The mechanical compliance of PEDOT:PSS films for their

use in flexible devices can be improved either by blending the conductive suspension with additives prior to film deposition[134, 281, 319] or by treating deposited films with additives.[318] Polar solvents, such as DMSO, MeOH and monoethylene glycol (EG) have proven ideal additives for increasing the conductivity by upwards of 300-fold.[317] Poly(ethylene glycol) (PEG) has become an effective plasticizer for decreasing the Young modulus and increasing the elongation at break of PEDOT:PSS films.[320, 321] Moreover, its intrinsic ion transport property can enhance the conductivity of PEDOT:PSS films.[134, 322] The mechanical and conductivity enhancements with PEG were exploited by S. Ghosh et al. to fabricate electronic fabrics.[323] They found that PEDOT phase separated from its PSS primary dopant when PEG was added. This led to better agglomerated PEDOT domains and enhanced electronic transport by hopping and tunneling. Similarly, Pengcheng et al. blended PEDOT:PSS with PEG-20K to increase the elongation of the conductive film at break to 55%.[324] The conductivity of the film could also be increased to 100 S/cm by treating the deposited film with DMSO, which forms PEDOT:PSS rich domains that can be described as gel-like particles in a pancake-like morphology that are surrounded by a PSS-rich matrix. Sulfuric acid treatment has emerged as a viable method to enhance the conductivity of PEDOT:PSS. While the exact mechanism that is responsible for increasing the electrical conductivity of PEDOT:PSS remains elusive,[287] the tangled polymeric domains nonetheless straighten when the excess insulating PSS is replaced with HSO_4^- ions when treated with sulfuric acid.[263, 325-327] This aside, both the stretchability and the conductivity of PEDOT:PSS films can be improved by combining PEG additives and acid treatment.

The limited flexibility and stretchability of contiguous thin films of PEDOT:PSS can in part be overcome with PEDOT fibers that are prepared by electrospinning. The fibers' aspect ratio, overall fiber thickness, and density can be regulated by adjusting the many electrospinning parameters. We recently demonstrated that the conductivity and the stretchability of fiber mats prepared from electrospun PEDOT:tosylate fibers are closely related to the fiber morphology. We highlighted the formation of fused fibers at their crossing nodes as a key factor in the electrical and mechanical properties in the resulting fiber mats. On one hand, fused fibers increased the conductivity by creating a network of fibers connected to one another. On the other hand, they reduced the degree of freedom of each fiber, resulting in a limited elongation at break. We leveraged this knowledge to fabricate stretchable OECTs and an all-organic electrochromic devices from electrospun

PEDOT:tosylate and PEDOT:PSS fibers, respectively. Although the devices were both stretchable and bendable, their performance was limited compared to their conventional counterparts. Indeed, the performance of the devices deteriorated with successive stretch/release cycles. We were therefore motivated to see whether the performance of stretchable OECTs prepared from electrospun PEDOT:PSS fibers could be improved by blending with an electrospinning additive and by acid treatment. Towards device performance enhancement and maintaining device operation over multiple stretch/release cycles, we investigated the effect of blending a PEG copolymer with PEDOT:PSS on the stretchability of electrospun PEDOT:PSS fibers. The conductivity effect of post treatment with sulfuric acid on the electrospun fiber mat was also examined towards producing highly stretchable and conductive fibers, whose conductivity could be maintained during successive applied stress/release cycles. Herein, we present the performance of stretchable OECTs prepared from electrospun fibers that were blended from poly(ethylene glycol)-poly(propylene glycol)-poly(ethylene glycol) (PEG-PPG-PEG) and PEDOT:PSS along with the device enhancement that was possible by secondary doping the conductive fibers with sulfuric acid.

1.4 MATERIALS AND METHODS

1.4.1 Reagents and materials

All reagents and materials were used as received. Polyethylene oxide (PEO) (1×10^6 Da and 5×10^6 Da), activated carbon (Norit, chemically activated), Nafion, poly(ethylene glycol)-poly(propylene glycol)-poly(ethylene glycol) copolymer (4.400 g/mol) (PEG-PPG-PEG), ethanol (100%) and concentrated sulfuric acid (H_2SO_4; 18 M) were purchased from Millipore Sigma. A PEDOT:PSS dispersion (CLEVIOS PH1000) was purchased from Heraeus Electronic Materials GmbH. Stretchable elastomeric VHB tape was purchased from 3M Canada. Glass slides and cloning cylinders were purchased from Corning. Carbon paper (Spectracarb 2050A) was obtained from Fuel Cell Store, USA and the silver ink (Flex 2, containing metallic silver, ethyl diglycol acetate and mineral salts) from Voltera.

1.4.2 Electrospinning

Electrospinning was done similar to previous reports, using a Linari RT collector.[328] Fibers were exclusively obtained without any visibldroplets by adjusting the spinning parameters. The mixture used for electrospinning consisted of Clevios PH1000 (77.8 wt%), DMF (4.9 wt%), and PEG-PPG-PEG (15.6 wt%) was adapted from previously reported work. The mixture was stirred for 1 hour, afterwards the electrospinning carrier PEO (1.7 wt%) was added, followed by stirring for 12 h at room temperature to complete homogenization. Various substrates were used for electrospinning contingent on the required measurement: glass slides for SEM, sheet resistance and transistor measurements; carbon paper for the electrochemistry; VHB tape for stretching tests and fabricating stretchable OECTs.

1.4.3 Spin coating

The electrospinning mixtures were diluted 2-fold for their spincoating (Ossila spincoater) as homogenous thin films (~200 to ~300 nm) on 25 mm^2 glass slides.

1.4.4 Characterization of fibers and films

Scanning electron microscopy (SEM), sheet resistance, conductivity, stretching, and electrochemical measurements were done similar to previous reports.[328] The thickness of the spincoated films was measured with a stylus profilometer (DektakXT Bruker). Cyclic voltammetry was done with electrospun fibers deposited on a 25 mm^2 carbon paper with an Ag wire pseudo-reference and platinum mesh counter electrodes. The NaCl (0.1 M) electrolyte solution used for electrochemical measurements was bubbled with N_2 prior to the measurements.

1.4.5 Transistor fabrication

Organic Electrochemical Transistors (OECTs) were prepared according to known methods by electrospinning fibers either on glass or stretchable VHB substrates.[328] Briefly, electrospun fiber mats were plasma etched to form OECTs channels and silver electrodes were printed as both drain and source electrodes. Conductivity enhancement of the deposited PEDOT:PSS was achieved by dropcasting sulfuric acid (18 M) on top of the fiber mats and allowing it to react for 1 minute. The substrates were then thoroughly rinsed 3 times with deionized water to remove the residual acid.

No visual alteration of the elastomeric VHB tape was observed after the acidic post treatment. Cloning cylinders were glued onto the channels to complete the solid OECTs fabrication. The stretchable OECTs were encapsulated by a second VHB tape over the channels after assembly. Three holes were next punched in the top VHB layer to create a flexible gate well and two wells for the drain and source electrodes (**Figure 6-1**).

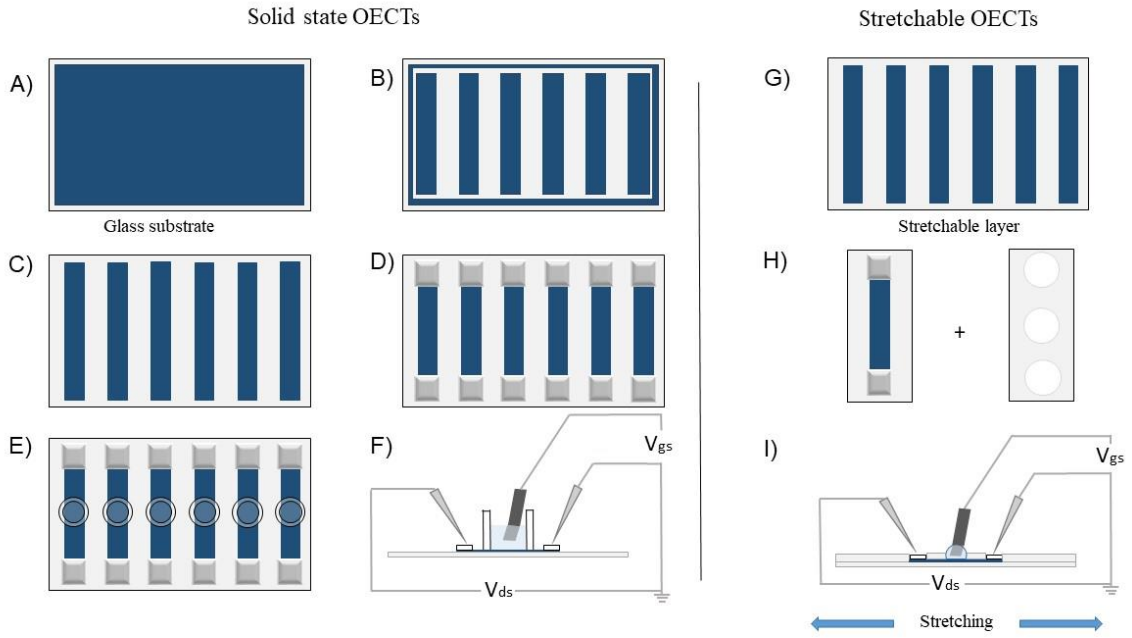

Figure 6-1. Schematic representation of OECT fabrication on glass substrates (left panel) and stretchable substrates (right panel). Left panel: deposition of fibers on the substrate (A), plasma etching (B), resulting fiber channels (C), electrodes printed on the channels (D), cloning cylinders glued on the channels to complete the OECTs (E), and electrical schematic of the final OECT (F). Right panel: electrospun fiber channels produced on a stretchable substrate by plasma etching (G), each channel isolated and the OECT is encapsulated with a top layer (H), and electrical schematic of the final OECT (I).

1.5 Results and discussion

1.5.1 Effect of PEG-PPG-PEG and H_2SO_4 on PEDOT:PSS fibers

Plasticizers are commonly used to enhance the flexibility and stretchability of otherwise brittle PEDOT:PSS films. Indeed, smooth flexible and stretchable PEDOT:PSS films are possible by blending a dispersion of the conductive polymer with ethylene glycol.[329, 330] Similarly, the stretchability and flexibility of PEDOT:PSS fibers can be improved by treating them with a plasticizer after they have been electrospun.[98, 329] To simplify the process of obtaining stretchable fibers, we added the plasticizer to the electrospinning mixture. PEG-PPG-PEG was selected over other plasticizers because it does not affect the viscosity of the spinning mixture, and hence, doesn't inhibit the fiber formation during the electrospinning process. This is the principal factor that affects the diameter of the fibers during electrospinning. Narrow fibers and a small diameter distribution are desired to optimize the conductivity of the mat. PEG-PPG-PEG is further advantageous because it can be blended upwards of 15%/wt to the spinning mixture and without causing defective fibers. In contrast, ethylene glycol can be blended only to 3%/wt before the fibers are defective. Moreover, both the stretchability and the conductivity are not improved when electrospinning with this plasticizer. Stacked fibers were targeted over fused fibers because they have fewer mechanical limitations. The electrospinning mixture composition was therefore optimized by reducing the PEO proportion to favor stacked fibers. Another benefit of the optimized spinning mixture composition was the instant drying of the fibers during electrospinning. The surfaces can therefore be evaluated or subjected to post-treatment without an additional drying step. A representative SEM image of the electrospun fiber from the optimized spinning mixture is seen in **Figure 6-2A**.

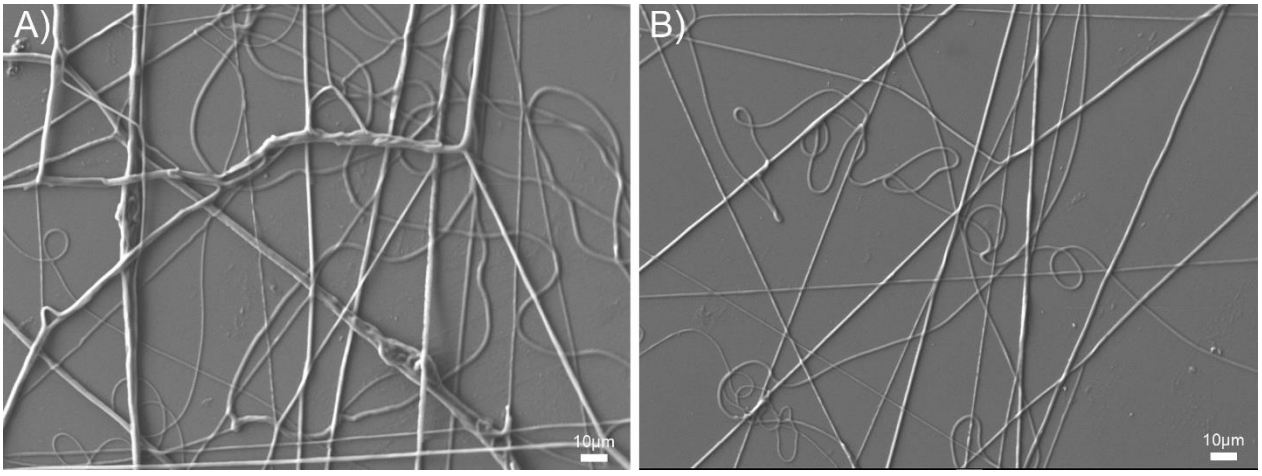

Figure 6-2. SEM image of electrospun PEG-PPG-PEG/PEDOT:PSS fibers before (A) and after treating with sulfuric acid (B).

Treatment of PEDOT:PSS films with sulfuric acid is well-known to increase the conductivity of PEDOT:PSS films. During this process the PSS dopant is assumed to be replaced by HSO_4^-.[331, 332] We initially investigated the possibility to increase the conductivity by adding H_2SO_4 to the PEG-PPG-PEG electrospinning mixture instead of immersing the fibers in acid after fiber deposition. Adding sulfuric acid in as low as 100 µL formed PEDOT aggregates and the heterogenous mixtures could not be electrospun. The most practical method for increasing the conductivity of the fibers by secondary doping was to briefly submerge the fiber mats directly in the acid. The diameter of the resulting acid-treated fibers was smaller than the untreated ones (**Figure 6-2B**). This can be attributed to two reasons. First, the excess insulating PSS is exchanged with the sulfuric acid. Second, both the PEG-PPG-PEG plasticizer and the PEO carrier are removed when the substrate is rinsed.[263] The density of the fibers also decreased because some fibers delaminated from the substrate when rinsed with deionized water.

The electrospinning mixture was further spincoated on glass slides to prepare smooth and homogenous films (**Figure 6-3A**). These were prepared to assess the conductivity enhancement of the film after acid post-treatment. The conductivity of the film increased over 600-fold (from 0.3 to 200 S/cm) with acid doping. This is consistent with the literature.[333] The film thickness decreased by around 10-fold with the ethanol rinsing steps. No further decrease in the film thickness was recorded with the acid exposure. This is from the selective removal of the copolymer (PEG-PPG-PEG), the carrying polymer (PEO) and the excess PSS. To better gauge the

conductivity enhancement, another spincoated film was prepared and it was rinsed exclusively with ethanol, as this treatment is also known to increase PEDOT:PSS conductivity.[334] Although the film thickness decrease after rinsing with ethanol was consistent with that observed with the acid treatment, the conductivity of the ethanol rinsed surface increased only ~10 times. The higher conductivity with sulfuric acid confirms its superior doping effect, partly explained by the absence of bulky insulating groups.

The sheet resistance of the fiber mats was also measured to assess their electronic conductivity enhancement with acid doping. As expected, their sheet resistance before the acidic treatment was high ($2x10^6$ Ω/sq). Similar to what was observed with the spincoated film, treating the mat with acid decreased the sheet resistance 300-fold (700 Ω/sq). Only a negligible drop in the sheet resistance ($1x10^6$ Ω/sq) was observed for ethanol rinsing.

The cyclic voltammogram of the same conductive mat with uniformly distributed PEDOT:PSS fibers was measured before and after treating with acid. (Figure S1) The cyclic voltammetry recorded for the acid-treated film showed the film retained its doping/dedoping character. Indeed, its capacitance was much greater than the untreated film. This is somewhat expected given the removal of insulating PSS with the washing step. The estimated specific capacitance (see Appendix 3 for details) of the untreated and acid treated electrode was ~310 and ~2 600 F/g, respectively.

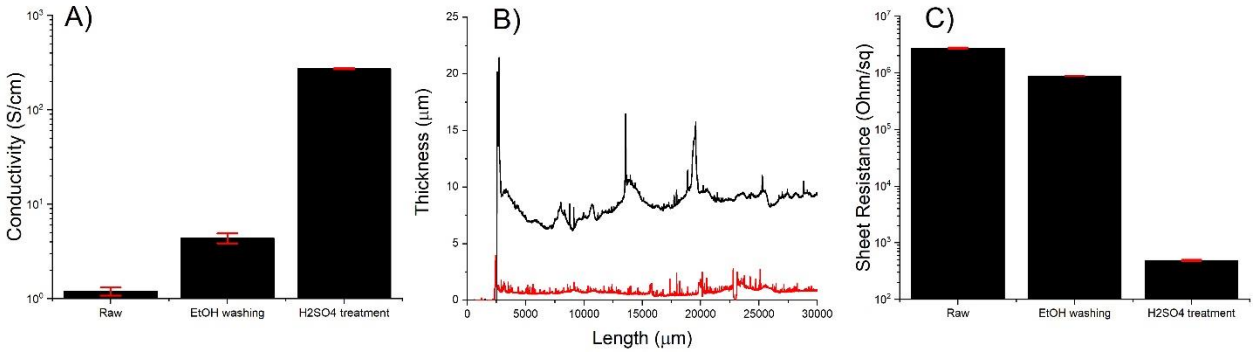

Figure 6-3. A) Conductivity of spincoated PEDOT:PSS films on glass substrates. B) Thickness of spincoated film before (—) and after rinsing with ethanol (—). C) Sheet resistance of electrospun PEDOT:PSS fibers on glass substrates.

1.5.2 Electromechanical testing

The stretchability and the ability of the electrospun fiber mats to retain their electrical conductance under strain were evaluated. These were done by monitoring the current during consecutive stretching cycles from 20% to 140% strain (**Figure 6-4A**). A reference sample was also prepared to benchmark the effect of the PEG-PPG-PEG carrier additive and the acidic treatment. For the reference sample, the PEDOT:PSS fibers were deposited on VHB tape without the PEG copolymer and they were not treated with the acid. A break in the electronic pathway occurred when stretching to 120% the untreated fibers, while the treated ones could be stretched up to 140% without breaking. PEDOT:PSS fibers also exhibited a more erratic behavior and they had pronounced drops in the current during the stretching phases. Meanwhile, the PEDOT:PSS/PEG fibers showed a quasi-linear decay in current with increasing applied strain. They retained 84% of their initial current at 140% strain. After being released from strain and allowed to rest for about one hour, the sample went back its initial length without any further current increase. No delamination of the fibers was observed, confirming the electrical pathway was damaged due to the strain. The plasticizing effect of the PEG-PPG-PEG on the PEDOT:PSS is clearly highlighted by the smoother decay of the current and the better stretchability of the PEDOT:PSS-PEG fibers compared the fibers without the plasticizer.

The current flowing through the PEDOT:PSS/PEG sample slowly increased after releasing the strain at the end of the measurement. This is from the fibers rearranging in the absence of a mechanical stress. The samples were further stretched to 160, 180, and 200% strain to additionally evaluate the fibers' conductive behavior. (**Figure 6-4B** to **D**). The stretching and releasing periods are highlighted in green, the 5-minute static stretch is highlighted in peach, and the sample returning to its original length after the strain was released corresponds to the blue region. As per **Figure 6-4**, the current significantly decreases when the mats are initially stretched. The decrease in current was contingent on the strain applied, with the biggest decrease being observed at 200% strain. This is a result of internal mechanical stresses that forces the fibers to realign and break the interfiber junctions. These nodes, where the fibers overlap, enable the electronic percolation, and in turn the current. In contrast, the current was constant when the strain was maintained. During this regime, the fibers glide and realign in the strain direction. The original current could be restored to 50% of its original value after releasing the applied strain and after a recovery period of ca. 17

minutes regardless of the applied strain. The delayed recovery in current can be assigned to the fibers rearranging by gliding to minimize the strain and restoring some of the original interfiber nodes that are required for electronic transport. The electromechanical tests demonstrate that the fiber mats can be stretched up to 200% without breaking while preserving their electrical conductive paths. As expected, adding PEG-PPG-PEG to the electrospinning mixture increased the stretchability the fibers upwards of 80% relative to the fibers prepared without the additive. Interestingly, the drop in current with stretching was less pronounced for the soft fibers. (**Figure 6-4A**) This can be from the soft regions that can readily absorb the mechanical stress. This dampens the stress felt by the rigid domains and prevents crack formation, ensuring the electrical pathways are preserved.

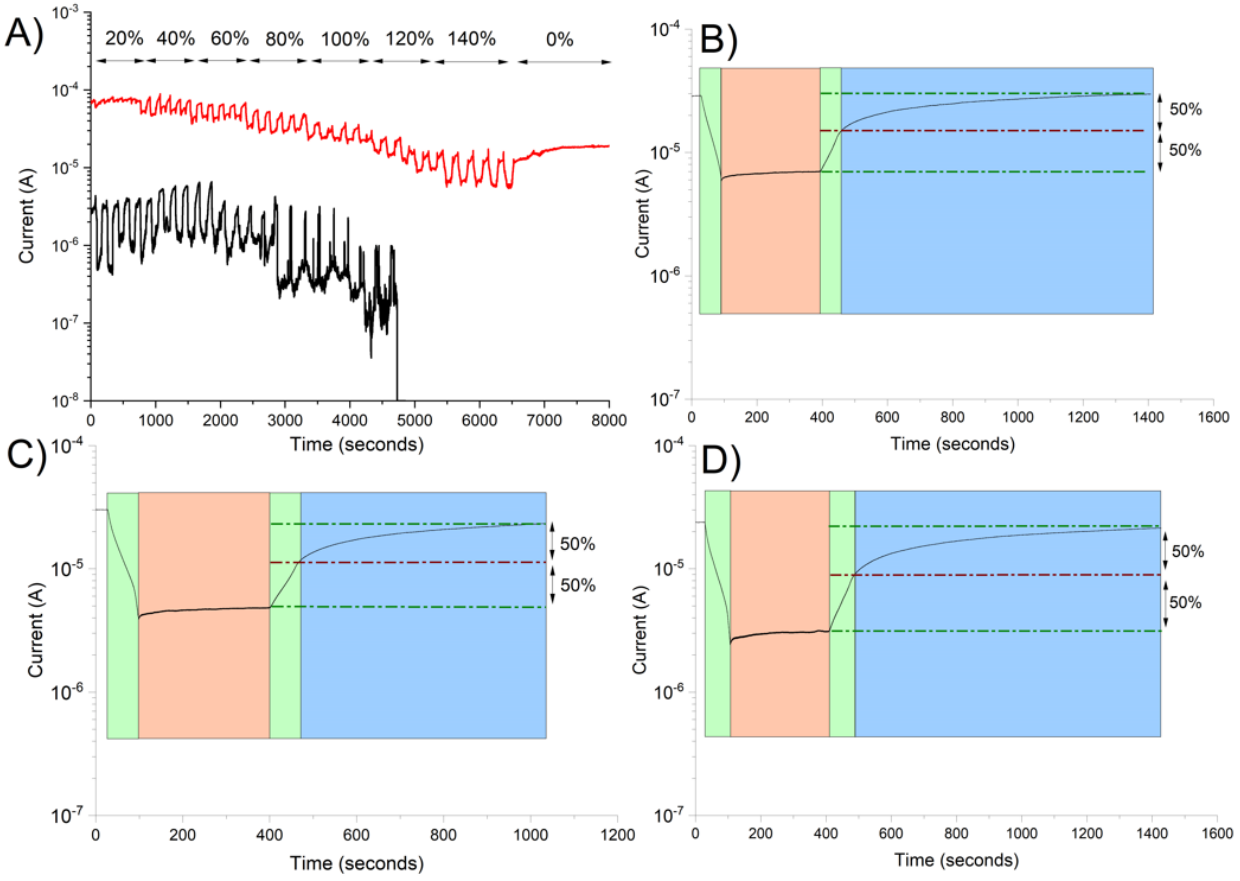

Figure 6-4. Current as a function of time of pristine PEDOT:PSS fibers (—) and PEDOT:PSS/PEG sulfuric acid treated fibers (—) (A) deposited on VHB stretchable substrate. The samples were stretched between 20% and 140% strain at 0.1 cm/s. Five consecutive

stretching/release cycles were done for each strain between 20% and 100%. The samples were kept in each state (stretched or released) for 1 minute. Current as a function of time of PEDOT:PSS fibers treated by sulfuric acid stretched to 160% (B), 180 % (C), and 200% strain (D). The colored zones correspond to the applied stress (lime green), maintaining the applied stretch for 5 minutes (peach), and recovery period after releasing the strain (blue).

1.5.3 Performance of OECT prepared from PEDOT:PSS/PEG fiber mats

The effect of the acid treatment on the OECTs' performance was investigated. To better understand the effect, OECTs were prepared from both electrospun fibers and spincoated films on glass substrates. Both samples were treated with acid and compared to their untreated counterparts. The acid-treated transistors that were prepared from the electrospun fibers had a higher On/Off ratio (~ 65) compared to the fibers that were rinsed only with ethanol (On/Off ratio ~ 8) (**Figure 6-5A**). The improved transistor performance is from the increased conductivity of PEDOT:PSS as a result of the acid treatment. (**Figure 6-5D**) The output curves of the acid-treated devices (**Figure 6-5C** and **F**) also showed better dedoping with increasing gate voltage compared to their untreated counterparts (**Figure 6-5B** and **E**). Interestingly, OECTs prepared from electrospun fibers exhibited better On/Off ratios and output characteristics than their film counterparts. Despite the spincoated films having a higher conductivity because of their homogeneous and contiguous surface coverage, these OECTs performed poorly relative to the devices prepared from fibers. Indeed, the On/Off ratios were ~65 and ~30 for the acid treated fibers and the smooth films, respectively. Similarly, albeit less pronounced, the On/Off ratio decreased from ~8 to ~ 3 for the ethanol rinsed fibers and spincoated films, respectively. The enhanced OECT performance can be explained by the greater specific area of fiber morphology. A greater number of contacts between the PEDOT:PSS fibers and the gate electrolyte is ensured by the greater specific area, leading to faster and easier redox reactions.

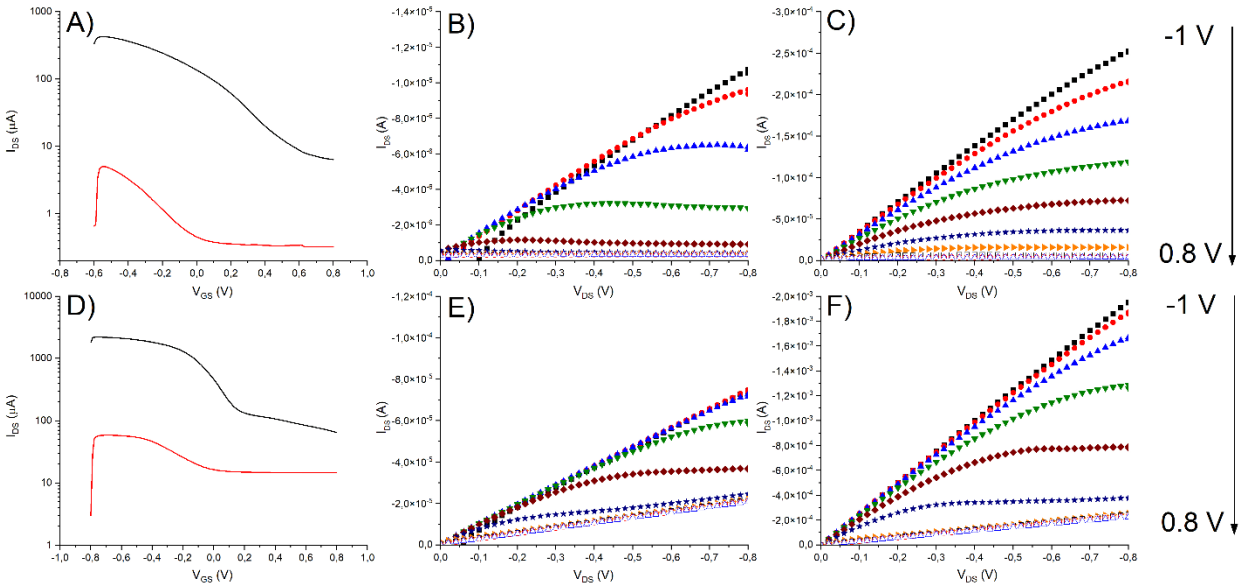

Figure 6-5. Transfer curves (A) of OECTs prepared from electrospun fibers treated with H_2SO_4 (▬) and ethanol (▬), and their corresponding output curves for electrospun fibers on glass substrates treated with either ethanol (B) or H_2SO_4 (C) and applied gate voltage: -1 (■), -0.8 (●), -0.6 (▲), -0.4 (▼), -0.2 (◆), 0 (★), 0.2 (►), 0.4 (□), 0.6 (○) and 0.6 (△) V. Transfer curves (D) of OECTs prepared by spincoating and treating with H_2SO_4 (▬) and ethanol (▬) and their corresponding output curves of spincoated films on glass substrates treated with ethanol (E) or H_2SO_4 (F) and applied gate voltage: -1 (■), -0.8 (●), -0.6 (▲), -0.4 (▼), -0.2 (◆), 0 (★), 0.2 (►), 0.4 (□), 0.6 (○) and 0.6 (△) V.

OECTs prepared by spincoating on stretchable substrates were investigated. These served as a reference to benchmark the stretchability and the transistor performances of the OECTs and compare them to devices prepared from fibers mat (**Figure 6-6**). Certain stretchable polymeric substrates are known to reduce the performance of OECTs. This is owing to the release of unreacted monomers among other species, within the polymer matrix when the substrate is stretched.[335, 336] These monomers inhibit the doping/dedoping process. The On/Off ratio with stretchable

substrate decreased from ≈32 to ≈20 and from ≈8 to ≈2 for the acid treated and untreated films, respectively.

The spincoated OECTs could be stretched up to 25% without a break in their electrical pathway. This is owing to the plasticizing effect of the PEG-PPG-PEG additive. However, the transistor behavior disappeared when the films were stretched. (**Figure 6-6A** and **D**) This is according to the On/Off ratio that was ≈1 for both the acid treated and untreated films.

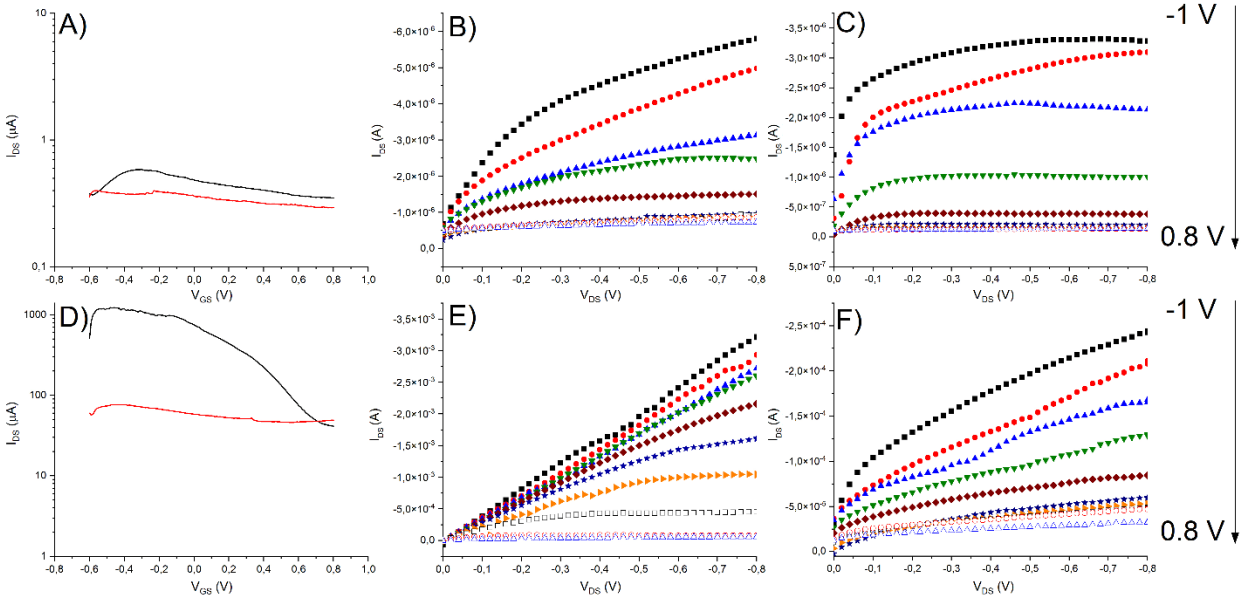

Figure 6-6. Transfer curve (A) of OECT prepared by spincoating and rinsing with ethanol in its initial state (▬) and stretched to 25% strain (▬). The corresponding output curves of the initial state (B) and under 25% strain (C) and applied gate voltage: -1 (■), -0.8 (●), -0.6 (▲), -0.4 (▼), -0.2 (◆), 0 (★), 0.2 (►), 0.4 (□), 0.6 (○) and 0.6 (△) V. Transfer curve (D) of OECT prepared by spincoating and treating with H_2SO_4 in the original state (▬) and stretched to 25% strain (▬). The corresponding output curves of the original state (E) and under 25% strain (F) and applied gate voltage: -1 (■), -0.8 (●), -0.6 (▲), -0.4 (▼), -0.2 (◆), 0 (★), 0.2 (►), 0.4 (□), 0.6 (○) and 0.6 (△) V.

OECTs were also prepared from fibers on the stretchable substrates and their transistor performance contingent on stretching was recorded (**Figure 6-7**). Although the On/Off ratio decreased when stretching to 100% strain (from ≈65 to ≈27), the transistor effect of the electrospun acid treated fiber OECT was preserved. (**Figure 6-7A**)

OECTs prepared from electrospun fibers were stretched to 50% and 100% strain. They were also held at 100% strain for 10 hours. The strain was then released and the devices returned to their original released state. Next, the devices were allowed to recover for 1 hour. Afterwards, the device performance was measured and compared to the benchmark values that were measured before stretching the devices. The On/Off ratio, derived from the transfer curves, decayed from 27 to 4 when the devices were strained to 100% strain (**Figure 6-7A**). The corresponding output curves followed the same trend with the current decreasing roughly 10-fold when the devices were stretched. (Figure S2 A-C) More interestingly, the device performance somewhat recovered when the OECT was held at 100% strain. This is apparent from the On/Off ratio that increased 16-fold when the device was immediately stretched (On/Off ≈4) and when maintaining the applied strain (~16). This was expected according to the electromechanical measurements (vide supra) and it implies the electrospun fibers can rearrange with an applied strain. Their movement is restricted in the solid state, leading to a slow recovery of their original orientation. After releasing the strain, the OECT recovered some of its initial device performance after a healing period with the On/Off ratio increasing to ~22. However, the original device performance could not be restored even after a 24h recovery period. This implies the fibers cannot regain their initial random orientation. They also cannot reform the original number of fibril nodes that are responsible for the electronic transport because they are irreversibly damaged with stretching.

Strain cycling tests were done by successively stretching the devices to 100% followed by releasing the strain. 100 stretch-release cycles were done and the OECTs performance was recorded before and after each applied strain (**Figure 6-7B**). The cycle test data were consistent with electromechanical testing data (**Figure 6-7C**). The performance of the OECTs was consistent throughout the 100 strain-release cycles. This is evidenced from the devices' high current and moderate On/Off ratio (≈5) that did not further decrease during continuous strain-release actions. The cycle tests confirmed that the electrospun fiber mats can continuously be stretched without comprising their performance. Rather, the fibers are damaged uniquely at the onset of testing,

during the first strain action, and their damage is not compounded with each strain-release cycle. The consistent performance even after repeated stretch/release cycles illustrates that electrospun fibers are suitable for use as conductive electrodes for stretchable organic electronics. Using fibers instead of homogenous thin films in stretchable OECTs has a two-fold advantage: the device performance is enhanced and the elongation at break is greater. These performance enhancements are a result of the fiber morphology and the large specific area of the fibers. Moreover, fibers can glide and rearrange with applied strain direction instead of breaking, in contrast with contiguous films.

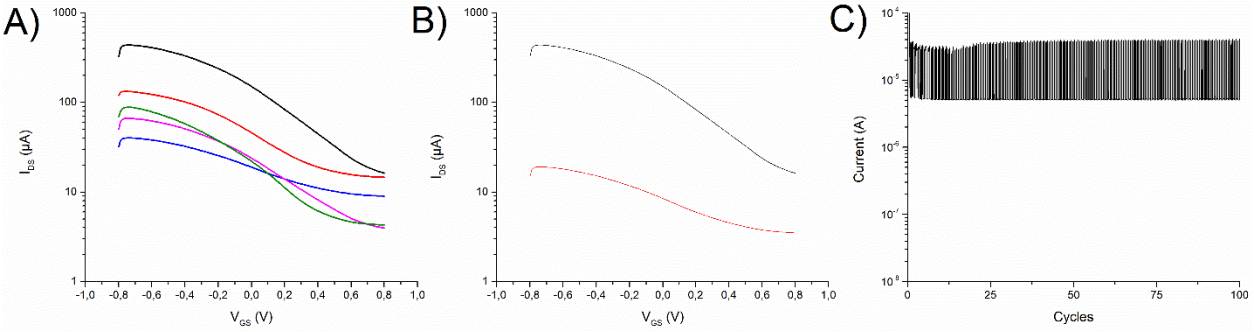

Figure 6-7. A) Transfer curves of OECTs prepared from electrospun fibers in the original state (—), stretched to 50% (—) and 100% strain (—), held at 100% strain for 10 hours (—), and released to the original state (—). B) Transfer curves of an OECT in the original state (—) and after 100 cycles of stretching to 100% strain and releasing (—). C) Current of an OECTs prepared from acid treated fibers as a function of stretch/release cycle.

1.6 Conclusions

PEDOT:PSS conductive fibers were successfully prepared by electrospinning. Their post-treatment with sulfuric acid increased the conductivity by 3 orders of magnitude compared to pristine PEDOT:PSS films. Blending the PEG-PPG-PEG copolymer in the electrospinning mixture improved the elasticity of the PEDOT:PSS fiber mats. The collective effects of the copolymer blending and post-spinning acid treatment increased the elasticity of the fiber mats up to 200% with a minimal reduction in current (≈20%) with stretching. More interestingly, the fibers could recover their current when the applied strain was released. This highlights the capacity of the fibers

to rearrange in the strain direction by gliding and minimizing the mechanical strain without breaking when stretched and released. OECTs prepared from electrospun conductive fibers had improved operating and elastic performances compared to conventional devices prepared from homogenous films. This illustrates that copolymer additives and secondary doping by acid treatment are viable processing methods for preparing electrospun PEDOT:PSS fibers that meet the elastic and electronic requirements to enable stretchable organic electronic devices that can withstand multiple stretch/release cycles. With the development of commercial scale electrospinning, the device performance enhancing processes can potentially be integrated in the large-scale production of elastic electronics that maintain their functionality during repetitive stress/release motions.

1.6.1 Conflict of interest

The authors declare that the research was conducted in the absence of any commercial or financial relationships that could be construed as a potential conflict of interest.

1.6.2 Acknowledgements

The Natural Sciences and Engineering Council Canada (NSERC) is acknowledged for Discovery Grants awarded to FC and WS that enabled this collaborative research. Equipment and infrastructure used for this research were acquired and maintained by the Canada Foundation for Innovation and Quebec Strategic Networks (CQMF-QCAM, RQMP, and GCM). This work is supported by Defence Research and Development Canada through an IDEaS Micronet (CFPMN1-008) grant awarded to F.C.

CHAPTER 7 GENERAL DISCUSSION

In the following, the results of Chapters 4 to 6 are discussed as a whole with reference to the literature presented in Chapter 2. A detailed study of the fundamental properties of PEDOT:PSS is presented in this thesis, and many insights are gained in terms of processing, conductivity and mechanical stretchability. We demonstrated that electrospinning is a facile and convenient method to produce stretchable organic electronics. We were able to produce stretchable OECTs from a brittle conjugated polymer (PEDOT:tos) by exploiting the fiber morphology. Advanced methods are developed to combine the intrinsically enhanced stretchability and conductivity of PEDOT:PSS and the fiber production to lead to the fabrication of highly stretchable OECTs and ECDs.

In the chapter 4, OECTs were fabricated on PDMS substrates via the combination of electrospinning and vapor phase polymerization. We turned a brittle conjugated polymer into a stretchable material by exploiting the fiber morphology. We hypothesized that the transistor performances and stretchability can be tuned by controlling the morphology of the electrospun fibers. As a result, in the article 1, we showed that the conductivity of the fiber mats is as expected dependant of the quantity of the deposited fibers, but a plateau is reached, limiting the conductivity. More importantly, we demonstrated the formation of two distinct morphologies with great impact on both the conductivity and the stretchability. On one side, the fibers are stacked on the top of each other at their crossing point, leading to free to move fibers. On the other side, they can be fused, forming rigid nodes interconnecting fibers in a kind of network. The formation of such nodes induced an enhanced conductivity in the fiber mats by simplifying the inter fiber electron motion but also reduced their stretchability as a trade-off. This one was also observed in the OECTs' mechanical and electronic performances, where the presence of rigid nodes led to the best transistor performances but the most limited stretchability.

The knowledge we gained in the article 1 inspired us to focus on the production of node-free fiber mats in order to maximize the stretchability of the devices. The limited conductivity of PEDOT:Tos can be overcome by replacing it by its poly(styrene sulfonate) doped counterpart : PEDOT:PSS. Poly(styrene sulfonate) increases the conductivity of PEDOT by enhancing the formation of PEDOT rich clusters along its insulating backbone. Moreover, the tunability of PEDOT:PSS solution is of great interest in order to increase both the stretchability and conductivity of the fibers.

In the article 2, we used PEDOT:PSS instead of PEDOT:Tos as the conducting material to take advantage of a higher conductivity and a better processability. The fiber production has been simplified by removing the VPP step. We demonstrated that PEDOT:PSS fibers deposited on PDMS elastomer substrates can be successfully used as a substitute to ITO as transparent electrodes for organic electronics. Our electrodes offer the advantage to be stretchable up to 100% strain. We assembled stretchable electrochromic devices and demonstrated a reversible behavior even under 100% strain. The stress procured by the mechanical deformation induced a diminution of the charge quantity injected from the electrode to the electrochrome, and hence limiting the redox reaction responsible of the color switching. A stretching beyond 150% strain led to the definitive break of the electronic pathway, and the irreversible damage of the device.

Taking this behavior in consideration, we hypothesized that PEDOT:PSS can be a good candidate to produce stretchable OECTs from electrospun fibers, if we are able to increase its conductivity and ductility. In article 3, we chose to tune the intrinsic properties of PEDOT:PSS to increase both its stretchability and its conductivity. We demonstrated that the combination of electrospinning, in situ PEDOT:PSS doping and post treatment is a successful strategy to produce highly stretchable OECTs. PEG copolymer used in the electrospinning mixture act as a plasticizer to softened PEDOT:PSS, while an acidic post treatment drastically increase its conductivity. The as produced fibers took advantage of softened PEDOT:PSS to be stretched up to 200% while losing only 20% of the initial current. OECTs prepared from fibers showed stable transistor performances up to 100% strain and better performances than their thin film counterparts thanks to an increase of the surface contact with the gate medium due to the fiber shape.

In general, the fabrication methods we described can produce stretchable OECTs and electrochromic devices in a fast and reliable way. The fiber morphology was found to be of great interest to increase the stretchability of PEDOT:PSS and PEDOT:tos, even without a secondary doping treatment. More interestingly, the greater specific surface area of the fibers was directly used to improve transistor performances due to an increase of the reaction sites between the ion-gating medium and the gate channel. This particularity might also be exploited in future electronic devices involving electrochemical reactions as it provides a better response to stimuli. We believe the strategy we adopted in the article 3 by combining PEDOT:PSS doping and the electrospinning to optimize both the intrinsic and extrinsic properties will pave the way to highly stretchable

electronic organics. Despite there are still limitations for the materials or devices, this thesis contributes to the advancement of technology in organic electronics and we believe significant improvements can be achieved in the near future to meet the requirements for a large scale production and a commercial application.

CHAPTER 8 CONCLUSION AND RECOMMENDATIONS

This thesis explored the possibility to use the electrospinning as a reliable technic to produce stretchable organic electronics. We focused our work on one specific conjugated polymer, PEDOT, thanks to its commercial availability, biocompatibility and versatility. We developed a protocol to fabricate OECTs from a fiber mats in a fast and reliable way by combining plasma etching and electrode printing. The fabrication of a stretchable all organic electrochromic device demonstrated that PEDOT:PSS fibers are a promising alternative to ITO as transparent electrodes. Finally, we improved the transistor performances and the stretchability of OECTs by combining spun fibers and PEDOT:PSS post treatment. Although the results in terms of stretchability and OECT performances didn't break any record, our goal was to demonstrate the viability of electrospinning as a cost-effective and reliable technic to produce stretchable electronics. Its processability and its large-scale production capability also open the door to the production of commercial stretchable organic electronics.

In all of the three articles presented in this thesis we deposited either PEDOT:tos or PEDOT:PSS fibers on an elastomeric substrate. Since we worked with mechanically compliant objects, we didn't consider the impact of the interfacial adhesion between the fibers and the substrate. However, this parameter is of great importance for stretchable electrodes. It is known that because of the large difference in the mechanical and surfaces properties between the conductive film and the elastomeric substrate, debonding or delamination often happens under stretching. [337, 338] This problem is enhanced by the hydrophobic nature of PDMS while PEDOT:PSS is hydrophilic, leading to an insufficient interfacial strength between the two layers. One interesting solution, proposed by Gang Li et al. was to graft poly(methacrylic acid) onto pre-strained PDMS in order to create hydrogen bonding with a transferred PEDOT:PSS film.[338] As a result, the as-prepared conductive electrode showed a great stability over 10.000 cyclic stretching at 100% strain. However, pre-strained substrates may cause surface wrinkling of folding, which leads to a high surface roughness with a haze problem, which is not desirable to fabricate transparent electrodes. On the other hand, improving the adhesion between the PDMS substrate and the PEDOT:PSS using chemicals like poly(methacrylic acid) is of great interest, especially in our group since we are working with mechanically compliant structures like fibers or printed buckled patterns. The biocompatibility shouldn't be neglected and the impact of the adhesion strength on the

stretchability and stability might be studied in order to offer a pertinent solution in the field of bioelectronics.

The successful use of sulfuric acid as a post-treatment to increase the conductivity of the PEDOT:PSS fibers was a keystone in the transistor performances of the stretchable OECTs. We demonstrated the compatibility of a post-treatment and the use of a plasticizer in the electrospinning mixture with the formation of fibers. Sulfonate and sulfonimide anions contained in ionic liquids were found to act as great stretchability and conductivity enhancers, leading to stretchable PEDOT:PSS films as high as 800%, with a conductivity of 2000 S/cm.[208] These compounds have the ability to soften the PSS domains and to promote a better conductivity and a higher crystallinity in PEDOT. The use of such ionic liquids e.g. 4-(3-butyl-1-imidazolio)-1-butanesulfonic acid triflate or l-butyl-3-methylimidazolium octyl sulfate, in the electrospinning mixture or as poste-treatment might be of great interest in order to drastically improve the performances of stretchable organic electronics. Improved stretchability will unfortunately lead to fabrication problems as the design of OETCs and ECDs involve the use of metallic electrodes. In this thesis, we used a printable silver paste which was flexible enough to undergo a 100% strain without visible crack. Beyond this value, the electrodes started to crack, breaking the electrical pathway. The design of organic electronic devices might be rethought to take in consideration this constraint. The removal of solid metallic electrodes might, moreover, offer the advantage to move the industry towards less expensive, less poisonous and more recyclable friendly resources. Our group is actually working on the development of PEDOT:PSS inks. We believe that PEDOT:PSS can be tuned to be intrinsically stretchable while being printable. This affordable solution has a great potential as the demand for stretchable electrodes will undeniably increases over the years.

REFERENCES

1. Ross, I.M., *The foundation of the silicon age.* Bell Labs technical journal, 1997. **2**(4): p. 3-14.1. Ross, I.M., *The foundation of the silicon age.* Bell Labs technical journal, 1997. **2**(4): p. 3-14.
2. Wong, W.S. and A. Salleo, *Flexible electronics: materials and applications*. Vol. 11. 2009: Springer Science & Business Media.
3. Sun, Y. and J.A. Rogers, *Inorganic semiconductors for flexible electronics.* Advanced materials, 2007. **19**(15): p. 1897-1916.
4. Huang, D., et al., *Plastic-compatible low resistance printable gold nanoparticle conductors for flexible electronics.* Journal of the electrochemical society, 2003. **150**(7): p. G412.
5. Wang, P., et al., *The evolution of flexible electronics: from nature, beyond nature, and to nature.* Advanced Science, 2020. **7**(20): p. 2001116.
6. Kim, T., et al., *Realizing stretchable OLEDs: a hybrid platform based on rigid island arrays on a stress-relieving bilayer structure.* Advanced Materials Technologies, 2020. **5**(11): p. 2000494.
7. Yang, J.C., et al., *Electronic skin: recent progress and future prospects for skin-attachable devices for health monitoring, robotics, and prosthetics.* Advanced Materials, 2019. **31**(48): p. 1904765.
8. Mackanic, D.G., M. Kao, and Z. Bao, *Enabling deformable and stretchable batteries.* Advanced Energy Materials, 2020. **10**(29): p. 2001424.
9. Yu, K.J., et al., *Inorganic semiconducting materials for flexible and stretchable electronics.* NPJ Flexible Electronics, 2017. **1**(1): p. 1-14.
10. Lee, H., et al., *Stretchable organic optoelectronic devices: Design of materials, structures, and applications.* Materials Science and Engineering: R: Reports, 2021. **146**: p. 100631.
11. Teo, M.Y., et al., *Highly stretchable and highly conductive PEDOT: PSS/ionic liquid composite transparent electrodes for solution-processed stretchable electronics.* ACS applied materials & interfaces, 2017. **9**(1): p. 819-826.
12. Yan, J., et al., *Plasticizer and catalyst co-functionalized PEDOT: PSS enables stretchable electrochemical sensing of living cells.* Chemical science, 2021. **12**(43): p. 14432-14440.
13. Oh, J.Y., et al., *Conducting polymer dough for deformable electronics.* Advanced Materials, 2016. **28**(22): p. 4455-4461.
14. Sun, J., et al., *Self-healable, stretchable, transparent triboelectric nanogenerators as soft power sources.* ACS nano, 2018. **12**(6): p. 6147-6155.
15. Takei, A., et al., *Stretchable and durable Parylene/PEDOT: PSS/Parylene multi-layer induced by plastic deformation for stretchable device using functionalized PDMS.* AIP Advances, 2020. **10**(2): p. 025205.
16. Won, Y., et al., *Biocompatible, Transparent, and High-Areal-Coverage Kirigami PEDOT: PSS Electrodes for Electrooculography-Derived Human–Machine Interactions.* ACS sensors, 2021. **6**(3): p. 967-975.
17. Guan, Y.-S., et al., *Kirigami-inspired conducting polymer thermoelectrics from electrostatic recognition driven assembly.* ACS nano, 2018. **12**(8): p. 7967-7973.
18. Diao, Y., et al., *Kirigami electrodes of conducting polymer nanofibers for wearable humidity dosimeters and stretchable supercapacitors.* Journal of Materials Chemistry A, 2021. **9**(15): p. 9849-9857.

19. Upadhyay, A. and S. Karpagam, *Movement of new direction from conjugated polymer to semiconductor composite polymer nanofiber.* Reviews in Chemical Engineering, 2019. **35**(3): p. 351-375.
20. Chen, J.-Y., et al., *Solvent effects on morphology and electrical properties of poly (3-hexylthiophene) electrospun nanofibers.* Polymers, 2019. **11**(9): p. 1501.
21. Babaie, A., et al., *Synergistic effects of conductive PVA/PEDOT electrospun scaffolds and electrical stimulation for more effective neural tissue engineering.* European Polymer Journal, 2020. **140**: p. 110051.
22. Huang, Y., et al., *Mini-LED, Micro-LED and OLED displays: Present status and future perspectives.* Light: Science & Applications, 2020. **9**(1): p. 1-16.
23. Zhu, H., et al., *Printable semiconductors for backplane TFTs of flexible OLED displays.* Advanced Functional Materials, 2020. **30**(20): p. 1904588.
24. Tsai, K.W., et al., *Solution-processed thermally activated delayed fluorescent OLED with high EQE as 31% using high triplet energy crosslinkable hole transport materials.* Advanced Functional Materials, 2019. **29**(15): p. 1901025.
25. Chen, C.H., et al., *Novel photoinduced recovery of OFET memories based on ambipolar polymer electret for photorecorder application.* Advanced Functional Materials, 2019. **29**(40): p. 1902991.
26. Ditte, K., et al., *Rapid detection of SARS-CoV-2 antigens and antibodies using OFET biosensors based on a soft and stretchable semiconducting polymer.* ACS Biomaterials Science & Engineering, 2021.
27. Nikolka, M. and H. Sirringhaus, *Conjugated polymer-based OFET devices.* Conjugated Polymers: Properties, Processing, and Applications, 2019: p. 1-20.
28. Soylemez, S., et al., *A multipurpose conjugated polymer: Electrochromic device and biosensor construction for glucose detection.* Organic Electronics, 2019. **65**: p. 327-333.
29. Li, M., et al., *Colorless to black electrochromic devices using subtractive color mixing of two electrochromes: A conjugated polymer with a small organic molecule.* Organic Electronics, 2020. **84**: p. 105748.
30. Zhang, L., et al., *Liquid/Liquid Interfacial Suzuki Polymerization Prepared Novel Triphenylamine-Based Conjugated Polymer Films with Excellent Electrochromic Properties.* ACS Applied Materials & Interfaces, 2021. **13**(17): p. 20810-20820.
31. Mariani, F., et al., *PEDOT: dye-based, flexible organic electrochemical transistor for highly sensitive pH monitoring.* ACS applied materials & interfaces, 2018. **10**(26): p. 22474-22484.
32. Wang, Y.-F., et al., *Fully printed PEDOT: PSS-based temperature sensor with high humidity stability for wireless healthcare monitoring.* Scientific reports, 2020. **10**(1): p. 1-8.
33. Savikhin, V., et al., *Impact of polymer side chain modification on OPV morphology and performance.* Chemistry of Materials, 2018. **30**(21): p. 7872-7884.
34. Yang, S.S., et al., *Toward High-Performance Polymer Photovoltaic Devices for Low-Power Indoor Applications.* Solar RRL, 2017. **1**(12): p. 1700174.
35. Gu, X., et al., *Roll-to-roll printed large-area all-polymer solar cells with 5% efficiency based on a low crystallinity conjugated polymer blend.* Advanced Energy Materials, 2017. **7**(14): p. 1602742.
36. Macher, S., et al., *New roll-to-roll processable PEDOT-based polymer with colorless bleached state for flexible electrochromic devices.* Advanced Functional Materials, 2020. **30**(6): p. 1906254.

37. Jadoun, S. and U. Riaz, *Conjugated polymer light-emitting diodes.* Polymers for Light-Emitting Devices and Displays, 2020: p. 77-98.
38. Ciocca, M., et al., *Colour-sensitive conjugated polymer inkjet-printed pixelated artificial retina model studied via a bio-hybrid photovoltaic device.* Scientific reports, 2020. **10**(1): p. 1-15.
39. Lo, L.-W., et al., *An inkjet-printed PEDOT: PSS-based stretchable conductor for wearable health monitoring device applications.* ACS Applied Materials & Interfaces, 2021. **13**(18): p. 21693-21702.
40. Nübling, F., H. Komber, and M. Sommer, *All-conjugated, all-crystalline donor–acceptor block copolymers p3ht-b-pndit2 via direct arylation polycondensation.* Macromolecules, 2017. **50**(5): p. 1909-1918.
41. Schiefer, D., R. Hanselmann, and M. Sommer, *All-conjugated P3HT donor PCDTBT acceptor graft copolymers synthesised via a grafting through approach.* Polymer Chemistry, 2017. **8**(30): p. 4368-4377.
42. Dianatdar, A., et al., *Polytriphenylamine composites for energy storage electrodes: effect of pendant vs. backbone polymer architecture of the electroactive group.* RSC Advances, 2021. **11**(56): p. 35187-35196.
43. Nad, S. and S. Malik, *Design, synthesis, and electrochromic behaviors of donor-acceptor-donor type triphenylamine-iso-naphthalenediimide derivatives.* ChemElectroChem, 2020. **7**(19): p. 4144-4152.
44. Lv, X., et al., *Colorless to Multicolored, Fast Switching, and Highly Stable Electrochromic Devices Based on Thermally Cross-Linking Copolymer*. ACS Applied Materials & Interfaces, 2021. **13**(35): p. 41826-41835.
45. Gueye, M.N., et al., *Progress in understanding structure and transport properties of PEDOT-based materials: A critical review.* Progress in Materials Science, 2020. **108**: p. 100616.
46. Luo, R., et al., *A simple strategy for high stretchable, flexible and conductive polymer films based on PEDOT: PSS-PDMS blends.* Organic Electronics, 2020. **76**: p. 105451.
47. Kayser, L.V. and D.J. Lipomi, *Stretchable conductive polymers and composites based on PEDOT and PEDOT: PSS.* Advanced Materials, 2019. **31**(10): p. 1806133.
48. Li, X., et al., *Electrospinning-based strategies for battery materials.* Advanced Energy Materials, 2021. **11**(2): p. 2000845.
49. Liu, T., et al., *Embedding amorphous lithium vanadate into carbon nanofibers by electrospinning as a high-performance anode material for lithium-ion batteries.* Journal of Colloid and Interface Science, 2020. **580**: p. 21-29.
50. Cai, M., et al., *Lithium ion battery separator with improved performance via side-by-side bicomponent electrospinning of PVDF-HFP/PI followed by 3D thermal crosslinking.* Journal of Power Sources, 2020. **461**: p. 228123.
51. Morais, P.V., et al., *High gas sensor performance of WO3 nanofibers prepared by electrospinning.* Journal of Alloys and Compounds, 2021. **864**: p. 158745.
52. Al-Hazeem, N.Z., et al., *Hydrogen gas sensor based on nanofibers TiO 2-PVP thin film at room temperature prepared by electrospinning.* Microsystem Technologies, 2021. **27**(1): p. 293-299.
53. Hittini, W., et al., *Ultrasensitive and low temperature gas sensor based on electrospun organic-inorganic nanofibers.* Organic Electronics, 2020. **81**: p. 105659.

54. Jayathilaka, W., A. Chinnappan, and S. Ramakrishna, *Electrospinning of luminescence nanofibers: Current and future trends in wearable light-emitting devices*, in *Electrospun Polymers and Composites*. 2021, Elsevier. p. 383-404.
55. Ercan, E., et al., *One-dimensional micro-scale patterned conjugated polymer structures in bilayer architecture and light emitting diode application.* Organic Electronics, 2020. **87**: p. 105965.
56. Xing, Y., et al., *Optoelectronic functional fibers: materials, fabrication, and application for smart textiles.* Journal of Materials Chemistry C, 2021. **9**(2): p. 439-455.
57. Kondawar, S.B., M.A. Haque, and C.N. Pangul, *Application of Electrospun Materials in LEDs.* Polymers for Light-Emitting Devices and Displays, 2020: p. 99-123.
58. Qin, Z., et al., *Enhancing physical properties of chitosan/pullulan electrospinning nanofibers via green crosslinking strategies.* Carbohydrate Polymers, 2020. **247**: p. 116734.
59. Shu, D., et al., *One-step electrospinning cellulose nanofibers with superhydrophilicity and superoleophobicity underwater for high-efficiency oil-water separation.* International Journal of Biological Macromolecules, 2020. **162**: p. 1536-1545.
60. Pakravan, M., M.-C. Heuzey, and A. Ajji, *A fundamental study of chitosan/PEO electrospinning.* Polymer, 2011. **52**(21): p. 4813-4824.
61. Rwei, S.-P. and C.-C. Huang, *Electrospinning PVA solution-rheology and morphology analyses.* Fibers and Polymers, 2012. **13**(1): p. 44-50.
62. Lyu, J.-Y., et al., *Fabrication of high-performance graphene oxide doped PVDF/CuO/Al nanocomposites via electrospinning.* Chemical Engineering Journal, 2019. **368**: p. 129-137.
63. Wang, W., et al., *Synthesis, morphology and electrochemical performances of perovskite-type oxide LaxSr1-xFeO3 nanofibers prepared by electrospinning.* Journal of Physics and Chemistry of Solids, 2019. **124**: p. 144-150.
64. Wang, D., L. Wang, and G. Shen, *Nanofiber/nanowires-based flexible and stretchable sensors.* Journal of Semiconductors, 2020. **41**(4): p. 041605.
65. Pan, J.-L., et al., *Ultrathin and strong electrospun porous fiber separator.* ACS Applied Energy Materials, 2018. **1**(9): p. 4794-4803.
66. Liu, L.-G. and J.-H. He, *Solvent evaporation in a binary solvent system for controllable fabrication of porous fibers by electrospinning.* Thermal Science, 2017. **21**(4): p. 1821-1825.
67. Lee, C.-G., et al., *Porous electrospun fibers embedding TiO2 for adsorption and photocatalytic degradation of water pollutants.* Environmental science & technology, 2018. **52**(7): p. 4285-4293.
68. Qin, Z., et al., *Coaxial electrospinning for flexible uniform white-light-emitting porous fibrous membrane.* Materials & Design, 2018. **147**: p. 175-181.
69. Huang, Y., et al., *Robust preparation of tubular PTFE/FEP ultrafine fibers-covered porous membrane by electrospinning for continuous highly effective oil/water separation.* Journal of Membrane Science, 2018. **568**: p. 87-96.
70. Yoon, J., et al., *Recent progress in coaxial electrospinning: New parameters, various structures, and wide applications.* Advanced Materials, 2018. **30**(42): p. 1704765.
71. Pant, B., M. Park, and S.-J. Park, *Drug delivery applications of core-sheath nanofibers prepared by coaxial electrospinning: a review.* Pharmaceutics, 2019. **11**(7): p. 305.
72. Han, D. and A.J. Steckl, *Coaxial electrospinning formation of complex polymer fibers and their applications.* ChemPlusChem, 2019. **84**(10): p. 1453-1497.
73. Reneker, D.H., et al., *Bending instability of electrically charged liquid jets of polymer solutions in electrospinning.* Journal of Applied physics, 2000. **87**(9): p. 4531-4547.

74. Taylor, G.I., *Electrically driven jets.* Proceedings of the Royal Society of London. A. Mathematical and Physical Sciences, 1969. **313**(1515): p. 453-475.
75. Alharbi, A.R., et al., *Highly hydrophilic electrospun polyacrylonitrile/polyvinypyrrolidone nanofibers incorporated with gentamicin as filter medium for dam water and wastewater treatment.* Journal of Membrane and Separation Technology, 2016. **5**(2): p. 38-56.
76. Zaarour, B., L. Zhu, and X. Jin, *Controlling the surface structure, mechanical properties, crystallinity, and piezoelectric properties of electrospun PVDF nanofibers by maneuvering molecular weight.* Soft Materials, 2019. **17**(2): p. 181-189.
77. Park, B.K. and I.C. Um, *Effect of molecular weight on electro-spinning performance of regenerated silk.* International journal of biological macromolecules, 2018. **106**: p. 1166-1172.
78. Jian, S., et al., *Nanofibers with diameter below one nanometer from electrospinning.* RSC advances, 2018. **8**(9): p. 4794-4802.
79. Angel, N., et al., *Effect of processing parameters on the electrospinning of cellulose acetate studied by response surface methodology.* Journal of Agriculture and Food Research, 2020. **2**: p. 100015.
80. Lasprilla-Botero, J., M. Álvarez-Láinez, and J. Lagaron, *The influence of electrospinning parameters and solvent selection on the morphology and diameter of polyimide nanofibers.* Materials Today Communications, 2018. **14**: p. 1-9.
81. Angammana, C.J. and S.H. Jayaram, *Analysis of the effects of solution conductivity on electrospinning process and fiber morphology.* IEEE Transactions on industry applications, 2011. **47**(3): p. 1109-1117.
82. Fan, L., et al., *Effect of salt concentration in spinning solution on fiber diameter and mechanical property of electrospun styrene-butadiene-styrene tri-block copolymer membrane.* Polymer, 2018. **153**: p. 61-69.
83. Bakar, S., et al. *Effect of voltage and flow rate electrospinning parameters on polyacrylonitrile electrospun fibers*. in *IOP Conference Series: Materials Science and Engineering*. 2018. IOP Publishing.
84. Joy, N., et al., *Coupling between voltage and tip-to-collector distance in polymer electrospinning: Insights from analysis of regimes, transitions and cone/jet features.* Chemical Engineering Science, 2021. **230**: p. 116200.
85. Motamedi, A.S., et al., *Effect of electrospinning parameters on morphological properties of PVDF nanofibrous scaffolds.* Progress in biomaterials, 2017. **6**(3): p. 113-123.
86. Drosou, C., M. Krokida, and C.G. Biliaderis, *Composite pullulan-whey protein nanofibers made by electrospinning: Impact of process parameters on fiber morphology and physical properties.* Food Hydrocolloids, 2018. **77**: p. 726-735.
87. Arifin, Z., S. Hadi, and S.D. Prasetyo. *Characteristics of ZnO nanofiber in double Layer (TiO2/ZnO) DSSC results of direct deposition electrospinning manufacturing: Variation of tip to collector distance*. in *IOP Conference Series: Materials Science and Engineering*. 2021. IOP Publishing.
88. Korycka, P., et al., *Effect of electrospinning process variables on the size of polymer fibers and bead-on-string structures established with a 23 factorial design.* Beilstein journal of nanotechnology, 2018. **9**(1): p. 2466-2478.
89. Veerabhadraiah, A., et al., *Development of polyvinyl acetate thin films by electrospinning for sensor applications.* Applied Nanoscience, 2017. **7**(7): p. 355-363.
90. Verpoorten, E., et al., *Electrospun PEO/PEDOT: PSS nanofibers for wearable physiological flex sensors.* Sensors, 2021. **21**(12): p. 4110.

91. Huang, C.-Y. and C.-W. Chiu, *Facile fabrication of a stretchable and flexible nanofiber carbon film-sensing electrode by electrospinning and its application in smart clothing for ECG and EMG monitoring.* ACS Applied Electronic Materials, 2021. **3**(2): p. 676-686.
92. Tseghai, G.B., et al., *PEDOT: PSS-based conductive textiles and their applications.* Sensors, 2020. **20**(7): p. 1881.
93. Fallahi, A., et al., *Flexible and Stretchable PEDOT-Embedded Hybrid Substrates for Bioengineering and Sensory Applications.* ChemNanoMat, 2019. **5**(6): p. 729-737.
94. Chotimah, C., et al., *Electrospun Nanofiber Poly (3, 4-ethylenedioxytriophene): poly (styrene sulfonate)/poly (vinyl alcohol) as Strain Sensor Application.* Journal of Science and Applicative Technology, 2021. **5**(2): p. 342-347.
95. He, X., et al., *PEDOT: PSS/CNT composites based ultra-stretchable thermoelectrics and their application as strain sensors.* Composites Communications, 2021. **27**: p. 100822.
96. Yan, Y., et al., *Electrospun Nanofibers for New Generation Flexible Energy Storage.* Energy & Environmental Materials, 2021. **4**(4): p. 502-521.
97. Yun, T.G., et al., *All-transparent stretchable electrochromic supercapacitor wearable patch device.* ACS nano, 2019. **13**(3): p. 3141-3150.
98. Cárdenas-Martínez, J., et al., *Flexible and transparent supercapacitors using electrospun PEDOT: PSS electrodes.* Synthetic Metals, 2020. **267**: p. 116436.
99. Park, Y.W., et al., *Electrical transport in doped polyacetylene.* The Journal of Chemical Physics, 1980. **73**(2): p. 946-957.
100. Heeger, A.J., *Semiconducting and metallic polymers: the fourth generation of polymeric materials (Nobel lecture).* Angewandte Chemie International Edition, 2001. **40**(14): p. 2591-2611.
101. Ouyang, J., *"Secondary doping" methods to significantly enhance the conductivity of PEDOT: PSS for its application as transparent electrode of optoelectronic devices.* Displays, 2013. **34**(5): p. 423-436.
102. Printz, A.D. and D.J. Lipomi, *Competition between deformability and charge transport in semiconducting polymers for flexible and stretchable electronics.* Applied Physics Reviews, 2016. **3**(2): p. 021302.
103. Noriega, R., et al., *A general relationship between disorder, aggregation and charge transport in conjugated polymers.* Nature materials, 2013. **12**(11): p. 1038.
104. Chiang, C.K., et al., *Electrical conductivity in doped polyacetylene.* Physical review letters, 1977. **39**(17): p. 1098.
105. Bredas, J.L. and G.B. Street, *Polarons, bipolarons, and solitons in conducting polymers.* Accounts of Chemical Research, 1985. **18**(10): p. 309-315.
106. Massuyeau, F., *Etudes photophysiques d'un polymère conjugué nanostructuré: du film nanocomposite à la nanofibre*. 2008, Université de Nantes.
107. Sirringhaus, H., *Device physics of solution-processed organic field-effect transistors.* Advanced Materials, 2005. **17**(20): p. 2411-2425.
108. Clemens, W., *Polymer electronics,* in *Technology Guide*. 2009, Springer. p. 84-87.
109. Devreese, J.T., *Polarons.* Encycl. Appl. Phys., 1996. **14**(cond-mat/0004497): p. 383-409.
110. BELJONNE, D. and J. CORNIL, *Senseurs chimiques et biologiques basés sur des polymères conjugués*. 2006: Ed. Techniques Ingénieur.
111. Shi, K., et al., *Toward high performance n-type thermoelectric materials by rational modification of BDPPV backbones.* Journal of the American Chemical Society, 2015. **137**(22): p. 6979-6982.

112. Wang, Y., et al., *Naphthodithiophenediimide–benzobisthiadiazole-based polymers: versatile n-type materials for field-effect transistors and thermoelectric devices.* Macromolecules, 2017. **50**(3): p. 857-864.
113. Reynolds, J.R., B.C. Thompson, and T.A. Skotheim, *Conjugated polymers: perspective, theory, and new materials*. 2019: CRC Press.
114. Diaz, A. and J. Logan, *Electroactive polyaniline films.* Journal of Electroanalytical Chemistry and Interfacial Electrochemistry, 1980. **111**(1): p. 111-114.
115. Diaz, A., K.K. Kanazawa, and G.P. Gardini, *Electrochemical polymerization of pyrrole.* Journal of the Chemical Society, Chemical Communications, 1979(14): p. 635-636.
116. Tourillon, G. and F. Garnier, *New electrochemically generated organic conducting polymers.* Journal of Electroanalytical Chemistry and Interfacial Electrochemistry, 1982. **135**(1): p. 173-178.
117. McCullough, R.D., *The chemistry of conducting polythiophenes.* Advanced Materials, 1998. **10**(2): p. 93-116.
118. MacDiarmid, A. and A.J. Epstein, *The concept of secondary doping as applied to polyaniline.* Synthetic metals, 1994. **65**(2-3): p. 103-116.
119. Kim, J., et al., *Enhancement of electrical conductivity of poly (3, 4-ethylenedioxythiophene)/poly (4-styrenesulfonate) by a change of solvents.* Synthetic Metals, 2002. **126**(2-3): p. 311-316.
120. Jönsson, S., et al., *The effects of solvents on the morphology and sheet resistance in poly (3, 4-ethylenedioxythiophene)–polystyrenesulfonic acid (PEDOT–PSS) films.* Synthetic metals, 2003. **139**(1): p. 1-10.
121. Ouyang, J., et al., *On the mechanism of conductivity enhancement in poly (3, 4-ethylenedioxythiophene): poly (styrene sulfonate) film through solvent treatment.* Polymer, 2004. **45**(25): p. 8443-8450.
122. Kim, Y.H., et al., *Highly conductive PEDOT: PSS electrode with optimized solvent and thermal post-treatment for ITO-free organic solar cells.* Advanced Functional Materials, 2011. **21**(6): p. 1076-1081.
123. Niu, Q., et al., *Understanding the mechanism of PEDOT: PSS modification via solvent on the morphology of perovskite films for efficient solar cells.* Synthetic Metals, 2018. **243**: p. 17-24.
124. Nardes, A.M., R.A. Janssen, and M. Kemerink, *A morphological model for the solvent-enhanced conductivity of PEDOT: PSS thin films.* Advanced Functional Materials, 2008. **18**(6): p. 865-871.
125. Döbbelin, M., et al., *Influence of ionic liquids on the electrical conductivity and morphology of PEDOT: PSS films.* Chemistry of materials, 2007. **19**(9): p. 2147-2149.
126. Xia, Y. and J. Ouyang, *Significant conductivity enhancement of conductive poly (3, 4-ethylenedioxythiophene): poly (styrenesulfonate) films through a treatment with organic carboxylic acids and inorganic acids.* ACS applied materials & interfaces, 2010. **2**(2): p. 474-483.
127. Meng, W., et al., *Conductivity enhancement of PEDOT: PSS films via phosphoric acid treatment for flexible all-plastic solar cells.* ACS Applied Materials & Interfaces, 2015. **7**(25): p. 14089-14094.
128. Xia, Y., K. Sun, and J. Ouyang, *Solution-processed metallic conducting polymer films as transparent electrode of optoelectronic devices.* Advanced materials, 2012. **24**(18): p. 2436-2440.

129. Kim, N., et al., *Highly conductive PEDOT: PSS nanofibrils induced by solution-processed crystallization.* Advanced materials, 2014. **26**(14): p. 2268-2272.
130. Kim, N., et al., *Highly conductive all-plastic electrodes fabricated using a novel chemically controlled transfer-printing method.* Advanced Materials, 2015. **27**(14): p. 2317-2323.
131. Lang, U., N. Naujoks, and J. Dual, *Mechanical characterization of PEDOT: PSS thin films.* Synthetic Metals, 2009. **159**(5-6): p. 473-479.
132. Dauzon, E., et al., *Conducting and stretchable PEDOT: PSS electrodes: Role of additives on self-assembly, morphology, and transport.* ACS applied materials & interfaces, 2019. **11**(19): p. 17570-17582.
133. Savagatrup, S., et al., *Plasticization of PEDOT: PSS by common additives for mechanically robust organic solar cells and wearable sensors.* Advanced Functional Materials, 2015. **25**(3): p. 427-436.
134. Li, Y., et al., *Highly stretchable PEDOT: PSS organic electrochemical transistors achieved via polyethylene glycol addition.* Flexible and Printed Electronics, 2019. **4**(4): p. 044004.
135. Zhang, S., et al., *Patterning of stretchable organic electrochemical transistors.* Chemistry of Materials, 2017. **29**(7): p. 3126-3132.
136. Wen, Z., et al., *A wrinkled PEDOT: PSS film based stretchable and transparent triboelectric nanogenerator for wearable energy harvesters and active motion sensors.* Advanced Functional Materials, 2018. **28**(37): p. 1803684.
137. Lipomi, D.J., et al., *Toward mechanically robust and intrinsically stretchable organic solar cells: Evolution of photovoltaic properties with tensile strain.* Solar energy materials and solar cells, 2012. **107**: p. 355-365.
138. Seol, Y.G., et al., *Nanocomposites of reduced graphene oxide nanosheets and conducting polymer for stretchable transparent conducting electrodes.* Journal of Materials Chemistry, 2012. **22**(45): p. 23759-23766.
139. Hansen, T.S., et al., *Highly stretchable and conductive polymer material made from poly (3, 4-ethylenedioxythiophene) and polyurethane elastomers.* Advanced functional materials, 2007. **17**(16): p. 3069-3073.
140. Teng, C., et al., *Polymer in situ embedding for highly flexible, stretchable and water stable PEDOT: PSS composite conductors.* Rsc Advances, 2013. **3**(20): p. 7219-7223.
141. Tang, Y. and J. Yin, *Design of cut unit geometry in hierarchical kirigami-based auxetic metamaterials for high stretchability and compressibility.* Extreme Mechanics Letters, 2017. **12**: p. 77-85.
142. Sun, B., et al., *Recent advances in flexible and stretchable electronic devices via electrospinning.* Journal of Materials Chemistry C, 2014. **2**(7): p. 1209-1219.
143. Lv, X., et al., *Ultra-stretchable membrane with high electrical and thermal conductivity via electrospinning and in-situ nanosilver deposition.* Composites Science and Technology, 2020. **200**: p. 108414.
144. Chen, J.-Y., et al., *Electrospinning-induced elastomeric properties of conjugated polymers for extremely stretchable nanofibers and rubbery optoelectronics.* Journal of Materials Chemistry C, 2020. **8**(3): p. 873-882.
145. Boubée de Gramont, F., et al., *Highly stretchable electrospun conducting polymer nanofibers.* Applied Physics Letters, 2017. **111**(9): p. 093701.
146. William, S., *Circuit element utilizing semiconductive material*. 1951, Google Patents.
147. White, H.S., G.P. Kittlesen, and M.S. Wrighton, *Chemical derivatization of an array of three gold microelectrodes with polypyrrole: fabrication of a molecule-based transistor.* Journal of the American Chemical Society, 1984. **106**(18): p. 5375-5377.

148. Ponder Jr, J.F., A.M. Osterholm, and J.R. Reynolds, *Conjugated polyelectrolytes as water processable precursors to aqueous compatible redox active polymers for diverse applications: electrochromism, charge storage, and biocompatible organic electronics.* Chemistry of Materials, 2017. **29**(10): p. 4385-4392.
149. Malti, A., et al., *An organic mixed ion–electron conductor for power electronics.* Advanced science, 2016. **3**(2): p. 1500305.
150. Bernards, D.A. and G.G. Malliaras, *Steady-state and transient behavior of organic electrochemical transistors.* Advanced Functional Materials, 2007. **17**(17): p. 3538-3544.
151. Rivnay, J., et al., *Organic electrochemical transistors.* Nature Reviews Materials, 2018. **3**(2): p. 1-14.
152. Khodagholy, D., et al., *High transconductance organic electrochemical transistors.* Nature communications, 2013. **4**(1): p. 1-6.
153. Torsi, L., et al., *Multi-parameter gas sensors based on organic thin-film-transistors.* Sensors and Actuators B: Chemical, 2000. **67**(3): p. 312-316.
154. Scheiblin, G., et al., *Referenceless pH sensor using organic electrochemical transistors.* Advanced Materials Technologies, 2017. **2**(2): p. 1600141.
155. Fenoy, G.E., et al., *PEDOT: Tosylate-Polyamine-Based Organic Electrochemical Transistors for High-Performance Bioelectronics.* Advanced Electronic Materials, 2021: p. 2100059.
156. Majak, D., J. Fan, and M. Gupta, *Fully 3D printed OECT based logic gate for detection of cation type and concentration.* Sensors and Actuators B: Chemical, 2019. **286**: p. 111-118.
157. Demuru, S., B.P. Kunnel, and D. Briand, *Thin film organic electrochemical transistors based on hybrid PANI/PEDOT: PSS active layers for enhanced pH sensing.* Biosensors and Bioelectronics: X, 2021. **7**: p. 100065.
158. Keene, S.T., et al., *Wearable organic electrochemical transistor patch for multiplexed sensing of calcium and ammonium ions from human perspiration.* Advanced healthcare materials, 2019. **8**(24): p. 1901321.
159. Coppedè, N., et al., *Ion selective textile organic electrochemical transistor for wearable sweat monitoring.* Organic Electronics, 2020. **78**: p. 105579.
160. van der Pol, T.P., et al., *The mechanism of dedoping PEDOT: PSS by aliphatic polyamines.* The Journal of Physical Chemistry C, 2019. **123**(39): p. 24328-24337.
161. Keene, S.T., et al., *Enhancement-Mode PEDOT: PSS Organic Electrochemical Transistors Using Molecular De-Doping.* Advanced Materials, 2020. **32**(19): p. 2000270.
162. Deb, S., *A novel electrophotographic system.* Applied Optics, 1969. **8**(101): p. 192-195.
163. Yin, Y., et al., *Design strategy for efficient solution-processable red electrochromic polymers based on unconventional 3, 6-bis (dodecyloxy) thieno [3, 2-b] thiophene building blocks.* Macromolecules, 2018. **51**(19): p. 7853-7862.
164. Stec, G.J., et al., *Multicolor electrochromic devices based on molecular plasmonics.* ACS nano, 2017. **11**(3): p. 3254-3261.
165. Chaudhary, A., et al., *Polythiophene–PCBM-based all-organic electrochromic device: fast and flexible.* ACS Applied Electronic Materials, 2019. **1**(1): p. 58-63.
166. Ling, H., et al., *Automatic light-adjusting electrochromic device powered by perovskite solar cell.* Nature communications, 2021. **12**(1): p. 1-8.
167. Chang, I., B. Gilbert, and T. Sun, *Electrochemichromic systems for display applications.* Journal of The Electrochemical Society, 1975. **122**(7): p. 955.

168. Yen, H.-J. and G.-S. Liou, *Novel blue and red electrochromic poly (azomethine ether) s based on electroactive triphenylamine moieties.* Organic Electronics, 2010. **11**(2): p. 299-310.
169. Lai, J.-C., et al., *A new multicolored and near-infrared electrochromic material based on triphenylamine-containing poly (3, 4-dithienylpyrrole).* Organic Electronics, 2014. **15**(12): p. 3735-3745.
170. Kim, K.-W., et al., *Novel triphenylamine containing poly-viologen for voltage-tunable multi-color electrochromic device.* Dyes and Pigments, 2021. **190**: p. 109321.
171. Lacroix, J., K. Kanazawa, and A. Diaz, *Polyaniline: A very fast electrochromic material.* Journal of the electrochemical society, 1989. **136**(5): p. 1308.
172. Wang, X.-J., et al., *In-situ characterization of electrochromism based on ITO/PEDOT: PSS towards preparation of high performance device.* Chinese Physics B, 2015. **25**(2): p. 028201.
173. Lv, X., et al., *Polymeric electrochromic materials with donor–acceptor structures.* Journal of Materials Chemistry C, 2017. **5**(1): p. 12-28.
174. Wan, Z., et al., *Multicolored, Low-Voltage-Driven, Flexible Organic Electrochromic Devices Based on Oligomers.* Macromolecular rapid communications, 2018. **39**(10): p. 1700886.
175. Soyleyici, H.C., *Electrochromic properties of multifunctional conductive polymer based on naphthalene.* Optical Materials, 2019. **90**: p. 208-214.
176. Sun, Y., et al., *Multicolored cathodically coloring electrochromism and electrofluorochromism in regioisomeric star-shaped carbazole dibenzofurans.* ACS Applied Materials & Interfaces, 2020. **12**(21): p. 24156-24164.
177. Liou, G.S., et al., *Synthesis and electrochromism of novel organosoluble polyarylates bearing triphenylamine moieties.* Journal of Polymer Science Part A: Polymer Chemistry, 2007. **45**(10): p. 2004-2014.
178. Yen, H.-J. and G.-S. Liou, *Enhanced near-infrared electrochromism in triphenylamine-based aramids bearing phenothiazine redox centers.* Journal of Materials Chemistry, 2010. **20**(44): p. 9886-9894.
179. Lin, H.-T., C.-L. Huang, and G.-S. Liou, *Design, synthesis, and electrofluorochromism of new triphenylamine derivatives with AIE-active pendent groups.* ACS applied materials & interfaces, 2019. **11**(12): p. 11684-11690.
180. Malagoli, M. and J.-L. Brédas, *Density functional theory study of the geometric structure and energetics of triphenylamine-based hole-transporting molecules.* Chemical Physics Letters, 2000. **327**(1-2): p. 13-17.
181. Zhan, C.-G., J.A. Nichols, and D.A. Dixon, *Ionization potential, electron affinity, electronegativity, hardness, and electron excitation energy: molecular properties from density functional theory orbital energies.* The Journal of Physical Chemistry A, 2003. **107**(20): p. 4184-4195.
182. Wang, J., et al., *Triarylamine: versatile platform for organic, dye-sensitized, and perovskite solar cells.* Chemical reviews, 2016. **116**(23): p. 14675-14725.
183. Kim, Y., et al., *Design of intrinsically stretchable and highly conductive polymers for fully stretchable electrochromic devices.* Scientific reports, 2020. **10**(1): p. 1-12.
184. Wang, M., et al., *Electrochromic smart windows can achieve an absolute private state through thermochromically engineered electrolyte.* Advanced Energy Materials, 2019. **9**(21): p. 1900433.

185. Xu, J.W., M.H. Chua, and K.W. Shah, *Electrochromic Smart Materials: Fabrication and Applications*. 2019: Royal Society of Chemistry.
186. Yu, H., et al., *Side-chain engineering of green color electrochromic polymer materials: toward adaptive camouflage application.* Journal of Materials Chemistry C, 2016. **4**(12): p. 2269-2273.
187. Rai, V., et al., *A review on recent advances in electrochromic devices: a material approach.* Advanced Engineering Materials, 2020. **22**(8): p. 2000082.
188. Chaudhary, A., et al., *Raw hibiscus extract as redox active biomaterial for novel herbal electrochromic device.* Solar Energy Materials and Solar Cells, 2020. **215**: p. 110588.
189. Lv, X., et al., *An all-solid-state polymeric electrochromic device based on two well-matched electrodes with fast switching time and excellent cycling stability.* Reactive and Functional Polymers, 2020. **156**: p. 104737.
190. Ko, I.J., et al., *An optically efficient full-color reflective display with an electrochromic device and color production units.* Journal of Information Display, 2019. **20**(3): p. 155-160.
191. Ko, I.J., et al., *High-Performance Reflective Electrochromic Device by Integrating White Reflector and High Optical Density Electrochromic System.* Advanced Materials Interfaces, 2019. **6**(18): p. 1900710.
192. Beaujuge, P.M. and J.R. Reynolds, *Color control in π-conjugated organic polymers for use in electrochromic devices.* Chemical reviews, 2010. **110**(1): p. 268-320.
193. Hassab, S., et al., *A new standard method to calculate electrochromic switching time.* Solar Energy Materials and Solar Cells, 2018. **185**: p. 54-60.
194. Neerinck, D. and T. Vink, *Depth profiling of thin ITO films by grazing incidence X-ray diffraction.* Thin Solid Films, 1996. **278**(1-2): p. 12-17.
195. Hamasha, M.M., et al., *Reliability of indium tin oxide thin films: Properties under mechanical and thermal loads*, in *Indium: Properties, Technological Applications and Health Issues*. 2013, Nova Science. p. 159-186.
196. Liu, J., et al., *Highly stretchable and flexible graphene/ITO hybrid transparent electrode.* Nanoscale research letters, 2016. **11**(1): p. 1-7.
197. Macher, S., et al., *Avoiding Voltage-Induced Degradation in PET-ITO-Based Flexible Electrochromic Devices.* ACS Applied Materials & Interfaces, 2020. **12**(32): p. 36695-36705.
198. Rakibuddin, M., M.A. Shinde, and H. Kim, *Sol-gel fabrication of NiO and NiO/WO3 based electrochromic device on ITO and flexible substrate.* Ceramics International, 2020. **46**(7): p. 8631-8639.
199. Lee, S.-M., et al., *Asymmetric ITO/Ag/ZTO and ZTO/Ag/ITO anodes prepared by roll-to-roll sputtering for flexible organic light-emitting diodes.* Surface and Coatings Technology, 2018. **343**: p. 115-120.
200. Bi, C., et al., *Efficient flexible solar cell based on composition-tailored hybrid perovskite.* Advanced Materials, 2017. **29**(30): p. 1605900.
201. Zhao, P., et al., *Stretchable electrochromic devices enabled via shape memory alloy composites (SMAC) for dynamic camouflage.* Optical Materials, 2019. **94**: p. 378-386.
202. Lee, C., et al., *Flash-induced nanowelding of silver nanowire networks for transparent stretchable electrochromic devices.* Scientific reports, 2018. **8**(1): p. 1-10.
203. Liu, H.-S., B.-C. Pan, and G.-S. Liou, *Highly transparent AgNW/PDMS stretchable electrodes for elastomeric electrochromic devices.* Nanoscale, 2017. **9**(7): p. 2633-2639.
204. Hao, T., et al., *Stretchable Electrochromic Devices Based on Embedded WO3@ AgNW Core-Shell Nanowire Elastic Conductors.* Chemical Engineering Journal, 2021: p. 130840.

205. Zhao, S.-Q., et al., *Self-supporting, ultra-thin and highly transparent conducting nickel grids for extremely flexible and stretchable electrochromic devices.* Optics Express, 2021. **29**(16): p. 25254-25269.
206. Lee, J., et al., *Improved electrochromic device performance from silver grid on flexible transparent conducting electrode prepared by electrohydrodynamic jet printing.* Journal of Materials Chemistry C, 2017. **5**(48): p. 12800-12806.
207. Lee, J.H., et al., *Highly conductive, stretchable, and transparent PEDOT: PSS electrodes fabricated with triblock copolymer additives and acid treatment.* ACS applied materials & interfaces, 2018. **10**(33): p. 28027-28035.
208. Wang, Y., et al., *A highly stretchable, transparent, and conductive polymer.* Science advances, 2017. **3**(3): p. e1602076.
209. Cui, Y., et al., *A Stretchable and Transparent Electrode Based on PEGylated Silk Fibroin for In Vivo Dual-Modal Neural-Vascular Activity Probing.* Advanced Materials, 2021. **33**(34): p. 2100221.
210. He, H., et al., *Enhancement in the Mechanical Stretchability of PEDOT: PSS Films by Compounds of Multiple Hydroxyl Groups for Their Application as Transparent Stretchable Conductors.* Macromolecules, 2021. **54**(3): p. 1234-1242.
211. Lu, B., et al., *Pure pedot: Pss hydrogels.* Nature communications, 2019. **10**(1): p. 1-10.
212. Ramadhan, Z.R., et al., *Conductive PEDOT: PSS on surface-functionalized chitosan biopolymers for stretchable skin-like electronics.* Organic Electronics, 2021. **94**: p. 106165.
213. Kai, H., et al., *Intrinsically stretchable electrochromic display by a composite film of poly (3, 4-ethylenedioxythiophene) and polyurethane.* ACS applied materials & interfaces, 2017. **9**(23): p. 19513-19518.
214. Linderhed, U., et al., *Fully screen printed stretchable electrochromic displays.* Flexible and Printed Electronics, 2021. **6**(4): p. 045014.
215. Heaney, M.B., *Electrical conductivity and resistivity*, in *Measurement, instrumentation, and sensors handbook*. 2017, CRC Press. p. 26-1-26-16.
216. Wang, T., et al., *Novel biodegradable and ultra-flexible transparent conductive film for green light OLED devices.* Carbon, 2021. **172**: p. 379-389.
217. Li, Y., et al., *High-Performance Semi-Transparent Organic Photovoltaic Devices via Improving Absorbing Selectivity.* Advanced Energy Materials, 2021: p. 2003408.
218. Hsu, L.-C., et al., *Stretchable OFET Memories: Tuning the Morphology and the Charge-Trapping Ability of Conjugated Block Copolymers through Soft Segment Branching.* ACS Applied Materials & Interfaces, 2021. **13**(2): p. 2932-2943.
219. Singh, B.P., S.K. Goyal, and P. Kumar, *Solar PV cell materials and technologies: Analyzing the recent developments.* Materials Today: Proceedings, 2021.
220. Wang, D., et al., *Roll-to-roll Fabrication of Highly Transparent Ca: Ag Top-Electrode towards Flexible Large-Area OLED Lighting Application.* Flexible and Printed Electronics, 2021.
221. Amruth, C., M. Pahlevani, and G.C. Welch, *Organic light emitting diodes (OLEDs) with slot-die coated functional layers.* Materials Advances, 2021.
222. Lim, M.S., et al., *Two-dimensionally stretchable organic light-emitting diode with elastic pillar arrays for stress relief.* Nano letters, 2020. **20**(3): p. 1526-1535.
223. Oh, J.Y., et al., *Intrinsically stretchable and healable semiconducting polymer for organic transistors.* Nature, 2016. **539**(7629): p. 411-415.
224. Qin, J., et al., *Recent progress in flexible and stretchable organic solar cells.* Advanced Functional Materials, 2020. **30**(36): p. 2002529.

225. Lu, Y., et al., *Stretchable and Twistable Resistive Switching Memory with Information Storage and Computing Functionalities.* Advanced Materials Technologies, 2021. **6**(1): p. 2000810.
226. Hsu, L.-C., et al., *Stretchable OFET Memories: Tuning the Morphology and the Charge-Trapping Ability of Conjugated Block Copolymers through Soft Segment Branching.* ACS Applied Materials & Interfaces.
227. Chen, S., et al., *Transparent, highly-stretchable, adhesive, and ionic conductive composite hydrogel for biomimetic skin.* Journal of Materials Science, 2021. **56**(3): p. 2725-2737.
228. Li, Y., et al., *Highly stretchable polystyrene sulfonate organic electrochemical transistors achieved via polyethylene glycol addition.* Flexible and Printed Electronics, 2019. **4**(4): p. 044004.
229. Morikawa, Y., et al., *Ultrastretchable kirigami bioprobes.* Advanced healthcare materials, 2018. **7**(3): p. 1701100.
230. Latonen, R.-M., et al., *Electrospinning of Electroconductive Water-Resistant Nanofibers of PEDOT–PSS, Cellulose Nanofibrils and PEO: Fabrication, Characterization, and Cytocompatibility.* ACS Applied Bio Materials, 2020.
231. Cárdenas-Martínez, J., et al., *Flexibleand transparent supercapacitors using electrospun PEDOT: PSS electrodes.* Synthetic Metals, 2020. **267**: p. 116436.
232. Norris, I.D., et al., *Electrostatic fabrication of ultrafine conducting fibers: polyaniline/polyethylene oxide blends.* Synthetic metals, 2000. **114**(2): p. 109-114.
233. Huang, H.J.n., et al., *Improved Performance of Thick Films Based Binary and Ternary Bulk Heterojunction Organic Photovoltaic Devices Incorporated with Electrospinning Processed Nanofibers.* Advanced Materials Interfaces, 2018. **5**(20): p. 1800914.
234. Román-Doval, R., et al., *Enhancing electrospun scaffolds of PVP with polypyrrole/iodine for tissue engineering of skin regeneration by coating via a plasma process.* Journal of Materials Science, 2019. **54**(4): p. 3342-3353.
235. Marega, C. and R. Saini, *Preparation and characterization of conductive polymer blends of polypyrrole and poly (ethylene oxide).* Journal of nanoscience and nanotechnology, 2018. **18**(2): p. 1283-1289.
236. Basri, N.A.F., M.N. Mustafa, and Y. Sulaiman, *Facile fabrication of PVA nanofiber coated with PEDOT as a counter electrode for dye-sensitized solar cell.* Journal of Materials Science: Materials in Electronics, 2019: p. 1-7.
237. Choi, G.M., et al., *PEDOT: PSS/Polyacrylamide Nanoweb–Highly Reliable Soft Conductors with Swelling-Resistance.* ACS applied materials & interfaces, 2019.
238. Zarrin, N., et al., *An investigation on the fabrication of conductive polyethylene dioxythiophene (PEDOT) nanofibers through electrospinning.* Synthetic metals, 2018. **244**: p. 143-149.
239. Haider, A., S. Haider, and I.-K. Kang, *A comprehensive review summarizing the effect of electrospinning parameters and potential applications of nanofibers in biomedical and biotechnology.* Arabian Journal of Chemistry, 2018. **11**(8): p. 1165-1188.
240. Chen, R., et al., *Transparent impact-resistant composite films with bioinspired hierarchical structure.* ACS applied materials & interfaces, 2019. **11**(26): p. 23616-23622.
241. Yanılmaz, M. and A.S. Sarac, *A review: effect of conductive polymers on the conductivities of electrospun mats.* Textile Research Journal, 2014. **84**(12): p. 1325-1342.
242. Laforgue, A. and L. Robitaille, *Production of conductive PEDOT nanofibers by the combination of electrospinning and vapor-phase polymerization.* Macromolecules, 2010. **43**(9): p. 4194-4200.

243. Jin, S., et al., *Synthesis of freestanding PEDOT: PSS/PVA@ Ag NPs nanofiber film for high-performance flexible thermoelectric generator.* Polymer, 2019. **167**: p. 102-108.
244. Tsai, N.C., et al., *Poly (3, 4-ethylenedioxythiophene) Polymer Composite Bioelectrodes with Designed Chemical and Topographical Cues to Manipulate the Behavior of PC12 Neuronal Cells.* Advanced Materials Interfaces, 2019. **6**(5): p. 1801576.
245. Verpoorten, E., et al., *Design and optimization of piezoresistive peo/pedot: Pss electrospun nanofibers for wearable flex sensors.* Nanomaterials, 2020. **10**(11): p. 2166.
246. Winther-Jensen, B., D.W. Breiby, and K. West, *Base inhibited oxidative polymerization of 3, 4-ethylenedioxythiophene with iron (III) tosylate.* Synthetic metals, 2005. **152**(1-3): p. 1-4.
247. Koski, A., K. Yim, and S. Shivkumar, *Effect of molecular weight on fibrous PVA produced by electrospinning.* Materials Letters, 2004. **58**(3-4): p. 493-497.
248. Bolin, M.H., et al., *Nano-fiber scaffold electrodes based on PEDOT for cell stimulation.* Sensors and Actuators B: Chemical, 2009. **142**(2): p. 451-456.
249. Bessaire, B., et al., *Synthesis of continuous conductive PEDOT: PSS nanofibers by electrospinning: A conformal coating for optoelectronics.* ACS applied materials & interfaces, 2017. **9**(1): p. 950-957.
250. Kiristi, M., et al., *Electrospun chitosan/PEDOT nanofibers.* Materials Science and Engineering: C, 2013. **33**(7): p. 3845-3850.
251. Mujib, S.B., et al., *Electrospun SiOC ceramic fiber mats as freestanding electrodes for electrochemical energy storage applications.* Ceramics International, 2020. **46**(3): p. 3565-3573.
252. Wang, H. and L. Pilon, *Physical interpretation of cyclic voltammetry for measuring electric double layer capacitances.* Electrochimica Acta, 2012. **64**: p. 130-139.
253. Travaglini, L., et al., *Single-Material OECT-Based Flexible Complementary Circuits Featuring Polyaniline in Both Conducting Channels.* Advanced Functional Materials, 2021. **31**(4): p. 2007205.
254. Shaker, A., et al., *Micropatterned flexible strain gauge sensor based on wet electrospun polyurethane/PEDOT: PSS nanofibers.* Smart Materials and Structures, 2019. **28**(7): p. 075029.
255. Kaiser, A.B., *Electronic transport properties of conducting polymers and carbon nanotubes.* Reports on Progress in Physics, 2001. **64**(1): p. 1.
256. Argun, A.A., et al., *Multicolored electrochromism in polymers: structures and devices.* Chemistry of materials, 2004. **16**(23): p. 4401-4412.
257. Shakhnov, V., A. Vlasov, and S. Tokarev. *Electrochromic thin-film components for information representation systems*. in *IOP Conference series: materials science and Engineering*. 2016. IOP Publishing.
258. Chaudhary, A., et al., *Pentafluorophenyl substituted fulleropyrrolidine: a molecule enabling the most efficient flexible electrochromic device with fast switching.* Journal of Materials Chemistry C, 2021. **9**(10): p. 3462-3469.
259. Yang, Y. and A. Heeger, *Polyaniline as a transparent electrode for polymer light-emitting diodes: Lower operating voltage and higher efficiency.* Applied Physics Letters, 1994. **64**(10): p. 1245-1247.
260. Yemata, T.A., et al., *Modulation of the doping level of PEDOT: PSS film by treatment with hydrazine to improve the Seebeck coefficient.* RSC Advances, 2020. **10**(3): p. 1786-1792.
261. de Izarra, A., et al., *Ionic liquid designed for PEDOT: PSS conductivity enhancement.* Journal of the American Chemical Society, 2018. **140**(16): p. 5375-5384.

262. Wu, F., et al., *Conductivity enhancement of PEDOT: PSS via addition of chloroplatinic acid and its mechanism.* Advanced Electronic Materials, 2017. **3**(7): p. 1700047.
263. Wang, X., et al., *Enhancement of thermoelectric performance of PEDOT: PSS films by post-treatment with a superacid.* RSC advances, 2018. **8**(33): p. 18334-18340.
264. Wang, C., et al., *Enhancement of Conductivity and Thermoelectric Property of PEDOT: PSS via Acid Doping and Single Post-Treatment for Flexible Power Generator.* Advanced Sustainable Systems, 2018. **2**(12): p. 1800085.
265. Dijk, G., A.L. Rutz, and G.G. Malliaras, *Stability of PEDOT: PSS-coated gold electrodes in cell culture conditions.* Advanced Materials Technologies, 2020. **5**(3): p. 1900662.
266. He, H., et al., *Biocompatible conductive polymers with high conductivity and high stretchability.* ACS applied materials & interfaces, 2019. **11**(29): p. 26185-26193.
267. Gadisa, A., et al., *Transparent polymer cathode for organic photovoltaic devices.* Synthetic metals, 2006. **156**(16-17): p. 1102-1107.
268. Jia, T., et al., *14.4% efficiency all-polymer solar cell with broad absorption and low energy loss enabled by a novel polymer acceptor.* Nano Energy, 2020. **72**: p. 104718.
269. Lee, D.J., et al., *Solution-processed semitransparent inverted organic solar cells from a transparent conductive polymer electrode.* ECS Journal of Solid State Science and Technology, 2019. **8**(2): p. Q32.
270. Cheng, Q., et al., *Construction of transparent cellulose-based nanocomposite papers and potential application in flexible solar cells.* ACS Sustainable Chemistry & Engineering, 2018. **6**(6): p. 8040-8047.
271. Argun, A.A., A. Cirpan, and J.R. Reynolds, *The first truly all-polymer electrochromic devices.* Advanced Materials, 2003. **15**(16): p. 1338-1341.
272. Qi, D., et al., *Stretchable electronics based on PDMS substrates.* Advanced Materials, 2021. **33**(6): p. 2003155.
273. Keum, K., et al., *Flexible/Stretchable supercapacitors with novel functionality for wearable electronics.* Advanced Materials, 2020. **32**(51): p. 2002180.
274. Lee, J., et al., *Recent advances in 1D stretchable electrodes and devices for textile and wearable electronics: materials, fabrications, and applications.* Advanced Materials, 2020. **32**(5): p. 1902532.
275. Zhai, W., et al., *Ultra-stretchable and multifunctional wearable electronics for superior electromagnetic interference shielding, electrical therapy and biomotion monitoring.* Journal of Materials Chemistry A, 2021. **9**(11): p. 7238-7247.
276. Dong, K., X. Peng, and Z.L. Wang, *Fiber/fabric-based piezoelectric and triboelectric nanogenerators for flexible/stretchable and wearable electronics and artificial intelligence.* Advanced Materials, 2020. **32**(5): p. 1902549.
277. Zhou, X., et al., *Self-healing, stretchable, and highly adhesive hydrogels for epidermal patch electrodes.* Acta Biomaterialia, 2021.
278. Cicoira, F. *Stretchable and Healable Bioelectronics*. in *ECS Meeting Abstracts*. 2020. IOP Publishing.
279. Choi, J., et al., *Electrospun PEDOT: PSS/PVP nanofibers as the chemiresistor in chemical vapour sensing.* Synthetic Metals, 2010. **160**(13-14): p. 1415-1421.
280. Zhao, W., B. Yalcin, and M. Cakmak, *Dynamic assembly of electrically conductive PEDOT: PSS nanofibers in electrospinning process studied by high speed video.* Synthetic Metals, 2015. **203**: p. 107-116.

281. Ding, Y., et al., *Scalable and facile preparation of highly stretchable electrospun PEDOT: PSS@ PU fibrous nonwovens toward wearable conductive textile applications.* ACS applied materials & interfaces, 2017. **9**(35): p. 30014-30023.
282. Lerond, M., et al., *Combining Electrospinning and Electrode Printing for Fabrication of Stretchable Electrochemical Transistors.* Frontiers in Physics: p. 437.
283. Hamsan, M., et al., *The study of EDLC device fabricated from plasticized magnesium ion conducting chitosan based polymer electrolyte.* Polymer Testing, 2020. **90**: p. 106714.
284. Kato, S.-i., et al., *Strongly red-fluorescent novel donor–π-bridge–acceptor–π-bridge–donor (D–π–A–π–D) type 2, 1, 3-benzothiadiazoles with enhanced two-photon absorption cross-sections.* Chemical communications, 2004(20): p. 2342-2343.
285. Son, W.K., et al., *The effects of solution properties and polyelectrolyte on electrospinning of ultrafine poly (ethylene oxide) fibers.* polymer, 2004. **45**(9): p. 2959-2966.
286. Tao, J., *Effects of Molecular weight and Solution Concentration on Electrospinning of PVA.* Worcester Polytechnic Institute, USA, 2003.
287. Hosseini, E., V.O. Kollath, and K. Karan, *The key mechanism of conductivity in PEDOT: PSS thin films exposed by anomalous conduction behaviour upon solvent-doping and sulfuric acid post-treatment.* Journal of Materials Chemistry C, 2020. **8**(12): p. 3982-3990.
288. Shin, M.K., et al., *Size-dependent elastic modulus of single electroactive polymer nanofibers.* Applied physics letters, 2006. **89**(23): p. 231929.
289. Liu, F., et al., *Electrochromism of novel triphenylamine-containing polyamide polymers.* Journal of Applied Polymer Science, 2019. **136**(15): p. 47264.
290. Lin, X., et al., *Multifunctional donor–acceptor conjugated polymers containing isoindigo and benzothiadiazole moieties for electrochromic, photoelectric sensor, 2, 4, 6-trinitrophenol detection and resistance memory device.* Journal of Materials Science, 2021. **56**(20): p. 12001-12017.
291. Justin Thomas, K., et al., *Color tuning in benzo [1, 2, 5] thiadiazole-based small molecules by amino conjugation/deconjugation: bright red-light-emitting diodes.* Advanced Functional Materials, 2004. **14**(1): p. 83-90.
292. Wałęsa-Chorab, M. and W. Skene, *Visible-to-NIR electrochromic device prepared from a thermally polymerizable electroactive organic monomer.* ACS Applied Materials & Interfaces, 2017. **9**(25): p. 21524-21531.
293. Wałęsa-Chorab, M., et al., *Suitability of alkyne donor-π-donor-π-donor scaffolds for electrofluorochromic and electrochromic use.* Journal of Materials Chemistry C, 2022.
294. Liang, Z., K. Nakamura, and N. Kobayashi. *Effect of Specific Surface Area of Counter Electrode in Hybrid Capacitor Type Electrochromic Device*. in *ECS Meeting Abstracts*. 2020. IOP Publishing.
295. Jia, Y., et al., *Multifunctional stretchable strain sensor based on polydopamine/reduced graphene oxide/electrospun thermoplastic polyurethane fibrous mats for human motion detection and environment monitoring.* Composites Part B: Engineering, 2020. **183**: p. 107696.
296. Wang, Y., et al., *Flexible electrically resistive-type strain sensors based on reduced graphene oxide-decorated electrospun polymer fibrous mats for human motion monitoring.* Carbon, 2018. **126**: p. 360-371.
297. Hsiang, E.L., et al., *Prospects and challenges of mini-LED, OLED, and micro-LED displays.* Journal of the Society for Information Display, 2021. **29**(6): p. 446-465.

298. Adetayo, A.E., et al., *Improvements of Organic Light-Emitting Diodes Using Graphene as an Emerging and Efficient Transparent Conducting Electrode Material.* Advanced Optical Materials, 2021. **9**(14): p. 2002102.
299. Ko, K.-J., et al., *Fabrication of an oxide/metal/oxide structured electrode integrated with antireflective film to enhance performance in flexible organic light-emitting diodes.* Materials Today Energy, 2021. **20**: p. 100704.
300. Cinquino, M., et al., *Effect of surface tension and drying time on inkjet-printed PEDOT: PSS for ITO-free OLED devices.* Journal of Science: Advanced Materials and Devices, 2021: p. 100394.
301. Liu, S., et al., *Efficient ITO-free organic light-emitting devices with dual-functional PSS-rich PEDOT: PSS electrode by enhancing carrier balance.* Journal of Materials Chemistry C, 2019. **7**(18): p. 5426-5432.
302. Tian, Y., et al., *High-Performance Transparent PEDOT: PSS/CNT Films for OLEDs.* Nanomaterials, 2021. **11**(8): p. 2067.
303. Fenoy, G.E., et al., *Functionalization Strategies of PEDOT and PEDOT: PSS Films for Organic Bioelectronics Applications.* Chemosensors, 2021. **9**(8): p. 212.
304. Dufil, G., et al., *Plant Bioelectronics and Biohybrids: The Growing Contribution of Organic Electronic and Carbon-Based Materials.* Chemical Reviews, 2021.
305. Wu, X. and H. Peng, *Polymer-based flexible bioelectronics.* Science Bulletin, 2019. **64**(9): p. 634-640.
306. Shim, H., et al., *Fully rubbery synaptic transistors made out of all-organic materials for elastic neurological electronic skin.* Nano Research, 2022. **15**(2): p. 758-764.
307. Khalifeh, S., *Polymers in Organic Electronics: Polymer Selection for Electronic, Mechatronic, and Optoelectronic Systems*. 2020: Elsevier.
308. Dauzon, E., et al., *Stretchable and transparent conductive PEDOT: PSS-based electrodes for organic photovoltaics and strain sensors applications.* Advanced Functional Materials, 2020. **30**(28): p. 2001251.
309. Cheng, P. and Y. Yang, *Narrowing the band gap: the key to high-performance organic photovoltaics.* Accounts of chemical research, 2020. **53**(6): p. 1218-1228.
310. Fenoy, G.E., et al., *PEDOT: Tosylate-Polyamine-Based Organic Electrochemical Transistors for High-Performance Bioelectronics.* Advanced Electronic Materials, 2021. **7**(6): p. 2100059.
311. Hempel, F., et al., *PEDOT: PSS organic electrochemical transistors for electrical cell-substrate impedance sensing down to single cells.* Biosensors and Bioelectronics, 2021. **180**: p. 113101.
312. Tang, K., W. Miao, and S. Guo, *Crosslinked PEDOT: PSS Organic Electrochemical Transistors on Interdigitated Electrodes with Improved Stability.* ACS Applied Polymer Materials, 2021. **3**(3): p. 1436-1444.
313. Song, J., et al., *High-conductivity, flexible and transparent PEDOT: PSS electrodes for high performance semi-transparent supercapacitors.* Polymers, 2020. **12**(2): p. 450.
314. Fan, X., et al., *PEDOT: PSS for flexible and stretchable electronics: modifications, strategies, and applications.* Advanced Science, 2019. **6**(19): p. 1900813.
315. Xu, S., et al., *High-performance PEDOT: PSS flexible thermoelectric materials and their devices by triple post-treatments.* Chemistry of Materials, 2019. **31**(14): p. 5238-5244.
316. Li, Y., et al., *Autonomic Self-Healing of PEDOT: PSS Achieved Via Polyethylene Glycol Addition.* Advanced Functional Materials, 2020. **30**(30): p. 2002853.

317. Shi, H., et al., *Effective approaches to improve the electrical conductivity of PEDOT: PSS: a review.* Advanced Electronic Materials, 2015. **1**(4): p. 1500017.
318. Jeong, W., et al., *Enhancing the conductivity of PEDOT: PSS films for biomedical applications via hydrothermal treatment.* Biosensors and Bioelectronics, 2021. **171**: p. 112717.
319. Kee, S., et al., *Highly stretchable and air-stable PEDOT: PSS/ionic liquid composites for efficient organic thermoelectrics.* Chemistry of Materials, 2019. **31**(9): p. 3519-3526.
320. Choi, K.-m., et al., *Plasticization of poly (lactic acid)(PLA) through chemical grafting of poly (ethylene glycol)(PEG) via in situ reactive blending.* European Polymer Journal, 2013. **49**(8): p. 2356-2364.
321. Kulinski, b. and E. Piorkowska, *Crystallization, structure and properties of plasticized poly (L-lactide).* Polymer, 2005. **46**(23): p. 10290-10300.
322. Geiculescu, O.E., et al., *The effect of low-molecular-weight poly (ethylene glycol)(PEG) plasticizers on the transport properties of lithium fluorosulfonimide ionic melt electrolytes.* The Journal of Physical Chemistry B, 2014. **118**(19): p. 5135-5143.
323. Ghosh, S., et al., *Fabrication and investigation of 3D tuned PEG/PEDOT: PSS treated conductive and durable cotton fabric for superior electrical conductivity and flexible electromagnetic interference shielding.* Composites Science and Technology, 2019. **181**: p. 107682.
324. Li, P., K. Sun, and J. Ouyang, *Stretchable and conductive polymer films prepared by solution blending.* ACS applied materials & interfaces, 2015. **7**(33): p. 18415-18423.
325. Sarabia-Riquelme, R., et al., *Highly conductive wet-spun PEDOT: PSS fibers for applications in electronic textiles.* Journal of Materials Chemistry C, 2020. **8**(33): p. 11618-11630.
326. Xia, Y. and J. Ouyang, *Significant different conductivities of the two grades of poly (3, 4-ethylenedioxythiophene): poly (styrenesulfonate), Clevios P and Clevios PH1000, arising from different molecular weights.* ACS applied materials & interfaces, 2012. **4**(8): p. 4131-4140.
327. Jang, W., et al., *Counterbalancing of morphology and conductivity of poly (3, 4-ethylenedioxythiophene) polystyrene sulfonate based flexible devices.* Nanoscale, 2016. **8**(47): p. 19557-19563.
328. Lerond, M., et al., *Combining Electrospinning and Electrode Printing for Fabrication of Stretchable Electrochemical Transistors.* Frontiers in Physics, 2021. **9**: p. 437.
329. Okuzaki, H., Y. Harashina, and H. Yan, *Highly conductive PEDOT/PSS microfibers fabricated by wet-spinning and dip-treatment in ethylene glycol.* European Polymer Journal, 2009. **45**(1): p. 256-261.
330. Lin, Y.-J., W.-S. Ni, and J.-Y. Lee, *Effect of incorporation of ethylene glycol into PEDOT: PSS on electron phonon coupling and conductivity.* Journal of Applied Physics, 2015. **117**(21): p. 215501.
331. Fan, Z., et al., *Significant enhancement in the thermoelectric properties of PEDOT: PSS films through a treatment with organic solutions of inorganic salts.* ACS applied materials & interfaces, 2016. **8**(35): p. 23204-23211.
332. Kim, J., et al., *Sulfuric acid vapor treatment for enhancing the thermoelectric properties of PEDOT: PSS thin-films.* Journal of Materials Science: Materials in Electronics, 2016. **27**(6): p. 6122-6127.

333. Jeong, M.H., et al., *Increasing the thermoelectric power factor of solvent-treated PEDOT: PSS thin films on PDMS by stretching.* Journal of Materials Chemistry A, 2018. **6**(32): p. 15621-15629.
334. Gueye, M.N., et al., *Structure and dopant engineering in PEDOT thin films: practical tools for a dramatic conductivity enhancement.* Chemistry of Materials, 2016. **28**(10): p. 3462-3468.
335. Dechene, J.M., *Surface modifications of poly (dimethylsiloxane) for biological application of microfluidic devices.* 2010.
336. Schwartz, G., et al., *Flexible polymer transistors with high pressure sensitivity for application in electronic skin and health monitoring.* Nature communications, 2013. **4**(1): p. 1-8.
337. Huang, S., et al., *Flexible electronics: stretchable electrodes and their future.* Advanced Functional Materials, 2019. **29**(6): p. 1805924.
338. Li, G., et al., *PEDOT: PSS/grafted-PDMS electrodes for fully organic and intrinsically stretchable skin-like electronics.* ACS applied materials & interfaces, 2019. **11**(10): p. 10373-10379.

APPENDICES

APPENDIX A COMBINING ELECTROSPINNING AND ELECTRODE PRINTING FOR THE FABRICATION OF STRETCHABLE ORGANIC ELECTROCHEMICAL TRANSISTORS

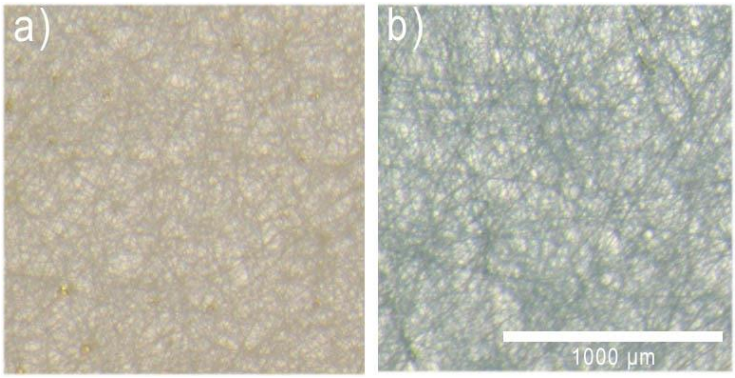

Supplementary Figure 1 : Optical image of electrospun fibers before (a) and after (b) vacuum vapor phase polymerization.

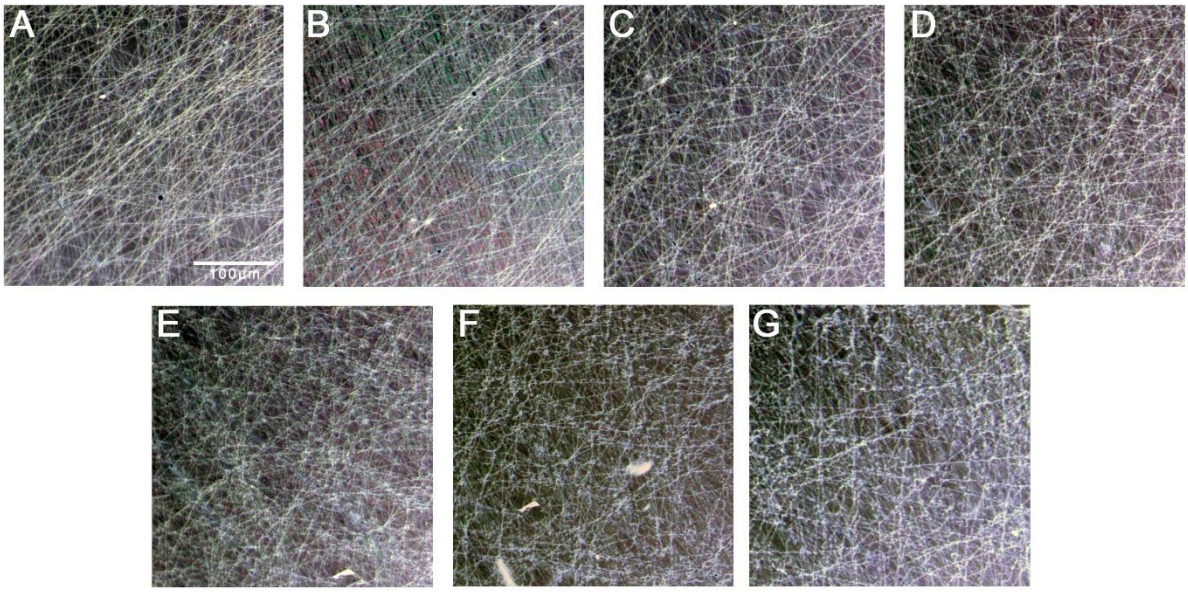

Supplementary Figure 2 : Optical pictures of electrospun fibers from mixture B under different strains: 0% (A), 20% (B), 40% (C), 60% (D), 80% (E), 100% (F) and 120% (G).

Specific Capacitance (C_p) calculation

The specific capacitance can be calculated from voltammograms with the following relation : $C_p = \frac{A}{m.k.\Delta V}$. Where A is the integrated area from the voltammograms, m the mass of PEDOT:Tos fibers, k the scan rate (20 mV/s) and ΔV the potential window (1.2V).

The mass m of deposited fibers on the electrode was estimated as following:

1. The flow rate of electrospinning is fixed at 0.1 mL/h and the electrospinning duration is known (either 700, 1000 or 1500 sec), allowing us to calculate the quantity of electrospun fibers: 22.9 mg, 31.9 mg and 49.2 mg regarding to the increasing electrospinning time.
2. This amount of fibers is supposed to be uniformly deposited on the cylindrical collector, allowing the calculation of a fiber density. The surface of the collector is of 113.1 cm^2, giving surface densities of $2.02*10^{-4}$ g/cm^2, $2.82*10^{-4}$ g/cm^2 and $4.35*10^{-4}$ g/cm^2 respectively.
3. The active surface of the electrode is fixed to 25 mm^2, then the amount of fibers involved in the electrochemical reaction is of $5.06*10^{-5}$ g, $7.04*10^{-5}$ g and $1.09*10^{-4}$ g respectively.

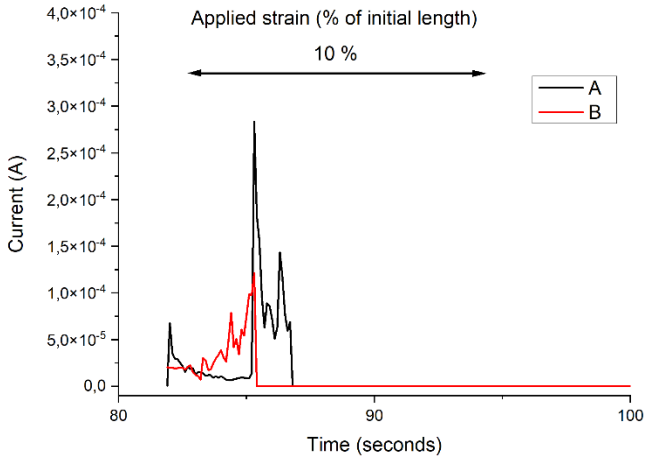

Supplementary Figure 3 : Current as a function of time for PEDOT :Tos spincoated films on PDMS of the Mixtures A (▬) and B (▬). The samples were stretched from 0 to 10% strain at 0.1 cm/s.

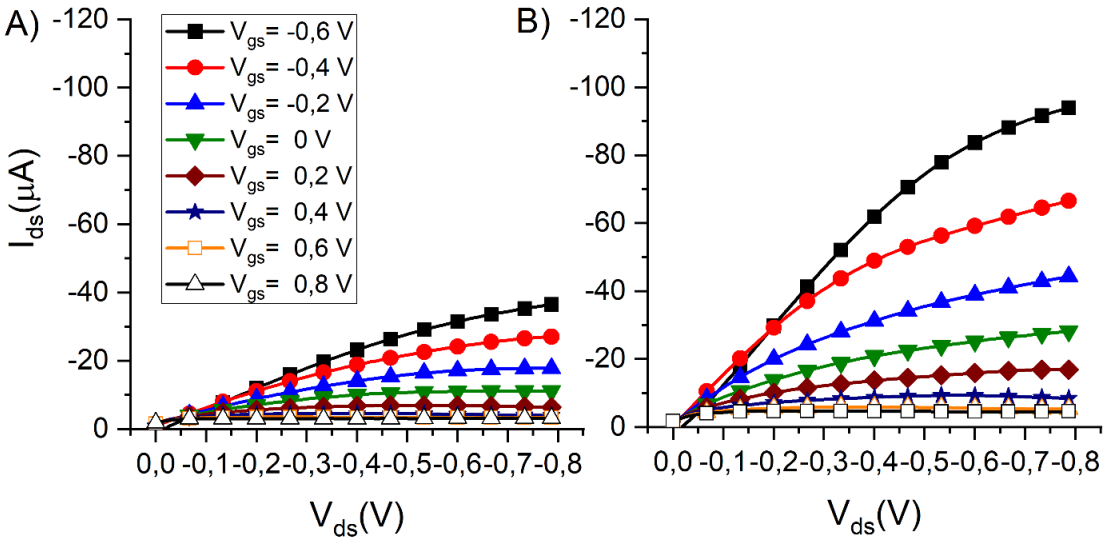

Supplementary Figure 4: Output curves of the transistors prepared from the mixture A after 700 seconds (A) and 1000 seconds (B) of electrospinning.

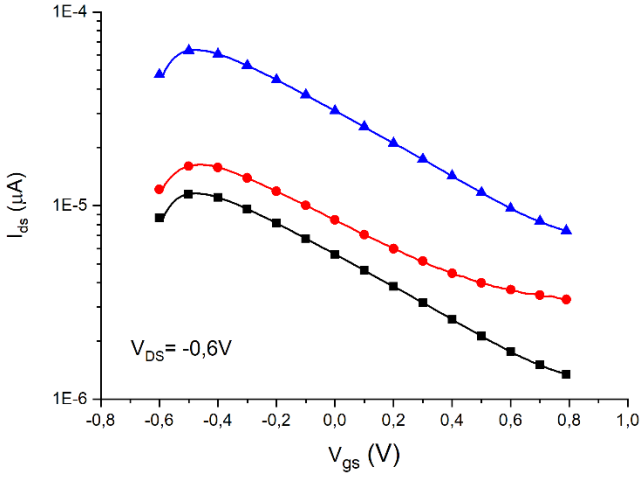

Supplementary Figure 5 : Transfer curves of the transistors prepared from the mixture A after 700 seconds (■), 1000 seconds (●) and 1500 seconds (▲) of electrospinning.

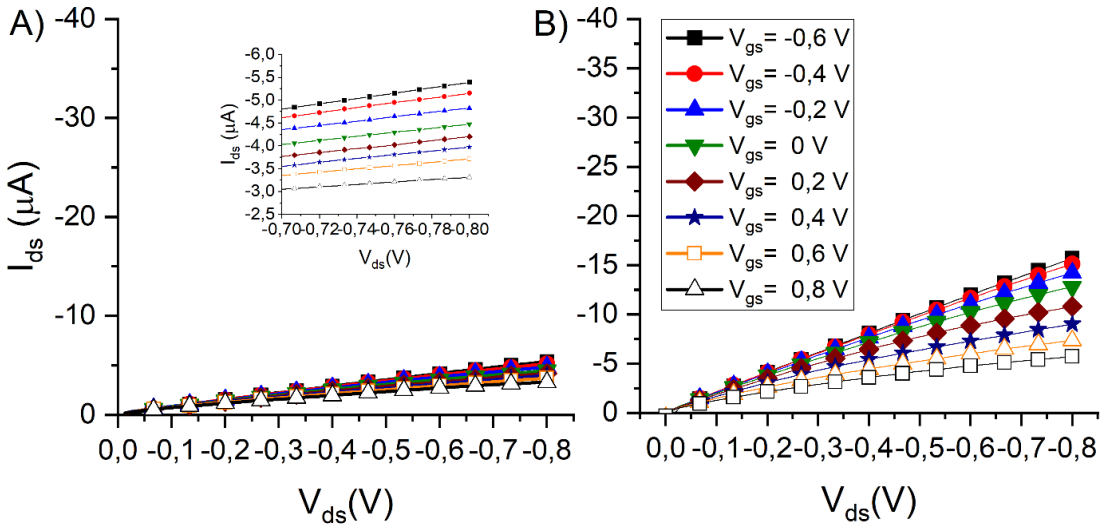

Supplementary Figure 6 : Output curves of the transistors prepared from the mixture B after 700 seconds (A) and 1000 seconds (B) of electrospinning.

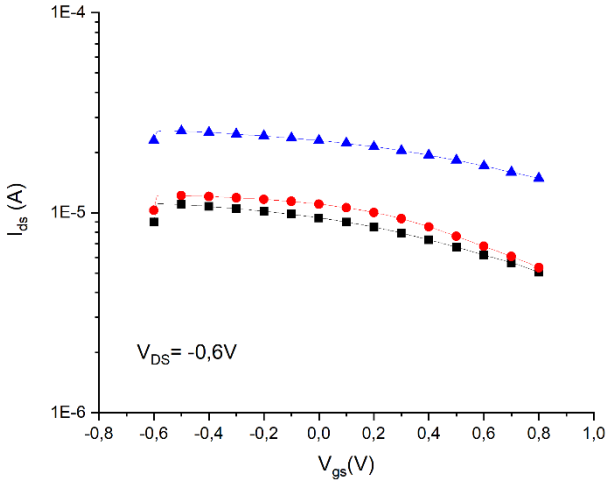

Supplementary Figure 7 : Transfer curves of the transistors prepared from the mixture B after (■), 1000 seconds (●) and 1500 seconds (▲) of electrospinning.

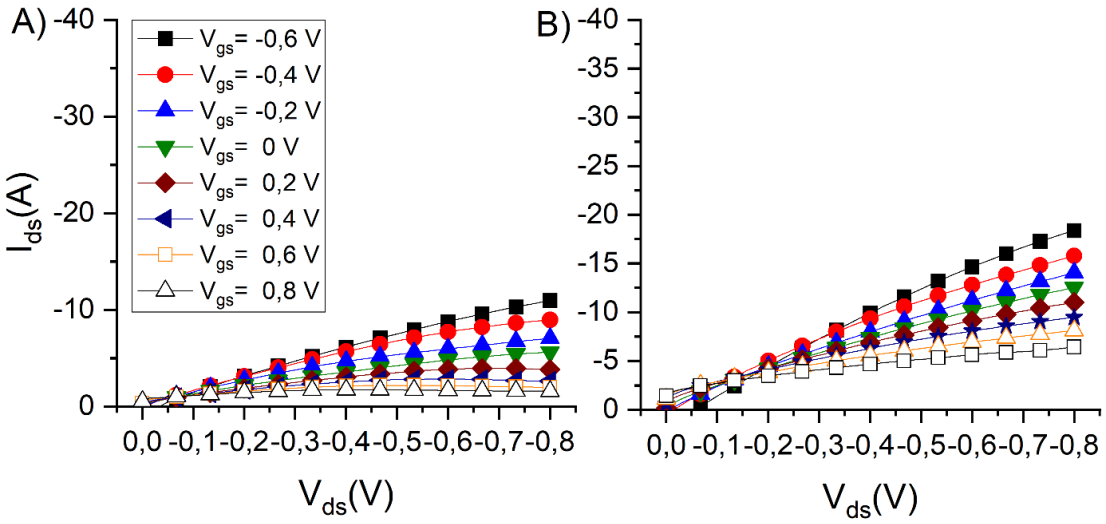

Supplementary Figure 8: Output curves of the transistors prepared from the mixture C after 700 seconds (A) and 1000 seconds (B) of electrospinning.

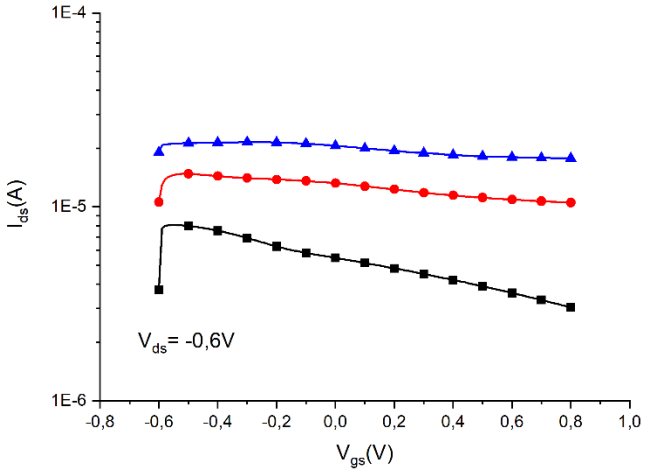

Supplementary Figure 9: Transfer curves of the transistors prepared from the mixture C after (■), 1000 seconds (●) and 1500 seconds (▲) of electrospinning.

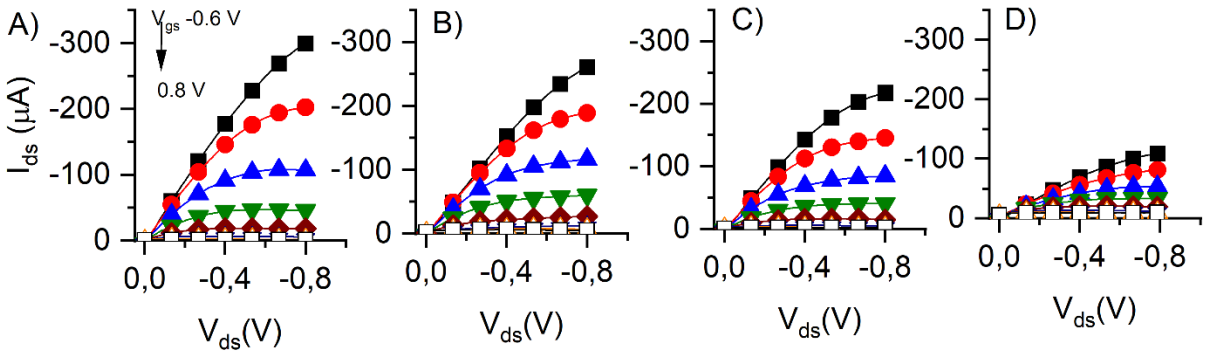

Supplementary Figure 10 : Output curves of a transistor prepared by electrospinning from the mixture A and stretched at 0% (A), 10% (B), 20% (C), 30% (D) strain.

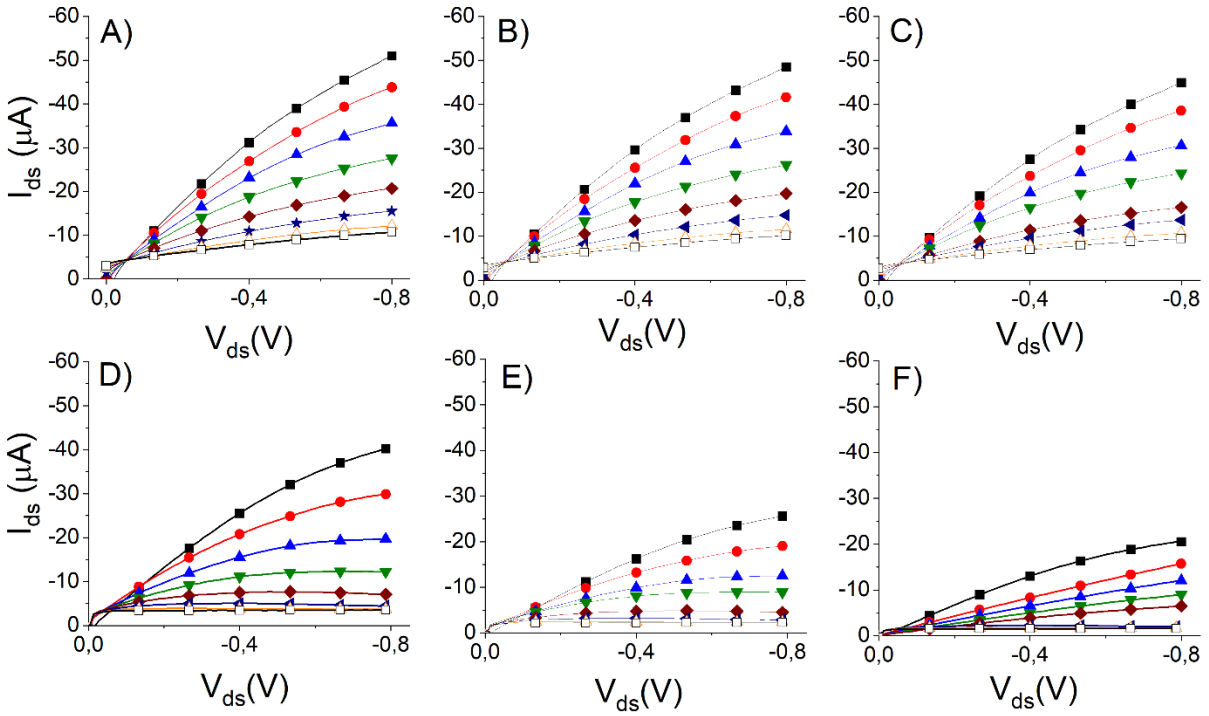

Supplementary Figure 11: Output curves of a transistor prepared by electrospinning from the mixture B and stretched at 0% (A), 10% (B), 20% (C), 30% (D), 40% (E) and 50% (F) strain.

APPENDIX B AN INTRINSICALLY STRETCHABLE AND BENDABLE ELECTROCHROMIC DEVICE

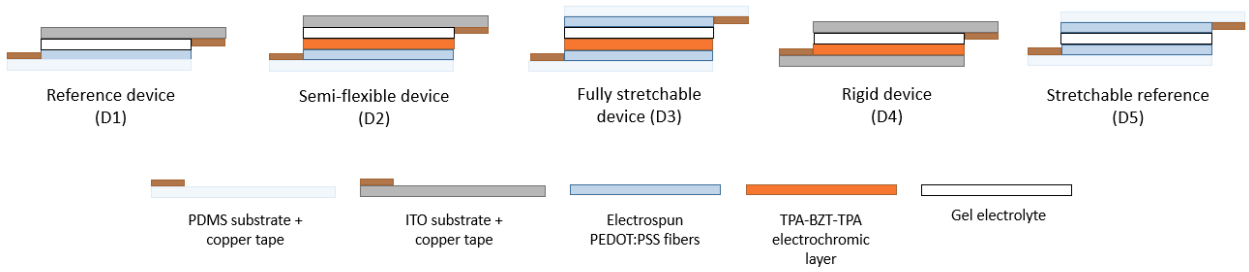

Figure S1. Schematic representation of the five electrochromic device architectures.

$$[\eta] = KM^{\alpha}$$

Equation S1. Mark-Houwink-Sakurada equation relating the viscosity [η] to the molecular weight M with the constants K and α for a given polymer and solvent system. K = 0.00125 and α =0.78 for PEO dissolved in water

$$[C]x[\eta] = 1$$

Equation S2. Critical chain overlap.

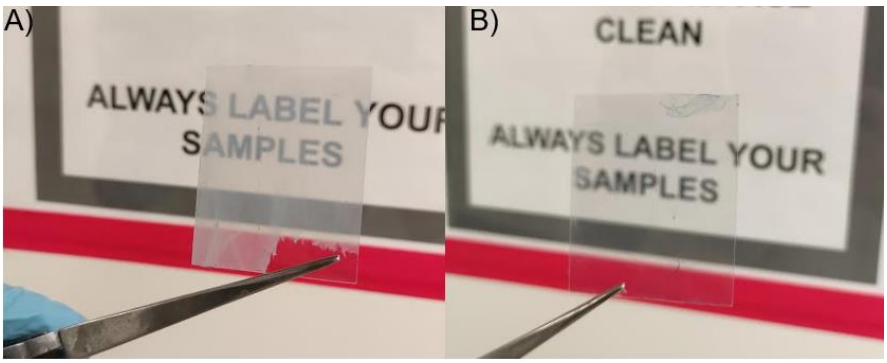

Figure S2. Photographs of a fiber mat before (A) and after (B) soaking in ethanol.

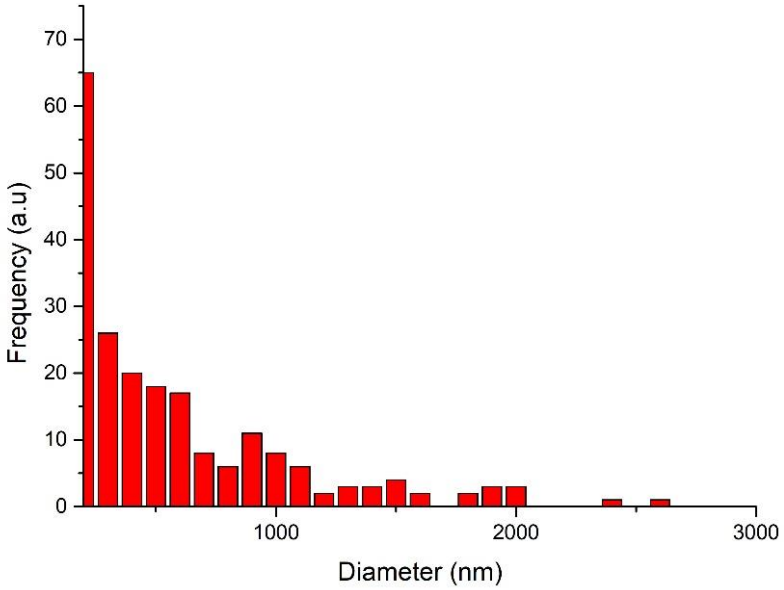

Figure S3. Pore diameter distribution of the fiber mats extracted from the SEM image with the Image J software.

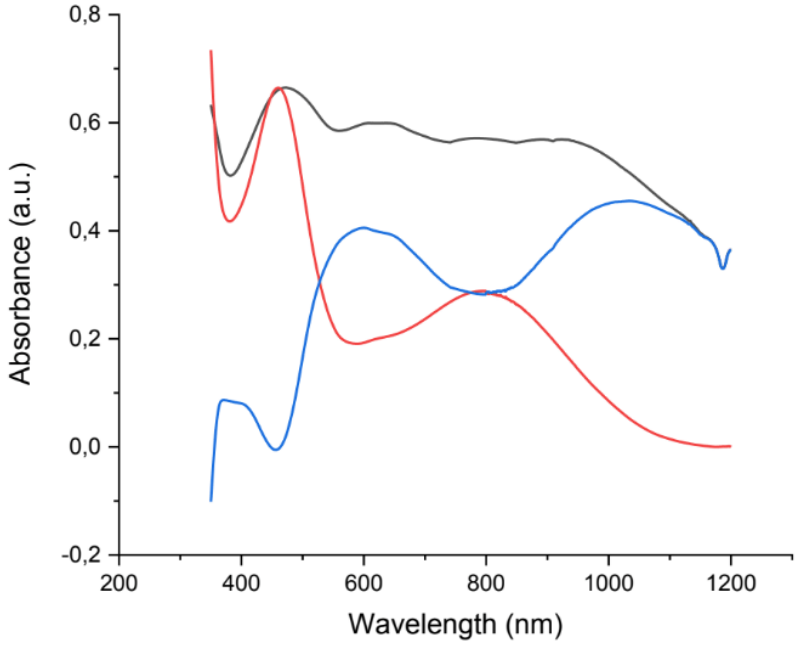

Figure S4. Absorption spectra of the oxidized state of a fully stretchable device (D3, black line), a semi-flexible device (D2, red line), and the resulting spectrum by subtracting the TPA-BTZ-TPA contribution from the fully stretchable device (D3, blue line).

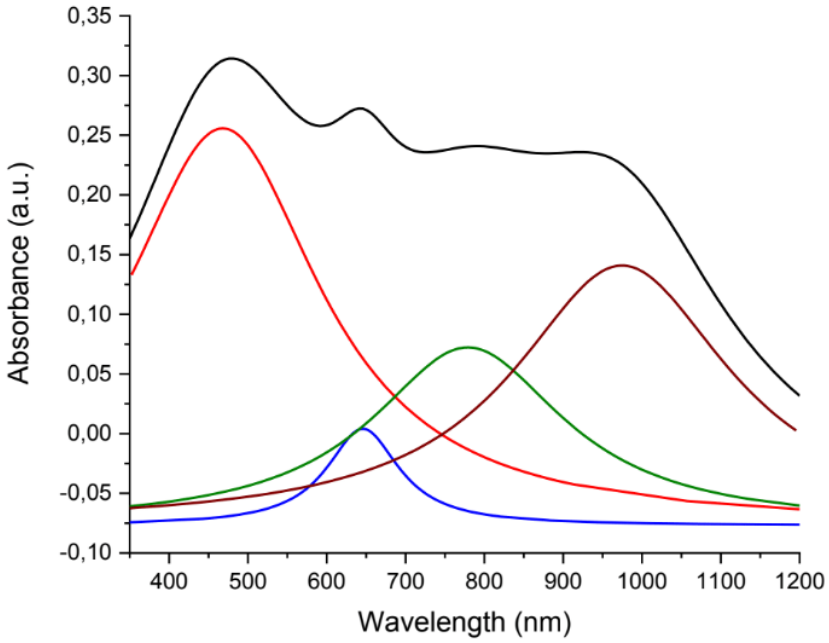

Figure S5. Reconvoluted absorption spectrum (black line) for the corresponding four contributions of the oxidized state of TPA-BZT-TPA (red and green lines) and the reduced PEDOT:PSS fibers (blue and wine lines).

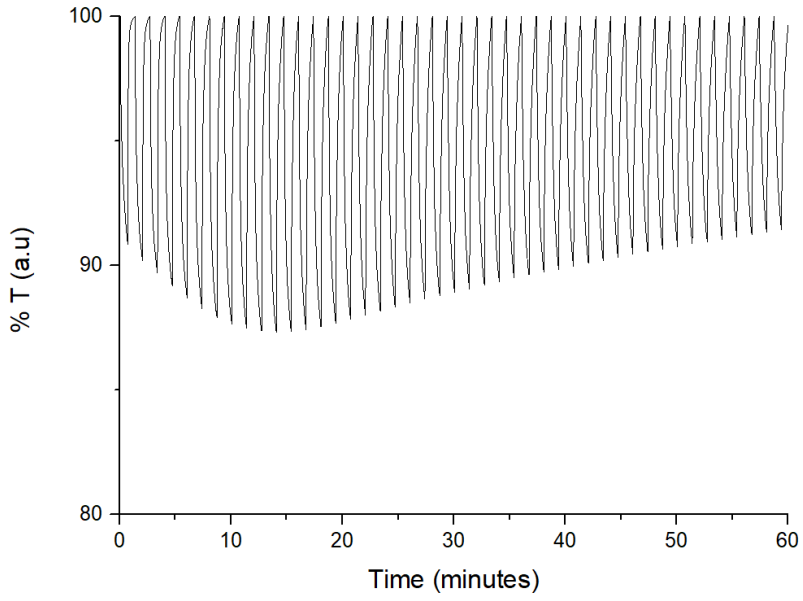

Figure S6. Change in transmittance percent of the rigid electrochromic device (D4) with applied potentials of 0 to +2.5 V switched at 30 sec intervals over 60 minutes and monitored at 952 nm.

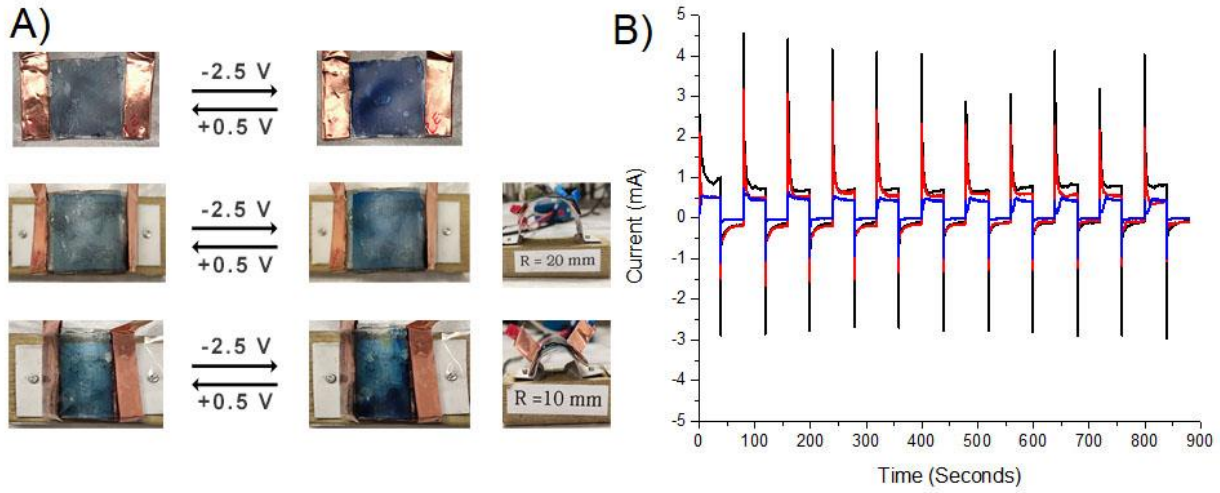

Figure S7. A) Pictures of the stretchable reference device (D5) switched between its bleached (oxidized) and colored (reduced) states and operating on a flat form (top) and bent to a curvature of 0.05 (middle) and 0.1 (bottom). B) Chronoamperometry of the stretchable (D5) reference device when switched between -2.5 and +0.5 V at 40 sec intervals over 11 cycles when bent at a 0 (—), and 10 (—), and 20 (—) mm radius of curvature.

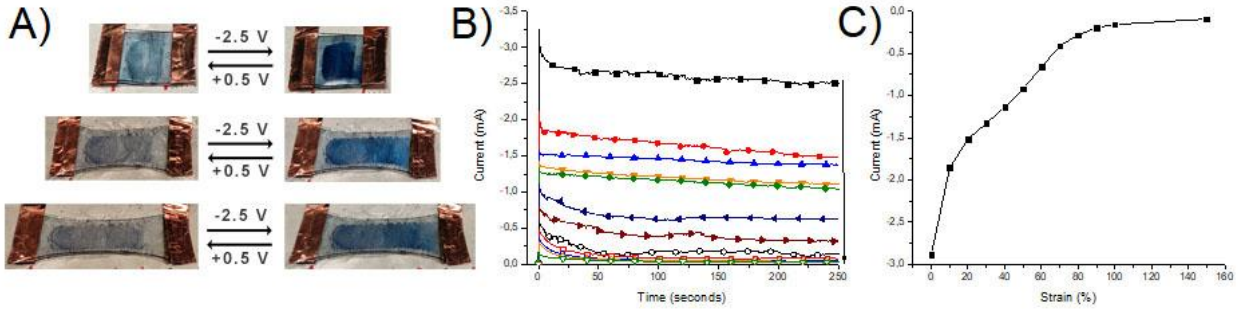

Figure S8. A) Pictures of the stretchable reference device (D5) when switched between its colored (left) and bleached (right) states and when stretched to 0% (top), 100% (middle), and 150% (bottom) strain. B) Chronoamperometry of the stretchable reference electrochromic device (D5) with an applied reduction potential when stretched from 0 to 150% of its initial strain with strains of 0% (—■—), 10% (—●—), 20% (—▲—), 30%(—▼—), 40% (—◆—), 50% (—◀—), 60% (—▶—), 70% (—□—), 80% (—○—), 90% (—△—), 100% (—▽—), and 150% (—◇—). C) Evolution of the measured current during the coloration of the functioning device with applied strains.

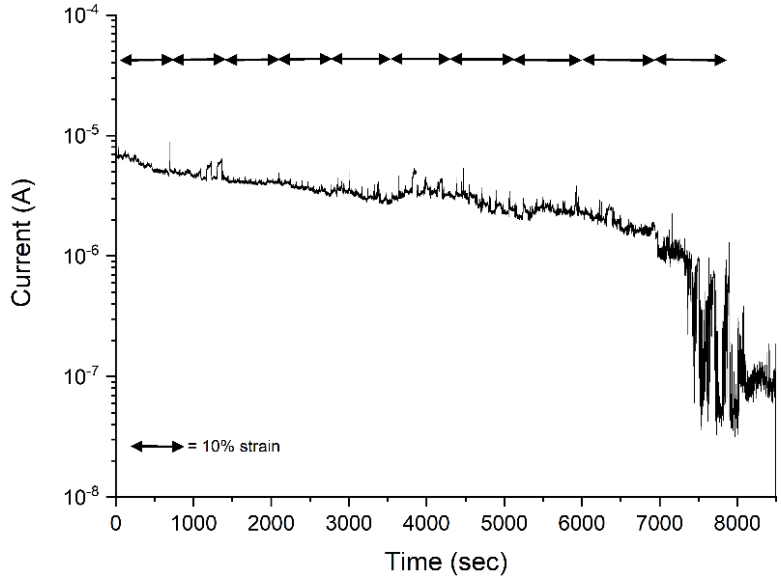

Figure S9. Current of the PEDOT:PSS fibers as a function of time with different strains. The samples were stretched between 10% and 100% strain at 0.1 cm/s. Five consecutive stretching/release cycles were done for each strain between 10% and 100%. The samples were kept in each state (stretched or released) for 1 minute.

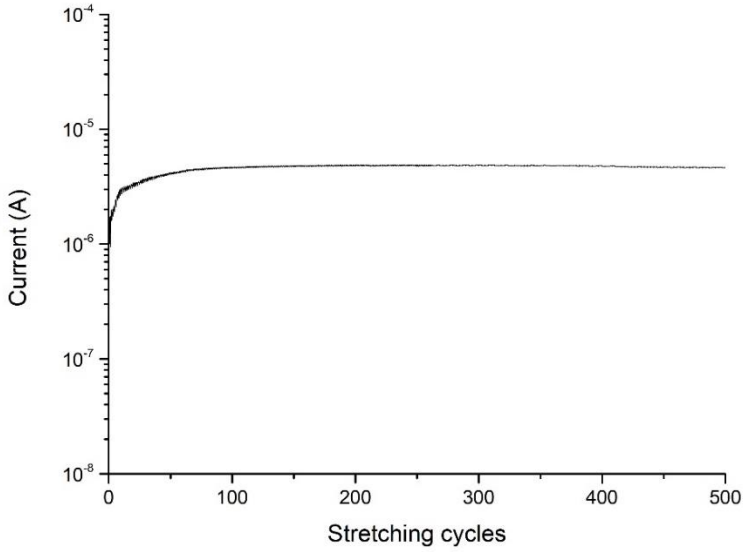

Figure S10. Current of the PEDOT:PSS fibers as a function stretching/releasing cycles. The sample was stretched to 50% strain at 0.1 cm/s and for 500 cycles of consecutive stretching/releasing.

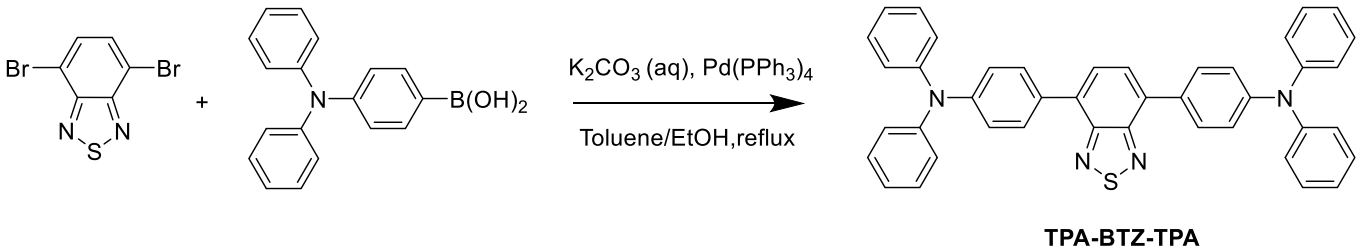

TPA-BTZ-TPA

Figure S11. Reaction scheme for the preparation of the TPA-BZT-TPA electrochrome.

4,7-Bis(4-diphenylaminophenyl)-2,1,3-benzothiaziazole (**TPA-BZT-TPA**).[284] In a dry 100 mL round bottom flask, 4,7-dibromobenzo[c][1,2,5]thiadiazole (1.00 g, 3.4 mmol) and 4-(diphenylamino)-phenyl boronic acid (2.2 g, 7.5 mmol) were dissolved in a toluene/ethanol 4:1 (v/v) mixture (50 mL) under N_2 atm. Then aqueous K_2CO_3 (5.1 mL, 2 M) was added. The reaction mixture was degassed with nitrogen and a catalytic amount of $Pd(PPh_3)_4$ was added under N_2 atm. The reaction mixture was stirred at 90 ˚C for overnight under nitrogen. Afterwards, it was cooled to room temperature. Dichloromethane (100 mL) was added and the mixture was washed with water and brine. The extracted organic layer was dried over $MgSO_4$, filtered, and the filtrate was evaporated under reduced pressure. The solid product was purified by silica gel column chromatography with dichloromethane:hexane (1:2 v/v) to title compound as a bright orange powder (1.3 g, 62%). ^{1} H NMR (400 MHz, $CDCl_3$) δ = 7.90 (d, *J* = 8.7 Hz, 4H), 7.77 (s, 2H), 7.32 (t, *J* = 7.3 Hz, 8H), 7.23 (t, *J* = 8.7 Hz, 12H), 7.10 (t, *J* = 7.3 Hz, 4H) ppm. ^{13}C NMR (100 MHz, $CDCl_3$) δ = 154.2, 147.9, 147.5, 132.2, 131.0, 129.9, 129.4, 127.4, 124.9, 123.29, 122.9 ppm. HR-MS: calc. 623.2264; found 623.2268 $(M + H)^+$.

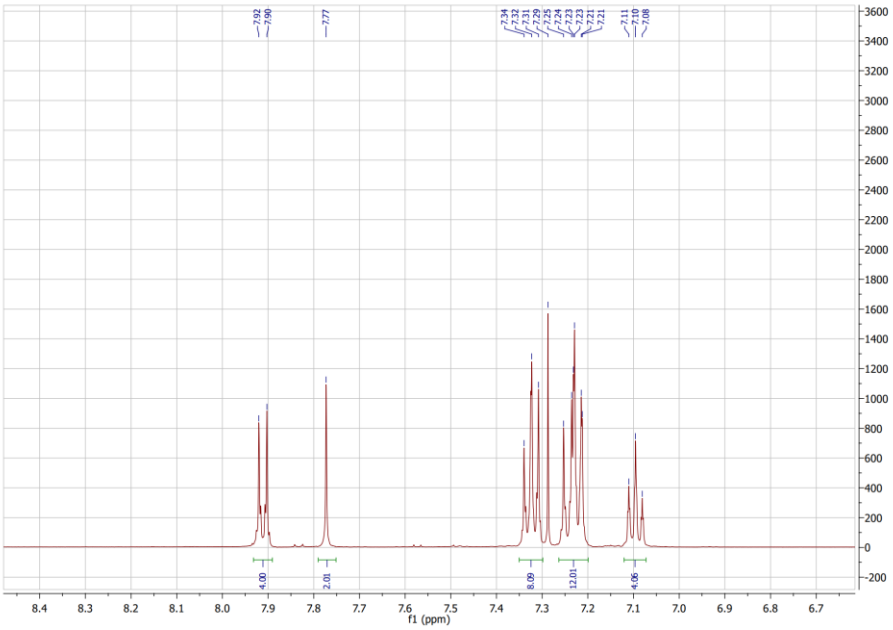

Figure S12. ^{1}H NMR spectrum of TPA-BZT-TPA in $CDCl_3$.

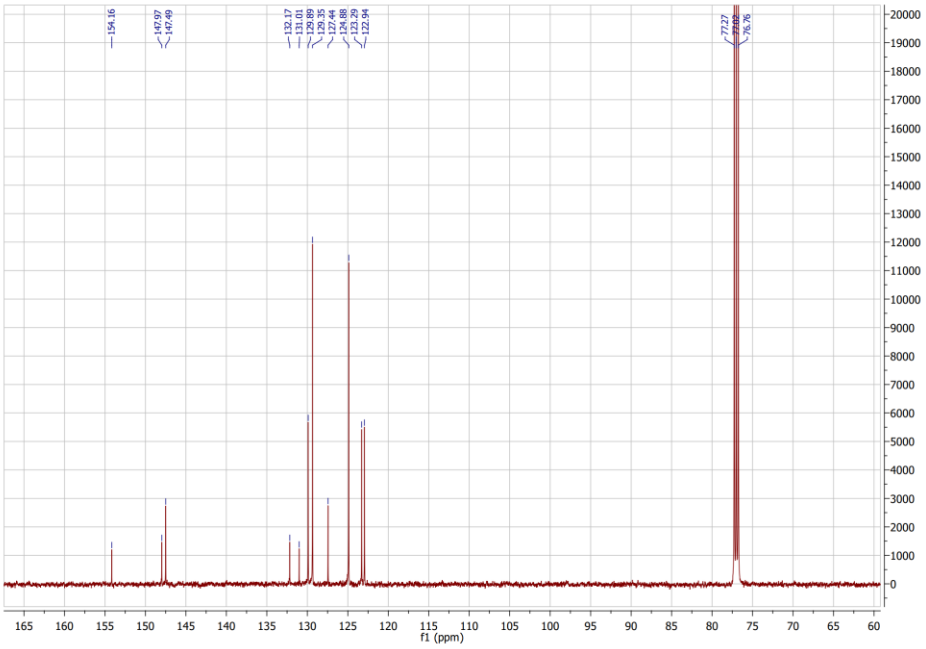

Figure S13. ^{13}C NMR spectrum of TPA-BZT-TPA in $CDCl_3$.

APPENDIX C ENHANCING THE PERFORMANCE OF TRANSPARENT AND HIGHLY STRETCHABLE ORGANIC ELECTROCHEMICAL TRANSISTORS BY ACID TREATMENT AND COPOLYMER BLENDING OF ELECTROSPUN PEDOT:PSS FIBERS

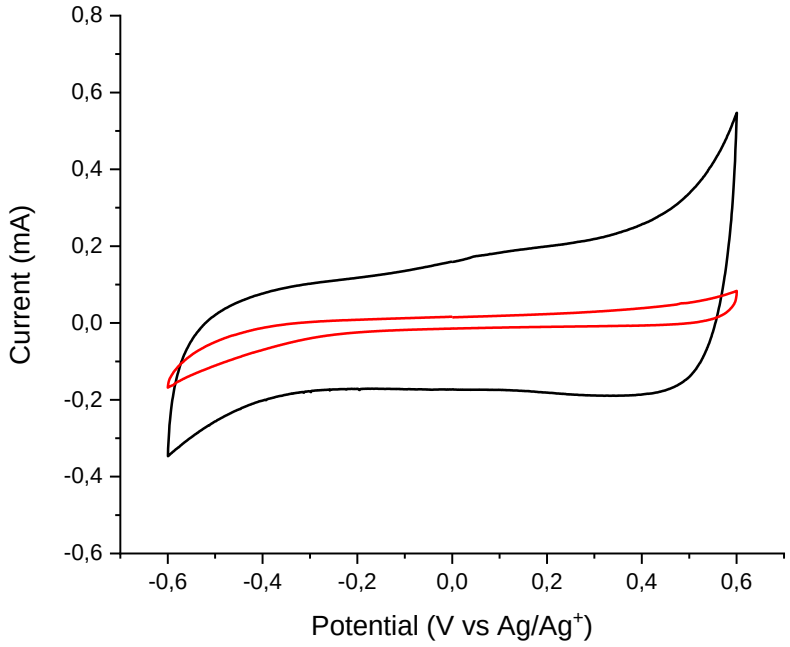

Figure S1. Cyclic voltammogram of acid treated fibers (—) and non-treated fibers (—) in NaCl (0.1 M) at a scan rate of 100 mV/s.

Specific Capacitance (C_p) calculation

The specific capacitance can be calculated form voltammograms with the following relation : $C_p = \frac{A}{m.k.\Delta V}$. Where A is the integrated area from the voltammograms, m the mass of PEDOT:PSS fibers, k the scan rate (100 mV/s) and ΔV the potential window (1.2V).

The mass m of deposited fibers on the electrode was estimated as following:

1. The flow rate of electrospinning is fixed at 0.1 mL/h and the electrospinning duration is known (2000 sec), allowing us to calculate the quantity of electrospun fibers: 0.055 mL or 0.058 g.

2. This amount of fibers is supposed to be uniformly deposited on the cylindrical collector, allowing the calculation of a fiber density. The surface of the collector is of 113.1 cm^2, giving a surface densities of $5.21*10^{-4}$ g/cm^2.
3. The active surface of the electrode is fixed to 25 mm^2, then the amount of fibers involved in the electrochemical reaction is of $1.30*10^{-5}$ g.

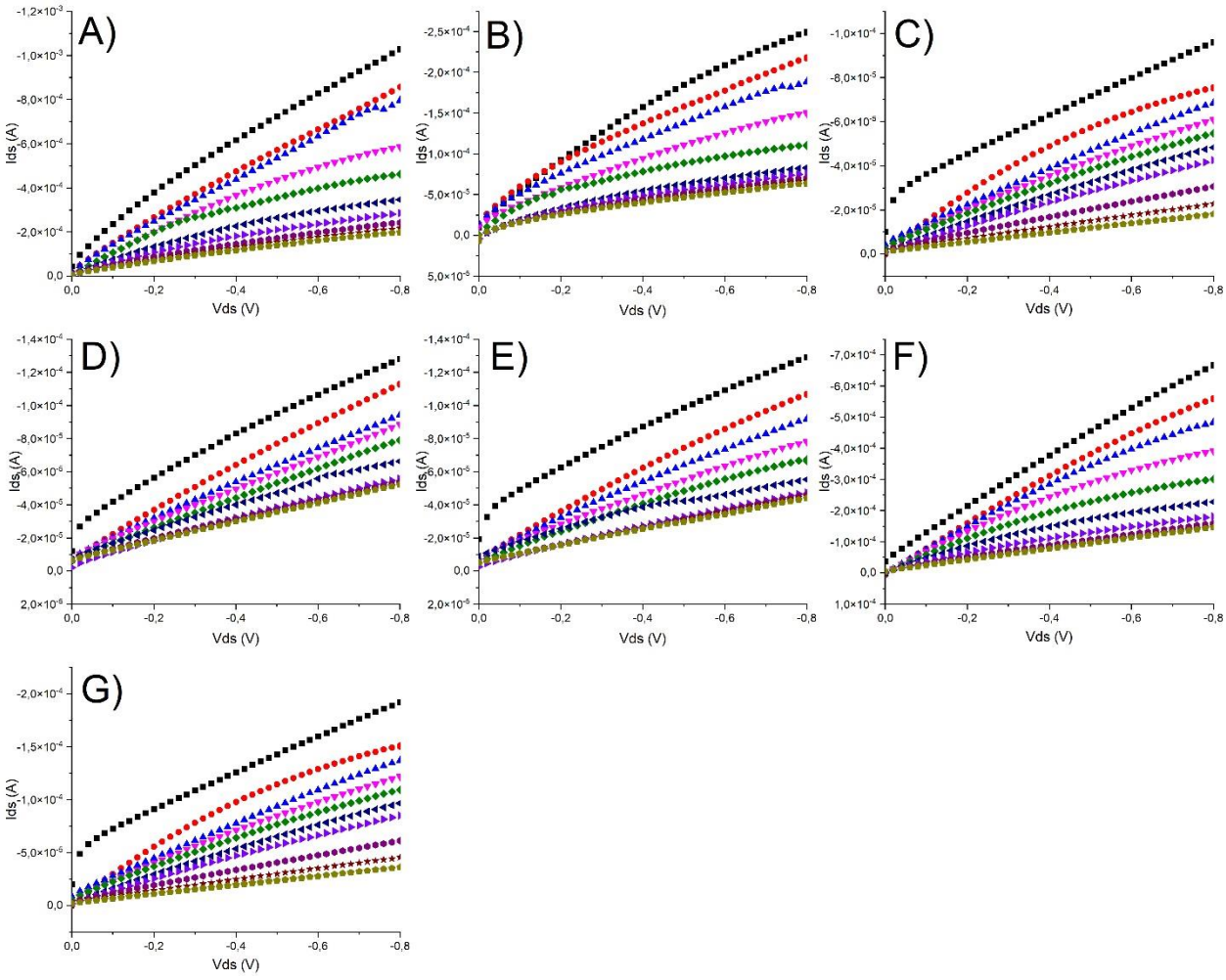

Figure S2. Output curves of stretchable OECTs in the initial state (A), stretched to 50% (B), 100% strain (C), held at 100% strain for 10 hours (D), released to initial state (E), before the cycling test (F) and stretched 100 times to 100% strain (G), and applied gate voltage: -1 (■), -0.8 (●), -0.6 (▲), -0.4 (▼), -0.2 (◆), 0 (★), 0.2 (►), 0.4 (□), 0.6 (○) and 0.6 (△) V